

Phylogeny and biogeography of Neotropical flowering plant tribe Citharexyleae (Verbenaceae)

Laura A. Frost

A dissertation

submitted in partial fulfillment of the
requirements for the degree of

Doctor of Philosophy

University of Washington

2018

Reading Committee:

Richard Olmstead, Chair

Caroline Strömberg

John Klicka

Program Authorized to Offer Degree:

Biology

©Copyright 2018

Laura A. Frost

University of Washington

Abstract

Phylogeny and biogeography of Neotropical flowering plant tribe Citharexyleae (Verbenaceae)

Laura A. Frost

Chair of the Supervisory Committee:

Richard Olmstead

Biology

The New World tropics, or Neotropics, located within tropical latitudes of North and South America, are one of the most diverse ecoregion in the world. However, this diversity is poorly understood in terms of described biodiversity—species numbers are uncertain and collection records are depauperate for many groups distributed in remote locations or dense forest—and patterns of evolution contributing to high diversity—factors underlying speciation in lineages are not well understood. A molecular phylogenetic and systematic study of the Neotropical flowering plant tribe Citharexyleae in the Verbena family (Verbenaceae), which also originated and diversified primarily in the Neotropics, was undertaken in order to describe diversity and understand patterns of evolution in an understudied Neotropical lineage. Chapter 1 comprises a systematic study of tribe Citharexyleae, which describes relationships between the three genera in the tribe (*Baillonia* (1 species), *Citharexylum* (ca. 70 species), and *Rehdera* (2 species)) as well as relationships within *Citharexylum*, the largest genus. *Baillonia* is included in

Citharexylum and *Rehdera* is retained distinct. A subgeneric classification including six subgenera system is proposed for *Citharexylum*, and morphological characters associated with each major clade described. In Chapter 2, the biogeographical patterns underpinning diversification in *Citharexylum* are explored. *Citharexylum* comprises ca. 70 species distributed widely throughout the Neotropics, from northern Mexico to southern Brazil and Argentina. Species occupy multiple biomes including continuously moist broadleaf forest, seasonally dry tropical forest, tropical coniferous forest, high elevation shrublands, and arid shrublands. The contributions of radiation within a biome and adaptation to/colonization of new biomes are compared. Both patterns have played important roles in the diversification of *Citharexylum*, and major lineages within *Citharexylum* display different patterns. The Mesoamerican clade exhibits a pattern of radiation within the ancestral biome with more recent, independent colonization events, whereas the South American clade exhibits a pattern of early colonization and radiation within biomes. Though diversification rates are higher in the Mesoamerican clade, both clades have produced similar taxonomic diversity in the same amount of time. Both patterns contribute equally to overall diversity in the genus. Chapter 3 incorporates molecular sequence data generated by the previous chapters with data generated in previous studies other lineages of Verbenaceae and newly generated data to produce an updated phylogeny of the Verbena family. Verbenaceae comprises ca. 770 species in 28 genera. A previous family-wide study sampled 7 chloroplast regions for 121 species. The expanded dataset encompasses twelve chloroplast regions, two nuclear ribosomal spacers, and eight low-copy nuclear loci for 366 species. Two new clades in Verbenaceae are described, including resurrection of the genus *Scleröon* Benth in Lindl.

ACKNOWLEDGEMENTS

I thank my committee for their advice, insight, and support throughout my time at the University of Washington. I especially thank my advisor, Richard Olmstead, for his academic, professional, and personal guidance during my graduate career. Without his encouragement and support, I may not be on the path I am today. I thank Toby Bradshaw for his mentorship during a rotation project and beyond, generosity with laboratory resources, and professional support. I thank Caroline Strömberg and John Klicka for their helpful comments on manuscripts and in meetings; the research truly benefitted from their input.

I thank my collaborators David Tank and Nataly O’Leary. Dave has been an invaluable source of methodological help and academic guidance. I thank him for opening his laboratory and his home to me during this project and his acceptance of my many, last-minute visits. I thank Nataly O’Leary for her insights on morphology and species divisions in *Citharexylum* and her many other contributions to the overall study of Verbenaceae. I thank her for her generosity in exchange of information and data; I hope that we continue to collaborate on projects.

I thank the past and present graduate students in the Olmstead lab for thoughtful conversations and advice about research, transmission of departmental and laboratory knowledge, and camaraderie: David Tank, Valerie Soza, Yuan Yaowu, Ryan Miller, Pat Lu-Irving, John Chau, Audrey Ragsac, and Ana Maria Bedoya. I also thank the many undergrads I have had the opportunity to work with and who have provided assistance in the lab: Ben Meersman, Wolf Rahfeldt, Sam Frankel, Sarah Tyson, Meng Lu, and Maxwell Haenel.

I thank the curators of the following herbaria for permitting us to sample specimens: F, HUH, MEX, MO, SI, TEX, USM, WTU; and the following people for assistance in the field: Carlos Burelo-Ramos, Warren Cardinal-McTeague, Itzue Caviedes-Solis, Ross Furbush, David Garcia, Johan Home, Diego Morales-Briones, Lenis Prado, Sarah Tyson, and Simon Uribe-Convers.

I thank the staff of the Biology Department, who have been tremendously helpful throughout the years. I especially thank Karen Bergeron for her guidance through submission of the NSF DDIG and Ben Wiggins for his instructional support during my stints as Instructor of Record. I thank the herbarium (WTU), especially David Giblin, for facilitating my work with specimens and for their financial and personal support. I also thank the Botany Greenhouse, especially Jeanette Milne and Doug Ewing, for allowing me to grow *Citharexylum* in Seattle, and Jason Lopez for facilitating the move of those plants from Seattle.

I thank the sources of financial support that have made this research possible: the Doctoral Dissertation Improvement Grant from the National Science Foundation; the Giles Botanical Field Research Award, Washington Research Foundation and Benjamin Hall Fellowship, and Melinda Denton Writing Fellowship from the UW Department of Biology; and student research grants from the American Society of Plant Taxonomists, Society of Systematic Biologists, and the Garden Club of America.

Lastly, I thank my friends and family for their unwavering support. I especially thank my sister Elizabeth, the first Dr. Frost for her guidance on getting in, getting through, and getting out of graduate school.

CONTENTS

CHAPTER 1. Phylogeny, classification, and character evolution of tribe Citharexyleae (Verbenaceae).....	1
CHAPTER 2. Is it faster to move or evolve? Comparing effects of niche conservatism and niche evolution on diversification rate in the Neotropical plant genus <i>Citharexylum</i> (Verbenaceae).....	55
CHAPTER 3. An updated phylogeny of Verbenaceae.....	124

CHAPTER 1:

Phylogeny, classification, and character evolution of tribe Citharexyleae (Verbenaceae)

ABSTRACT

- *Premise of the study:* Tribe Citharexyleae comprises three genera: *Baillonia*, *Citharexylum*, and *Rehdera*. While there is good support for these genera as a clade, relationships between genera remain unresolved due to low sampling of the largest genus, *Citharexylum*. A molecular phylogenetic approach was taken to resolve intergeneric relationships in Citharexyleae and infrageneric relationships in *Citharexylum*.
- *Methods:* Seven chloroplast regions, two nuclear ribosomal spacers, and six low-copy nuclear loci were analyzed for 64 species of Citharexyleae. Phylogenetic analyses were conducted using maximum likelihood, Bayesian inference, and Bayesian multi-species coalescent approaches. The following morphological traits were examined to identify diagnostic characters for clades within *Citharexylum*: habit, presence/absence of thorns, inflorescence architecture, flower color, fruit color, and geography.
- *Key results:* Intergeneric relationships are resolved as *Rehdera* sister to *Citharexylum* and *Baillonia* nested within *Citharexylum*. Two species, *C. oleinum* and *C. tetramerum*, fell outside of Citharexyleae. Six well-supported clades within *Citharexylum* are reconstructed; clades are best defined by geography, fruit color/maturation, and inflorescence architecture.
- *Conclusions:* *Baillonia* is included in *Citharexylum*; *Rehdera* is retained as a distinct genus. A subgeneric classification for *Citharexylum* is proposed.

Key words: *Baillonia*, *Citharexylum*, Citharexyleae, classification, microfluidic PCR, molecular phylogenetics, Neotropics, *Rehdera*, Verbenaceae

INTRODUCTION

Prior to molecular phylogenetics, there was disagreement on the division and definition of groups within Verbenaceae. Authorities employing different criteria (e.g., gynoeceal structure, inflorescence architecture, fruit characteristics) arrived at different divisions of the family. Despite conflict in these morphology-based classifications of Verbenaceae, all recognized a group including *Citharexylum*, *Duranta*, and *Rhaphithamnus* (Bentham, 1839; Schauer, 1847; Briquet, 1895; Moldenke, 1971; Troncoso, 1974; Sanders, 2001; Atkins, 2004) on the basis of woody habit, fleshy fruit, and the presence of a staminode. Though these genera share a strong morphological affinity, molecular studies indicated that each genus is more closely related to other taxa that differ in one or more of these traits (Marx et al., 2010; Yuan et al., 2010; O’Leary et al. 2012).

Tribe Citharexyleae, as most recently circumscribed, comprises ca. 133 spp. of Neotropical trees and shrubs in three genera: *Baillonia* (1 spp.), *Citharexylum* (130 spp.), and *Rehdera* (2 spp.) (Marx et al., 2010). *Baillonia* is distributed in Brazil and Paraguay, *Citharexylum* is widespread throughout the Neotropics from Northern Mexico to Southern Brazil and Argentina, and *Rehdera* is distributed in Central America. All genera share a woody habit, extra-floral nectaries, terminal inflorescences, minute floral bracts, short pedicellate flowers, and the presence of a staminode. However, none of these traits are exclusive to these genera in Verbenaceae, and morphological synapomorphies that define the tribe have not been identified (Marx et al. 2010; O’Leary et al., 2012).

The three genera are distinguished from each other by carpel number and fruit type. *Citharexylum* and *Rehdera* have bi-carpellate ovaries that develop into fruits with two, two-

seeded mericarps. Species of *Rehdera* were previously classified as *Citharexylum*, but were segregated by Moldenke (1935) on the basis of having dry, dehiscent fruits. *Citharexylum* and *Baillonia* both produce fleshy, drupaceous fruits. *Baillonia* was traditionally classified in tribe Lantaneae on the basis of having one carpel that aborts during development, giving rise to a unicarpellate, two-seeded fruit (Briquet, 1895). Its affinity for *Citharexylum* was suggested by Moore (1895) and Junell (1934). Additionally, species of *Citharexylum* exhibit cryptic dioecy (Tomlinson and Fawcett, 1972; Rocca and Sazima, 2006; Rueda and Hammil, in prep.). Flowers contain both stamens and pistils, but one whorl of reproductive parts is sterile so that individuals are functionally male or female. This characteristic has not been noted in other genera of Verbenaceae.

Molecular studies identified Citharexyleae as described above (Marx et al. 2010, O’Leary 2012), but, to date, no study has included sufficient sampling to confidently assess relationships among the tribe’s genera. Marx et al. (2010), the only study to include all three genera and sample multiple species of *Citharexylum* and both species of *Rehdera*, inferred that *Baillonia* is included within *Citharexylum* and *Rehdera* is sister to *Citharexylum* with high support. However, because only 11 species in Citharexyleae were sampled and only chloroplast data were used, assessment of intergeneric relationships was left for further study. Greater taxonomic and genetic sampling is needed to fully resolve generic relationships.

Since the tribe is dominated by *Citharexylum*, resolution of generic relationships by necessity involves more thorough sampling of *Citharexylum*, which provides a further opportunity to understand relationships within the genus. Estimated to comprise 130 species (Atkins 2004), it is one of the largest genera of Verbenaceae, though there are suggestions that

this estimate is inflated (Sanders, 2001; O’Leary and Frost, in prep.). Despite the size of the genus, it has been poorly studied and described. Moldenke published a series of notes (1957-1959) preparatory to a monograph, but never completed a monograph of *Citharexylum*. Similarly, divisions of species into infrageneric groups have been suggested, but not validly published. Walpers (1845) divided taxa into two major sections: *Spinosa* and *Inermia*, based on the presence or absence of spines, respectively. Section *Inermia* was further divided by calyx morphology. Section *Spinosa* included five taxa that have been reduced to three taxa recognized today as *C. flexuosum*, *C. montevidense*, and *Rhaphithamnus spinosus* (now distinct from *Citharexylum*); section *Inermia* encompassed the remaining 29 taxa in the treatment. Moldenke (1957-1959) mirrored Walpers’ sections in a dichotomous key, adding *C. andinum*, *C. herrerae*, and *C. weberbaueri* to section *Spinosa* and listing over 100 taxa in section *Inermia*. With the vast majority of taxa in section *Inermia*, this division provides little insight into relationships between species that further vary in traits such as habit, flower color, inflorescence architecture, and fruit color.

This study includes both greater taxonomic and genetic sampling than has been used previously. Microfluidic PCR was used to target seven chloroplast regions and two nuclear rDNA spacers. Broader sampling allows us to (1) resolve relationships between genera of Citharexyleae, (2) identify major clades of *Citharexylum* and the characters that unite them, (3) infer trait evolution within the tribe, and (4) establish a subgeneric classification for *Citharexylum*.

MATERIALS AND METHODS

Taxon sampling—One hundred eighty-two accessions representing 67 species of Citharexyleae were included in this study: one accession of monotypic *Baillonia*, 176 accessions of 64 *Citharexylum* species, and five accessions of two *Rehdera* species. Nine species from across the Verbenaceae served as the outgroup. Vouchers and GenBank accession numbers may be found in Appendix S1 (see the Supplementary Data with this article). Herbaria acronyms follow Index Herbariorum (Thiers, constantly updated: <http://sweetgum.nybg.org/science/ih/>).

Microfluidic PCR Primer Design and Validation—Targeted loci were selected for their phylogenetic utility and use in previous studies of Verbenaceae (O’Leary et al., 2009; Marx et al., 2010; Yuan et al., 2008, 2010; Lu-Irving and Olmstead, 2013; Lu-Irving et al. 2014; Frost et al., 2017). Seven chloroplast regions (cpDNA: *matK*, *ndhF*, *rbcL*, *rpl32*, *rpoC2*, *trnT-trnL*, and *trnL-trnF*), two spacer regions (ETS and ITS) of nuclear 18S/26S rDNA (nrDNA), and five low-copy nuclear genes (*waxy*, PPR 24, PPR 62, PPR 70, and PPR 123) were included in this study.

Primer design and validation followed Uribe-Convers et al. (2016), with the exception that primer sequences were designed by eye from alignments of published data pulled from genbank (ncbi.nlm.nih.gov). Each primer pair was designed to amplify 500 +/- 100 bp DNA segments. Validation reactions were performed with four experimental samples: two *Citharexylum* species (*C. schottii* and *C. myrianthum*) to test performance in the in-group, one outgroup taxon (*Duranta coriacea*) to test the potential for family-wide utility, and a negative control. Sixteen primer pairs were selected for seven chloroplast regions. One primer pair was used for each of the nrDNA and low-copy nuclear loci except for *waxy*, which was amplified

with two. Primer pair sequences can be found in Appendix S2 (see the Supplementary Data with this article).

DNA extraction, Microfluidic PCR, and sequencing—Genomic DNA was extracted from field-collected, silica-gel-dried tissues using a modified CTAB method (Doyle and Doyle, 1987) or from herbarium specimens using a DNeasy plant mini kit (Qiagen, Valencia, California, USA). A total of 7603 bp of cpDNA were targeted for amplification and sequencing, including: 890 bp of *matK* in two segments, 1823 bp of *ndhF* in four segments, 1029 bp of *rbcL* in two segments, 525 bp of *rpl32* in one segment, 1893 bp of *rpoC2* in four segments, 512 bp of *trnT* in one segment, and 931 bp of *trnLF* in two segments. A total of 5,132 bp of nuclear DNA were targeted for amplification and sequencing, including: 859 bp of nrDNA (400 bp of ETS and 459 bp of ITS) and 4,274 bp for low-copy nuclear regions (332 bp of PPR24, 534 bp of PPR62, 341 bp of PPR70, 595 bp of PPR123, 967 bp of waxy haplotype 1, and 968 bp of waxy haplotype 2).

Microfluidic PCR was performed in two separate runs on an Access Array System (Fluidigm), one with a 48.48 Access Array IFC and another with a Juno 192.24 IFC. The same primer pairs were submitted for each IFC. Amplicons were harvested and pooled as described in Uribe-Convers et al. (2016). For each IFC, the resulting pools were multiplexed in an Illumina Miseq using the Reagent Kit v3 600 cycles. Microfluidic PCR in the Access Array System, downstream quality control, and Illumina sequencing were performed in the University of Idaho (Moscow, ID) Institute for Bioinformatics and Evolutionary Studies (ibest) Genomic Resources Core facility.

Data processing—Reads from the Illumina Miseq runs were processed using the Fluidigm2PURC pipeline for processing paired-end Illumina data generated using the Fluidigm platform (Blischak et al., in review). Reads were demultiplexed using the program dbcAmplicons (Uribe-Convers et al., 2016). Paired reads were separated by locus, with the fluidigm2purc script (github.com/pblischak/fluidigm2PURC). Each locus was processed using PURC’s purc_recluster.py script (github.com/pblischak/fluidigm2PURC; Edgar, 2004, 2010; Camacho et al., 2009; Edgar et al., 2011; Martin 2011; Rothfels et al., 2016) to iteratively run chimera detection and sequence clustering to produce a set of putative haplotypes, or clusters. Reads were processed with clustering thresholds of 0.975, 0.99, 0.995, 0.997 and a size threshold of 5 (i.e. only clusters with ≥ 5 identical reads were retained). The clusters were run through the crunch-clusters script to infer haplotypes (github.com/pblischak/fluidigm2PURC).

Chloroplast regions were processed as haploid. Reads from nuclear loci were processed with “unknown” ploidy, meaning all possible haplotypes were kept and haplotype number could vary by sample. Gene trees were generated with RAxML ver. 8.2.11 (Stamatakis, 2014) to process the haplotypes for nuclear loci. For individuals with haplotypes that nested together—haplotypes that exhibited sequence similarity, but differed in amplicon length or a few heterogeneous sites—either the longest read or largest cluster was selected to represent the individual. For individuals with haplotypes that nested in different clades throughout the tree, all haplotypes were retained.

Raw reads for each locus were parsed into separate files by the purc_recluster.py script. In the instances that raw data were available, but with insufficient coverage to meet the filters set in purc_recluster.py, data were assessed and incorporated manually. For regions with a single

haplotype, a consensus sequence was generated for the available reads. For regions with multiple haplotypes, reads were analyzed individually in a phylogenetic context; consensus sequences were generated for reads that formed unique clades.

Four datasets were assembled for each region with different tiers of quality: 1) the original output from data processing, 2) the former plus individuals/haplotypes with ≥ 5 reads, 3) the former plus individuals/haplotypes with 2-4 reads, and 4) the former plus individuals/haplotypes with only a single read. Phylogenetic analyses were performed for each tier with RAxML ver. 8.2.11 to assess effects of the supplemented data on support values and topology. This supplementation technique was used only for individuals that had sufficient data to be included in the study, but were missing data for some loci due to low coverage. No additional individuals were added to the study as a result of these low-coverage reads.

Phylogenetic analyses

Gene tree analyses—Sequences were aligned using AliView ver. 1.18.1 (Larsson, 2014); alignments were inspected and manually adjusted where necessary. Individual alignments were analyzed with jModelTest 2.1.7 (Darriba et al., 2012; Guindon and Gascuel, 2003) to select the best-fit model of nucleotide substitution. The GTR + G model was selected and applied to all datasets. Alignments were concatenated using Geneious R7 7.0.6 (Biomatters, Auckland, New Zealand) and treated as a single dataset for regions with shared evolutionary histories: *ndhF*, *rpoC2*, *trnT-trnL-trnF*, *rbcL*, *matK*, and *rpl32* are part of the haploid chloroplast genome (cp); ETS and ITS are tightly linked in the nuclear rDNA repeat (nr). In the instance of that multiple haplotypes were recovered for a region, haplotypes were separated and treated as independent

datasets. Eight independent datasets were analyzed: cp, nr, PPR24, PPR62, PPR70, PPR123, waxy haplotype1, and waxy haplotype 2.

Phylogenetic reconstructions were conducted using maximum likelihood and Bayesian approaches, as implemented in RAxML and MrBayes ver. 3.2.6 (Ronquist & Huelsenbeck, 2003), respectively, for individual datasets, low-copy nuclear genes combined, and all data combined. Maximum likelihood analyses consisted of bootstrap analyses with 500 replicates for each dataset. Datasets were partitioned into individual gene regions with individual parameters unlinked in Bayesian analyses. Analyses consisted of two replicate runs, each with four chains, which were run for at least one million generations, sampling every 200 generations. Runs were assessed for convergence and stationarity in Tracer v1.6.0 (Rambaut et al., 2014); runs were considered to have converged when effective sample sizes (ESS) for parameter values were above 200 for combined files. For each run, the first 20% of sampled trees were discarded as burn-in and the remaining trees were summarized into a majority rule consensus tree with all compatible groups.

Species tree analyses—Species tree estimation was performed on the ingroup using the multispecies coalescent (MSC) model implemented in *BEAST (BEAST v1.8.4; Drummond et al. 2012). Substitution models and clock models were unlinked for the fourteen individual alignments. The GTR+G substitution model, empirical base frequencies, and a random local clock (Drummond and Suchard, 2010) were applied to each. Trees were linked based on shared evolutionary history, in the case of cp and nr datasets, or based on gene tree topology for lowcopy nuclear genes. Two partitions were set for lowcopy nuclear genes: (1) those where

Central American species form a monophyletic group (PPR24, PPR123, waxy haplotype 2) and (2) those where Central American species form a paraphyletic group with respect to South American species (PPR62, PPR70, waxy haplotype 1). Chloroplast data were treated as an organellar (haploid) locus with half the effective population size of a bi-parentally inherited locus. The birth-death process was used as the species tree prior. Replicate runs were performed for 500 million generations, sampling every 25,000. Runs were assessed for convergence and stationarity in Tracer v1.6.0 (Rambaut et al., 2014) and considered to have converged when effective sample sizes (ESS) for parameter values were above 200 for combined files. Between 25 and 50 million sampled tree states were discarded from each run as burn-in. Accessions of *C. bourgeauianum*, *C. flabellifolium*, *C. guatemalense*, *C. oleinum*, *C. reticulatum*, and *C. tetramerum* were excluded from the species tree analyses due to large amounts of missing data or because they were inferred to belong with the outgroup.

Morphology—Characters examined were habit, presence/absence of thorns, inflorescence architecture, flower number, corolla color, fruit color, and geography. For habit, species were scored as shrubs or trees. Species were considered shrubs if less than six m tall and with multiple main stems. Species over six m tall and/or with a single trunk were considered trees. To better describe the variability in inflorescence architecture, terminal and axillary inflorescences were scored separately. Each inflorescence type was scored as absent, simple, or compound. Average flower number per inflorescence was categorized >20, 10-20, or <10. Corolla color was categorized as solid white, solid yellow, solid purple, or white/yellow with purple/orange on the abaxial surface of the petal lobes. Fruit color through maturation was

categorized as green to red-orange, green to red to black in a two-phase maturation process, or green directly to black. Geographic range was divided into three regions: Central America, Caribbean, and South America. Ancestral character reconstructions were performed for terminal inflorescence architecture, axillary inflorescence architecture, flower number, flower color, and fruit color using the R package *phytools*, which employs a continuous-time Markov chain model. Habit and geography were used as descriptive characters, but ancestral character reconstructions were not performed. The biogeography of *Citharexylum* is of interest and will be addressed in a separate, more detailed study. Character data were pooled from Moldenke (1957-1959); field observations; herbarium records via personal visits to HUH, F, MEXU, MO, and USM; and online databases GBIF, CV Starr Virtual Herbarium (NYBG), SEINET, and Tropicos.

RESULTS

Dataset characteristics— The total concatenated dataset consisted of 12 927 aligned bp and 176 accessions, including 167 accessions in *Citharexyleae*. Among the characters, 4 140 were variable, of which 2 398 were potentially parsimony-informative. One hundred thirty-nine accessions had sequence data for at least five of the eight loci, with 82 of these having data for at least seven loci. All accessions included in the concatenated dataset had data for both cpDNA and nrDNA. Nine accessions of *Citharexylum* with insufficient data to be included in the concatenated analyses, but representing species not otherwise included, were retained in individual gene tree analyses. Characteristics of individual loci are shown in Table 1.

Phylogenetic analyses

Gene tree analyses—All gene trees support the monophyly of Citharexyleae, except for two species (*C. oleinum* and *C. tetramerum*), which nested in the outgroup. Within Citharexyleae, *Rehdera* was reconstructed as the sister to *Citharexylum*, and *Baillonia* nested within *Citharexylum* in all trees. *Citharexylum altamiranum* (clade vi) was reconstructed as sister to the rest of the genus (Figs. 2 and 3), which comprised two major clades (A and B; Fig. 3). Six smaller clades were consistently recovered in individual and combined gene trees, but relationships between these clades varied. Groups reconstructed within *Citharexylum* with high support for all datasets included: (i) a large clade including *C. ellipticum*, *C. hidalgense*, *C. moccinoi*, *C. roxanae*, and *C. schottii*; (ii) a clade composed of *C. brachyanthum*, *C. lycioides*, *C. racemosum* and *C. rosei*; (iii) a clade composed of *C. affine*, and *C. hintonii*; (iv) a clade including *Baillonia amabilis*, *C. microphyllum*, and *C. montanum*; (v) a clade/grade including *C. dentatum*, *C. flexuosum*, *C. herrerae*, and *C. montevidense*; and (vi) *C. altamiranum* (Figs. 2 and 3, but see Fig. 3 for tip labels). Clade A included clades i, ii, and iii in the chloroplast, lowcopy nuclear combined, and all data combined trees. In other trees, the placement of clades ii and iii varied. For the remainder of the paper Clade A will be referred to as the Central American clade (geography, Fig. 4) and will refer to the clade including clade i. In all trees, clade B included clade iv and clade/grade v, though relationships between taxa in clade/grade v differ among datasets (Supplemental trees with tip labels). Clade B is largely composed of South American species (geography, Fig. 4), and will from now on be referred to as the South American clade.

Citharexylum spinosum, the type species for the genus, nested within different clades for different datasets. All three accessions nested within the Central American clade in cpDNA,

PPR70, and PPR123 trees. Accessions were split, with some nesting in the Central American clade and some in the South American clade, in nrDNA, PPR24, and PPR62 trees. Two accessions of *C. spinosum* had an additional copy for each of the waxy of haplotypes (i.e. four total copies of the waxy gene, two copies of haplotype 1 and two copies of haplotype 2). For each haplotype, one copy nested within the Central American and another nested within the South American clade. One accession also showed this pattern in PPR62.

Species tree analyses—The species tree topology was consistent with the topology reconstructed by the all combined dataset (Fig. 4). The same six major clades were inferred with high support in the species tree as in the individual and combined gene trees. The split between the Central American clade and the South American clade was also well supported in the species tree. *Citharexylum spinosum*, which nested in both the Central American and South American clade in gene tree analyses, is placed in the Central American clade by the MSC.

Morphology—Observations were available for all characters for all species except fruit color in *C. racemosum* (Fig. 4). Thorns were present only in species in the Andean shrub clade. Ancestral character estimations supported two origins of thorns in clade ν (Appendix S9), the first either in a clade or grade—depending on the analysis—including *C. andinum*, *C. flexuosum*, *C. joergensenii*, *C. kobuskianum*, *C. montevidense*, and *C. weberbaueri* and the second in *C. herrerae*. Terminal inflorescences were lost in *C. subflavescens* and *C. montanum* (Appendix S10). Terminal inflorescences varied within species as whether they were simple or compound. Only *Rehdera penninervia* was found to consistently have compound terminal inflorescences.

Similarly, there was variation within species for presence/absence of axillary inflorescences. Almost half (27) of the species included individuals with axillary inflorescences. Of those, 12 species were observed to consistently have axillary inflorescences, and 6 of those species included individuals with compound axillary inflorescences. Again, *Rehdera penninervia* was the only species for which members consistently had compound axillary inflorescences. Axillary inflorescences were lost in the ancestor of the two major clades of *Citharexylum* and regained nine times (Appendix S11). Reduction of flower number per inflorescence from >20 to <20 is estimated to have occurred in *C. altamiranum*, *C. alanii* and *C. mircophyllum*, clade *ii*, and clade *v* (Appendix S12). Flowers with at least partial purple coloration arose six times throughout the genus (Appendix S13). Red fruits were estimated to be the ancestral fruit color in *Citharexylum*; black fruits arose in *C. altamiranum* and two or three times in clade *v* (Appendix S14). Ancestral reconstructions supported three separate origins of black fruits with a red-orange intermediate in the Central American clade. Red fruits were estimated to be the most likely ancestral state of this clade. Black fruits with a red-orange intermediate was the second-most probable ancestral state in the reconstructions.

DISCUSSION

Intergeneric relationships—Phylogenetic reconstructions infer *Rehdera* to be sister to *Citharexylum* and support the inclusion of *Baillonia* in *Citharexylum*. This is consistent with previous studies of Verbenaceae and is bolstered by increased sampling of species in Citharexyleae. Two species of *Citharexylum*, *C. oleinum* and *C. tetramerum*, nested with the

outgroup; preliminary results suggest these species belong to Duranteae, but further investigation is needed.

Infrageneric relationships— The Mexican species *Citharexylum altamiranum* is sister to the rest of the genus. The remaining species of *Citharexylum* form two major clades defined by geography: (A) the Central American clade and (B) the South American clade. Each of these major clades contains about half of the taxonomic diversity of *Citharexylum*. The Central American clade comprises three smaller, well-supported clades (clades *i*, *ii*, and *iii* in previous sections). The largest Central American subclade, clade *i*, contains 25-30 species of moist to seasonally dry forest trees and shrubs. *Citharexylum bourgeauianum* and *C. guatemalense*, which were not included in MSC analyses due to large amounts of missing data, were also placed in this clade in gene tree analyses. These relationships are supported by geography and morphology. Clade *ii* includes four species of arid-adapted shrubs distributed in Central Mexico, and clade *iii* is made up of two to three species of purple-flowered trees. Based on gene tree results, *Citharexylum flabellifolium* belongs to the Central American clade, but its placement in a subclade is unresolved. In the nrDNA tree, *C. flabellifolium* nests within clade *i*. The same accession nests in clade *iii* in the PPR70 tree. *Citharexylum flabellifolium* is an arid-adapted species distributed in Baja California Sur and Sonora; it is morphologically distinct from other species in the genus. Like *C. affine* and *C. hintonii*, the other species in clade *iii*, *C. flabellifolium* has purple flowers. However, there are also purple-flowered species in clade *i*, making it difficult to place without better phylogenetic resolution.

Two well-supported clades are inferred within the South American clade: (*iv*) a clade of tall, mesic-forest trees with many flowers, and (*v*) a clade of Andean shrubs with reduced inflorescences. With the exception of two Caribbean shrub species, clade *iv* includes large-leaved species distributed in Amazonia, the Brazilian Atlantic coast forest, and mid elevations of the northern Andes. Not sampled in the MSC, *C. reticulatum* is placed in this moist forest clade by nrDNA. This species would be difficult to place by morphology alone, since it shares characters of both the moist forest trees and the Andean shrubs. Distributed from Ecuador to Peru, it grows at higher elevations and is smaller in stature than is typical of the South American moist forest clade. The species does have long, many-flowered inflorescences with white flowers, which are typical of the moist forest trees. However, it is reported to have black fruits (Moldenke, 1957-1959), which are common in the Andean shrub clade, instead of red fruits typical of the moist forest clade.

Morphology— *Rehdera* is the earliest diverging lineage of Citharexyleae and is distinguished by having dry schizocarpous fruits, whereas *Citharexylum* and *Baillonia* have fleshy drupes. As suggested by Marx et al. (2010), *Baillonia amabilis* appears to be a species of *Citharexylum* in which only two of four ovules mature. It is ambiguous as to how the two mature ovules in *Baillonia* are derived (O’Leary et al., 2012). Traditionally, *Baillonia* is described as having one carpel abort early in development, the remaining carpel with two ovules matures. However, dissection of fruits from Rojas 7368 (SI) reveal two carpels, each with one mature ovule. Fruit dissections of closely related species *C. poepigii* reveal most individuals have four mature ovules, as expected, but one individual, Phillipson 1380 (US), appears to have one

abortive carpel (Nataly O’Leary, personal communication). Further investigation of mature carpel/ovule number is needed in *Baillonia* and *Citharexylum* to determine how prevalent abortion of carpels/ovules is throughout the genus.

Citharexylum represents an independent origin of fleshy fruits in Verbenaceae (O’Leary et al., 2012). Fruits either mature from green to red-orange, green to red to black in a two-phase maturation process, or green directly to black. The two major clades of *Citharexylum* are distinguished by fruit maturation. The South American clade consists of species with a single mature fruit color; fruits either mature to red or to black without an intermediate color. The moist forest trees typically have red fruits; black fruits are common in the Andean shrubs. The Central American clade includes species with a two-step fruit maturation process. Red-orange is an intermediate color as the fruits mature to black, and both colors of fruits are observed simultaneously in the infructescences. In some Central American species, only red-orange has been recorded as the mature fruit color; it is unclear if fruits of those species mature at the red-orange stage, or if observations for fully mature black fruits are lacking. Likewise, *C. altamiranum* is only reported as having black fruits; it is uncertain if the fruits mature from green to black or if the intermediate color has not been observed. It seems probable that single-phase maturation would be the ancestral state of the genus, and that *C. altamiranum*, as the earliest diverging lineage, would mature to black without an intermediate color. Without more observations, it cannot be concluded if two-phase maturation was lost in the South American clade or arose in the Central American clade

Dioecy needs further investigation throughout *Citharexylum*. Species have been confirmed as dioecious in the literature, including *C. spinosum* (Tomlinson and Fawcett, 1972),

C. myrianthum (Rocca and Sazima, 2006), Costa Rican species (Rueda and Hammil, in prep.), and dioecy has been observed in the field for many others (L. Frost, personal observation).

Dioecy can be inferred in *Citharexylum* because in male plants the entire flower disarticulates from the pedicel at senescence, leaving naked racemes. In female plants, the calyx becomes lignified as the fruits mature and is retained on the pedicel, even as fruits are eaten or fall off.

This pattern is observed in specimens of *Baillonia* (see Palmer 1853-6 (Orrell and Howell, 2018) and Hassler 2683a (MNHN, 2018a) for putative male and Prance et al. 15 (Tulig, 2017) and Weddell 3193 (MHNH, 2018b) for putative female specimens), but more detailed study is needed to determine if the species is dioecious.

A broader study is also needed to determine if all members of *Citharexylum* are dioecious or only some species/clades. Variation in inflorescence architecture provides further evidence of dioecy for some species. Functionally male plants often have greater investment in production of attractive, reproductive structures, which can translate as a greater number of flowers produced overall than female individuals (Mayer and Charlesworth, 1991). Variation within species of *Citharexylum* for presence/absence of compound or axillary inflorescences may be related to sex. In these variable species, male individuals could increase flower production either through the development of axillary inflorescences, or compound inflorescences, or both. Variation between sexes is easily observed for species with large, many-flowered inflorescences, but is difficult to detect in shrub species with reduced inflorescences. These species have simple, few-flowered inflorescences that terminate short, axillary branches. One individual does not obviously produce more flowers or more inflorescences than another. It is also more difficult in general to infer the

sex of individuals in these few-flowered species using the observations described above. Further investigation of dioecy in the Andean and arid-adapted Mexican shrubs is warranted.

In addition, cryptic dioecy is not always readily observable and may be more widespread in the family. A hand-written note on the label of G. Diggs & M. Nee 2473 (F) collection of *C. oleinum* reads, “4 epipetalous, ± sessile stamens. Style short, functionally a male flower?” *Citharexylum oleinum* and *C. tetramerum* consistently fall outside of Citharexyleae. Further work is needed to determine the exact placement of these species in Verbenaceae, but our evidence suggests that these species do not belong in *Citharexylum*. *Citharexylum* is the only genus in Verbenaceae in which dioecy has been documented, but *C. oleinum* and *C. tetramerum*, if found to be dioecious, would represent a separate origin in Verbenaceae.

Spines or thorns, arising as modified axillary shoots, were the first character used to suggest a subgeneric classification scheme for *Citharexylum*. Thorns are only present in the Andean shrub clade and may have arisen twice in that group. They may have evolved as a defense mechanism against large herbivores in the more open vegetation of inter-Andean dry valleys. Thorns are retained in the more mesic, low-land tree species *C. montevidense*, which is distributed in eastern Argentina, Paraguay, and Uruguay. The second origin of thorns is in *C. herrerae*, which is nested within a group of unarmed Andean cloud forest shrubs. Beyond the production of thorns, *C. herrerae* is morphologically distinct in this clade by having red fruits, whereas the unarmed shrubs have black fruits, and stems that remain green for several years (the latter trait is also distinct within the genus, shared only by *C. roxanae*, a distantly-related, arid-adapted shrub distributed in Baja California Sur and Sonora). Though not technically thorn-bearing, some species outside of the Andean shrub clade also have sharp defenses. *Baillonia*

amabilis, which inhabits the Brazilian cerrado, has spiny sterigmata at leaf bases (Moldenke, 1941), and the arid-adapted Mexican shrubs (*C. brachyanthum*, *C. flabeillifolium*, *C. lycioides*, *C. racemosum*, and *C. rosei*) have relatively short, pointed, branches.

Classification—We present a subgeneric classification of the revised *Citharexylum* including *Baillonia*, which was transferred recently to *Citharexylum* (Christenhusz et al., 2018). Six well-supported, monophyletic subgenera are identified. The type species *C. spinosum* is suspected to be of hybrid origin with parental lineages from separate subgenera. This poses a taxonomic problem, since two clades contain representatives of the type. However, chloroplast DNA, MSC analyses, fruit morphology, and a predominant distribution in the Caribbean (including southern Florida) support the placement of *C. spinosum* in clade *i* of the Central American clade.

Citharexyleae Briquet

I. *Citharexylum* L., Sp. Pl. 1: 625. 1753. Type: *Citharexylum spinosum* L.

1. C. subgenus ***Citharexylum*** L.A. Frost, subg. nov. Type: *Citharexylum spinosum* L.

Trees and shrubs, thorns absent; inflorescences terminal or terminal and axillary, simple or compound; flowers many, corolla white, pale yellow-green, or purple; fruits maturing from orange to black.

Distribution: Central America, Caribbean, Northern South America

Estimated species: 25-30

2. C. subgenus ***Mexicanum*** L.A. Frost, subg. nov. Type: *Citharexylum brachyanthum*

(A.Gray ex Hemsl.) A.Gray

Shrubs, thorns absent; inflorescences terminal and simple, terminating very short branchlets; flowers few, corolla white; fruits red-orange at maturity or maturing from orange to black.

Distribution: Central Mexico

Estimated species: 4

3. C. subgenus ***Affine*** L.A. Frost, subg. nov. Type: *Citharexylum affine* D.Don.

Trees, thorns absent; inflorescences terminal and axillary, simple or compound; flowers many, corolla purple; fruits maturing from orange to black.

Distribution: Central America (primarily Mexico)

Estimated species: 2-3

4. C. subgenus ***Sylvaticum*** L.A. Frost, subg. nov. Type: *Citharexylum myrianthum* Cham.

Trees or shrubs, thorns absent; inflorescences terminal, axillary, or terminal and axillary, simple or compound; flowers few or many, corolla white; fruits red.

Distribution: South America, the Carribean

Estimated species: 15 - 18

5. C. subgenus ***Andinum*** L.A. Frost, subg. nov. Type: *Citharexylum flexuosum* Moldenke

Shrubs, thorns present or absent; inflorescences terminal and simple; flowers few to submany, corollas white to pale yellow-green, some with lobes tipped purple or orange in bud; fruits red or black.

Distribution: Andean South America

Estimated species: 14-16

6. C. subgenus *Altamiranum* L.A. Frost, subg. nov. Type: *Citharexylum altamiranum*

Greenm.

Shrubs, thorns absent; inflorescences terminal and axillary, simple; flowers few, corollas purple; fruits black.

Distribution: Mexico

Estimated species: 1

II. *Rehdera* Moldenke, Repert. Spec. Nov. Regni Veg. 39: 48–50. 1935. Type: *Rehdera trinervis*

S.F. Blake

ACKNOWLEDGEMENTS

The authors thank the curators of the following herbaria for permitting us to sample specimens:

F, HUH, MEX, MO, SI, TEX, USM, WTU; the following people for assistance in the field:

Carlos Burelo-Ramos, Warren Cardinal-McTeague, Itzue Caviedes-Solis, Ross Furbush, David

Garcia, Johan Home, Diego Morales-Briones, Lenis Prado, Sarah Tyson, and Simon Uribe-

Convers; and anonymous reviewers. This study was supported by NSF grants DEB 0542493,

DEB 0710026, and DEB 1020369 to RGO and DEB 1500919 to LAF and RGO.

LITERATURE CITED

- Atkins, S. 2004. Verbenaceae. Pp. 449-468 In: *The Families and Genera of Flowering Plants*, Vol. 7 (J. W. Kadereit, ed.). Springer-Verlag, Berlin.
- Bentham, G. 1839. Enumeration of plants collected by Mr. Schomburgk in British Guiana. *The Annals and Magazine of Natural History* 2:441-451.
- Blischak, P. D., M. Latvis, D. F. Morales-Briones, J. C. Johnson, V. S. Di Stilio, A. D. Wolfe, and D. C. Tank. In Review. Fluidigm2PURC: automated processing and haplotype inference for double-barcoded PCR amplicons. *bioRxiv*. doi: 10.1101/242677.
- Briquet, J. 1895. Verbenaceae. In *Die natürlichen Pflanzenfamilien* (A. Engler and K. Prantl, eds), Teil 4/3a, pp. 132-182. Engelmann, Leipzig, Germany.
- Camacho, C., G. Coulouris, V. Avagyan, N. Ma, J. Papadopoulos, et al. 2009. BLAST+: Architecture and applications. *BMC Bioinformatics* 10: 421.
- Darriba, D., G. L. Taboada, R. Doallo, and D. Posada. 2012. jModelTest 2: more models, new heuristics and high-performance computing. *Nature Methods* 9(8): 772.
- Doyle, J. J., and J. L. Doyle. 1987. A rapid isolation procedure for small quantities of fresh leaf tissue. *Phytochemical Bulletin* 19: 11–15.
- Drummond, A. J., and M. A. Suchard. 2010. Bayesian random local clocks, or one rate to rule them all. *BMC Biology* 8:114. doi: 10.1186/1741-7007-8-114
- Drummond, A. J., M. A. Suchard, D. Xie, and A. Rambaut. 2012. Bayesian Phylogenetics with BEAUti and the BEAST 1.7. *Molecular Biology and Evolution* 29(8): 1969–1973. doi: 10.1093/molbev/mss075

- Edgar, R.C. 2004. MUSCLE: Multiple sequence alignment with high accuracy and high throughput. *Nucleic Acids Research* 32:1792-1797.
- Edgar, R.C. 2010. Search and clustering orders of magnitude faster than BLAST. *Bioinformatics* 26(19), 2460-2461
- Edgar, R.C., B.J. Haas, J.C. Clemente, C. Quince, R. Knight. 2011. UCHIME improves sensitivity and speed of chimera detection, *Bioinformatics* 27(16), 2194-2200.
- Frost, L. A., Tyson, S. M., Lu-Irving, P., O’Leary, N. and Olmstead, R. G. (2017), Origins of North American arid-land Verbenaceae: More than one way to skin a cat. *American Journal of Botany*, 104: 1708-1716. doi:10.3732/ajb.1700292
- Guindon, S., and O. Gascuel. 2003. A simple, fast, and accurate algorithm to estimate large phylogenies by maximum likelihood. *Systematic Biology* 52(5): 696-704.
- Höhna, S., T.A. Heath, B. Boussau, M.J. Landis, F. Ronquist, J.P. Huelsenbeck. 2014. Probabilistic graphical model representation in phylogenetics. *Systematic Biology* 63:753–771.
- Höhna, S., M.J. Landis, T.A. Heath, B. Boussau, N. Lartillot, B.R. Moore, J.P. Huelsenbeck, and F. Ronquist. 2016. RevBayes: Bayesian Phylogenetic Inference Using Graphical Models and an Interactive Model-Specification Language. *Systematic Biology* 65(4): 726-736.
- Junell, S. 1934. Zur Gynaceummorphologie und Systematik der Verbenaceen und Labiaten. *Symb. Bot. Upsal.* 4: 1-219.
- Larsson, A. (2014). AliView: a fast and lightweight alignment viewer and editor for large data sets. *Bioinformatics* 30(22): 3276-3278. doi:10.1093/bioinfor.

- Lu-Irving, P., and R. G. Olmstead. 2013. Investigating the evolution of Lantaneae (Verbenaceae) using multiple loci. *Botanical Journal of the Linnean Society* 171: 103-119. doi:10.1111/j.1095-8339.2012.01305.x
- Lu-Irving, P., O’Leary, N., O’Brien, A. and R. G. Olmstead. 2014. Resolving the genera *Aloysia* and *Acantholippia* within the tribe Lantaneae (Verbenaceae), using chloroplast and nuclear sequence data. *Systematic Botany* 39: 644-655. doi: 10.1600/036364414X680816
- Martin, M. 2011. Cutadapt removes adapter sequences from high-throughput sequencing reads. *EMBnet.journal* 17:10-12.
- Marx, H., N. O’Leary, Y.-W. Yuan, P. Lu-Irving, D. Tank, M.E. Múlgura, and R. G. Olmstead. 2010. A molecular phylogeny and classification of Verbenaceae. *American Journal of Botany* 97(10): 1647–1663.
- MNHN - Museum national d'Histoire naturelle. 2018a. The vascular plants collection (P) at the Herbarium of the Muséum national d'Histoire Naturelle (MNHN - Paris). Version 69.53. Occurrence Dataset <https://doi.org/10.15468/nc6rxy> accessed via GBIF.org on 2018-03-05. <https://www.gbif.org/occurrence/1019625478>.
- MNHN - Museum national d'Histoire naturelle. 2018b. The vascular plants collection (P) at the Herbarium of the Muséum national d'Histoire Naturelle (MNHN - Paris). Version 69.53. Occurrence Dataset <https://doi.org/10.15468/nc6rxy> accessed via GBIF.org on 2018-03-05. <https://www.gbif.org/occurrence/439496996>.
- Moldenke, H. N. 1941. A monograph of the genus *Baillonia*. *Darwiniana*, 5: 166-177.
- Moldenke, H. N. 1958a. Materials towards a monograph of the genus *Citharexylum* I. – *Phytologia* 6: 242–256.

- Moldenke, H. N. 1958b. Materials towards a monograph of the genus *Citharexylum* II. – *Phytologia* 6: 262–320.
- Moldenke, H. N. 1958c. Materials towards a monograph of the genus *Citharexylum* III. – *Phytologia* 6: 332–368.
- Moldenke, H. N. 1958d. Materials towards a monograph of the genus *Citharexylum* IV. – *Phytologia* 6: 383–432.
- Moldenke, H. N. 1959a. Materials towards a monograph of the genus *Citharexylum* V. – *Phytologia* 6: 448–505.
- Moldenke, H. N. 1959b. Materials towards a monograph of the genus *Citharexylum* VI. – *Phytologia* 7: 7–48.
- Moldenke, H. N. 1959c. Materials towards a monograph of the genus *Citharexylum* VII. – *Phytologia* 7: 49–73.
- Moldenke, H. N. 1971. A fifth summary of the Verbenaceae, Avicenniaceae, Stilbaceae, Dicrostylidaceae, Symphoremataceae, Nyctanthaceae, and Eriocaulaceae of the world as to valid taxa geographic distribution, and synonymy. 2 vols. Publ. by the author.
- Moore, Sp. Le M. 1895. The Phanerogamic Botany of the Matto Grosso Expedition, 1891-92. Transactions of the Linnean Society of London (Botany) Ser. 2 (4).
- O'Leary, N., Y.-W. Yuan, A. Chemisquy, and R. G. Olmstead. 2009. Reassignment of Species of Paraphyletic *Junellia* s. l. to the New Genus *Mulguraea* (Verbenaceae) and New Circumscription of Genus *Junellia*: Molecular and Morphological Congruence. *Systematic Botany*, 34(4): 777-786.

- O'Leary, N., C. I. Calviño, S. Martínez, P. Lu-Irving, R. G. Olmstead, and M. E. Múlgura. 2012. Evolution of morphological traits in Verbenaceae. *American Journal of Botany*, 99: 1778–1792. doi:10.3732/ajb.1200123.
- Orrell T, Hollowell T (2018). NMNH Extant Specimen Records. Version 1.14. National Museum of Natural History, Smithsonian Institution. Occurrence Dataset <https://doi.org/10.15468/hnhrg3> accessed via GBIF.org on 2018-03-05. <https://www.gbif.org/occurrence/1322362840>.
- Rambaut, A., M. A. Suchard, D. Xie, and A. J. Drummond. 2014. Tracer v1.6. Available from <http://beast.bio.ed.ac.uk/Tracer>.
- Rocca, M., and M. Sazima. 2006. The dioecious, sphingophilous species *Citharexylum myrianthum* (Verbenaceae): Pollination and visitor diversity. *Flora* 201: 440-450.
- Ronquist, F., and J. P. Huelsenbeck. 2003. MrBayes 3: Bayesian phylogenetic inference under mixed models. *Bioinformatics* 19(12): 1572–1574. doi:10.1093/bioinformatics/btg180
- Rothfels, C.J., K.M. Pryer, and F-W. Li. 2016. Next-generation polyploidy phylogenetics: rapid resolution of hybrid polyploid complexes using PacBio single-molecule sequencing. *New Phytologist*
- Sanders, R. W. 2001. The genera of Verbenaceae in the southeastern United States. *Harvard Papers in Botany* 5: 303-358.
- Schauer, J. C. 1847. Verbenaceae. In: A. P. De Candolle, Prodr. 11: 522-700.
- Stamatakis, A. 2014. RAxML version 8: a tool for phylogenetic analysis and post-analysis of large phylogenies. *Bioinformatics* 30(9): 1312–1313. doi:10.1093/bioinformatics/btu033.
- Tomlinson, P.B., & Fawcett, P. 1972. Dioecism in *Citharexylum* (Verbenaceae). *Journal of the Arnold Arboretum*. 53(3): 386-389.

- Troncoso, N. S. 1974. Los generos de Verbenacea de Sudamerica extratropical. *Darwiniana* 18: 295-412.
- Tulig M, Ramirez J, Watson K (2017). The New York Botanical Garden Herbarium (NY). The New York Botanical Garden. Occurrence Dataset <https://doi.org/10.15468/6e8nje> accessed via GBIF.org on 2018-03-05. <https://www.gbif.org/occurrence/1097308086>.
- Uribe-Convers, S., M. L. Settles, and D. C. Tank. 2016. A Phylogenomic Approach Based on PCR Target Enrichment and High Throughput Sequencing: Resolving the Diversity within the South American Species of *Bartsia* L. (Orobanchaceae). *PLOS ONE* 11(2): e0148203. doi: 10.1371/journal.pone.0148203
- Yuan, Y.-W., and R. G. Olmstead. 2008a. A species-level phylogenetic study of the *Verbena* complex (Verbenaceae) indicates two independent intergeneric chloroplast transfers. *Molecular Phylogenetics and Evolution* 48: 23-33.
- Yuan, Y.-W., C. Liu, H. E. Marx, and R. G. Olmstead. 2009. The PPR (pentatricopeptide repeat) gene family, a tremendous resource for plant phylogenetic studies. *New Phytologist* 182: 272-283.
- Yuan, Y.-W., C. Liu, H. E. Marx, and R. G. Olmstead. 2010. An empirical demonstration of using PPR (pentatricopeptide repeat) genes as phylogenetic tools: phylogeny of Verbenaceae and the *Verbena* complex. *Molecular Phylogenetics and Evolution* 54: 23-35.

TABLES

Table 1. Characteristics of individual datasets

Alignment	No. of taxa	Proportion of taxa	Alignment length (bp)	% missing data	No. of variable sites	Proportion of variable sites	No. of parsimony informative sites	Proportion of parsimony informative sites	GC content
all comb.	645	1.000	27794	74.00	11139	0.401	7270	0.262	0.392
cpDNA	627	0.972	16961	69.45	5176	0.305	3175	0.187	0.358
nrDNA	580	0.899	1401	43.94	906	0.647	764	0.545	0.592
PPR11	204	0.316	1461	29.76	866	0.593	621	0.425	0.401
PPR62	151	0.234	1452	44.65	717	0.494	457	0.315	0.411
PPR70	202	0.313	1128	52.35	697	0.618	464	0.411	0.382
PPR81	123	0.191	1180	7.96	652	0.553	433	0.367	0.395
PPR90	72	0.112	986	3.29	314	0.318	182	0.185	0.405
PPR91	45	0.070	1306	8.74	524	0.401	335	0.257	0.394
PPR97	62	0.096	747	5.47	266	0.356	158	0.212	0.41
PPR123	241	0.374	1394	31.18	739	0.53	533	0.382	0.405

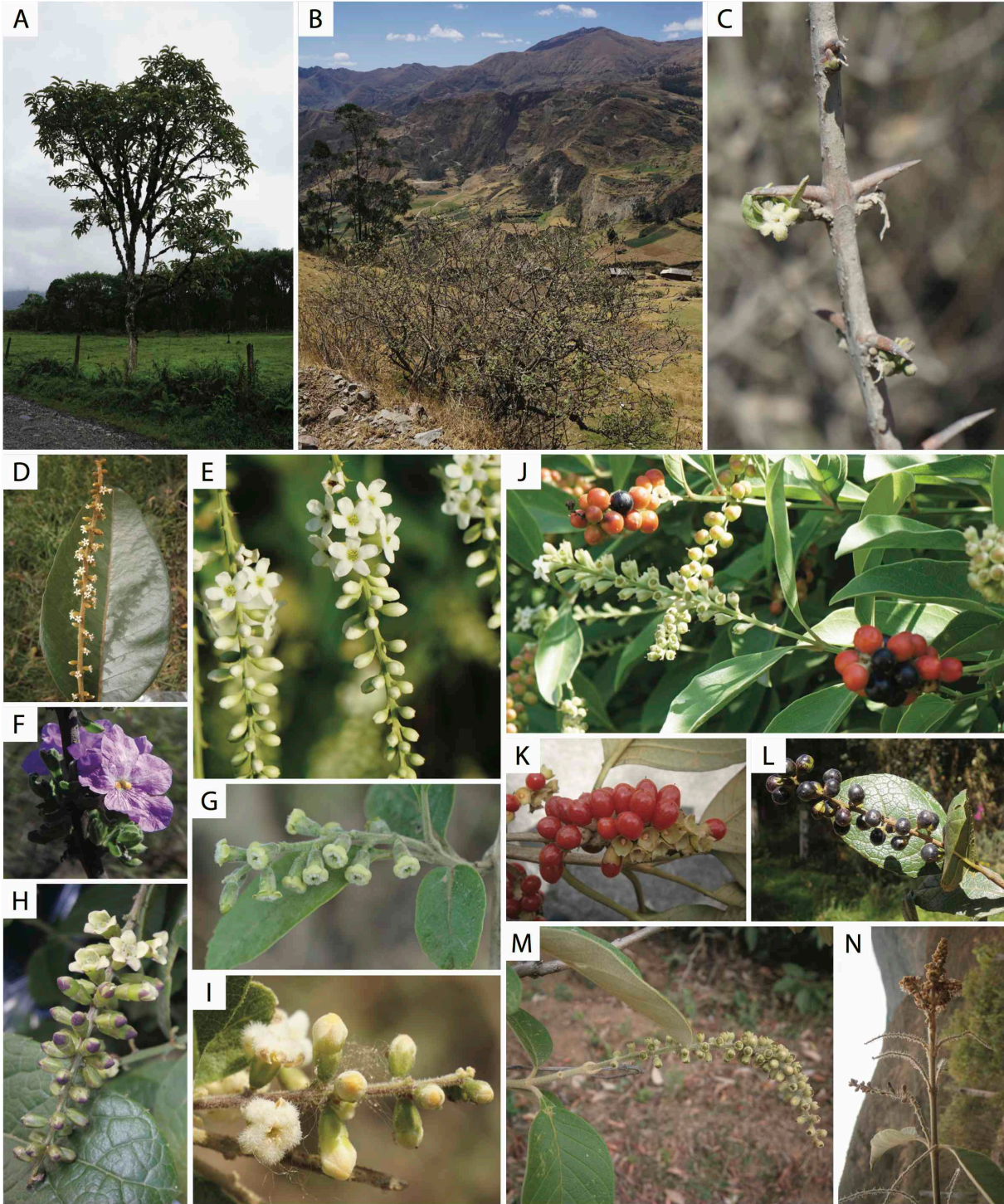
FIGURE CAPTIONS

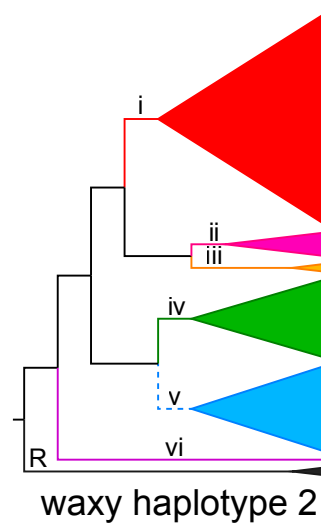
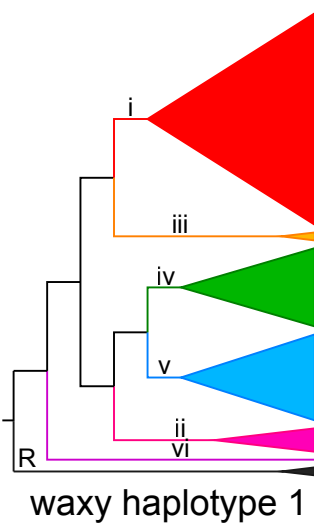
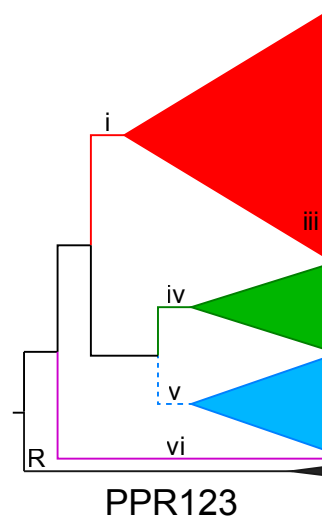
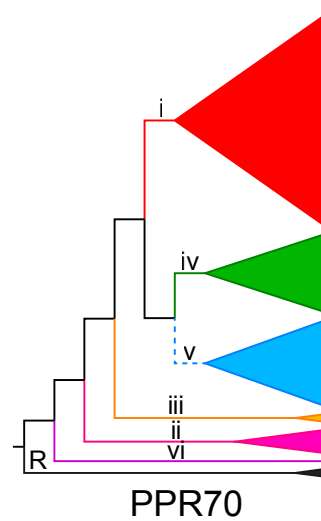
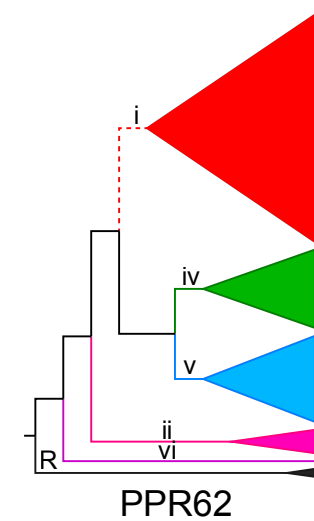
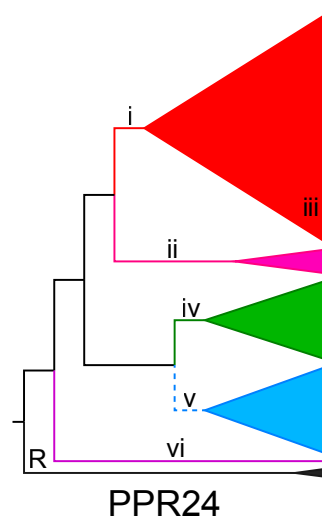
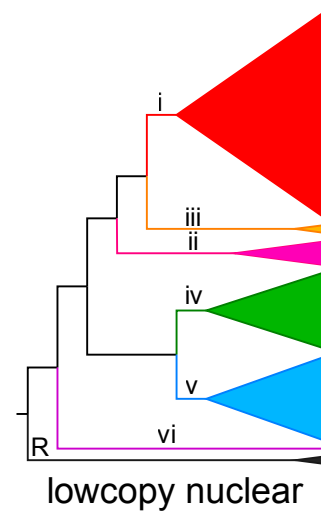
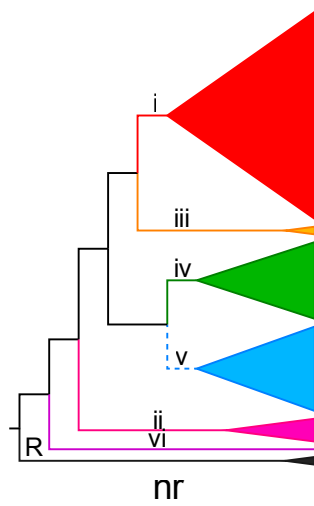
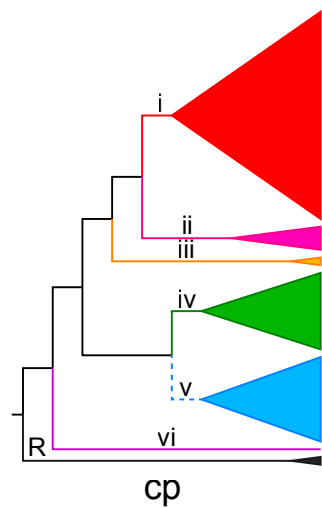
Fig. 1. Morphological diversity of *Citharexylum*. Habit (A-B): (A) tree (*C. montanum*), (B) shrub (*C. weberbaueri*); Thorns (C; *C. flexuosum*); Flower color (D-I): (D, E) white (*C. subflavescens*, *C. hexangulare*), (F) purple (*C. flabellifolium*), (G) pale yellow-green (*C. kobuskianum*), (H) pale with purple-tipped buds (*C. sulcatum*), (I) white with orange-tipped buds (*C. peruvianum*); Fruit color (J-L): (J) two-phase maturation from green to orange to black (*C. ellipticum*), (K) green to red (*C. montanum*), (L) green directly to black (*C. sulcatum*); Inflorescence (M-N; *C. kunthianum*): (M) female inflorescence with simple terminal raceme (N) male inflorescence with compound terminal racemes and simple axillary racemes.

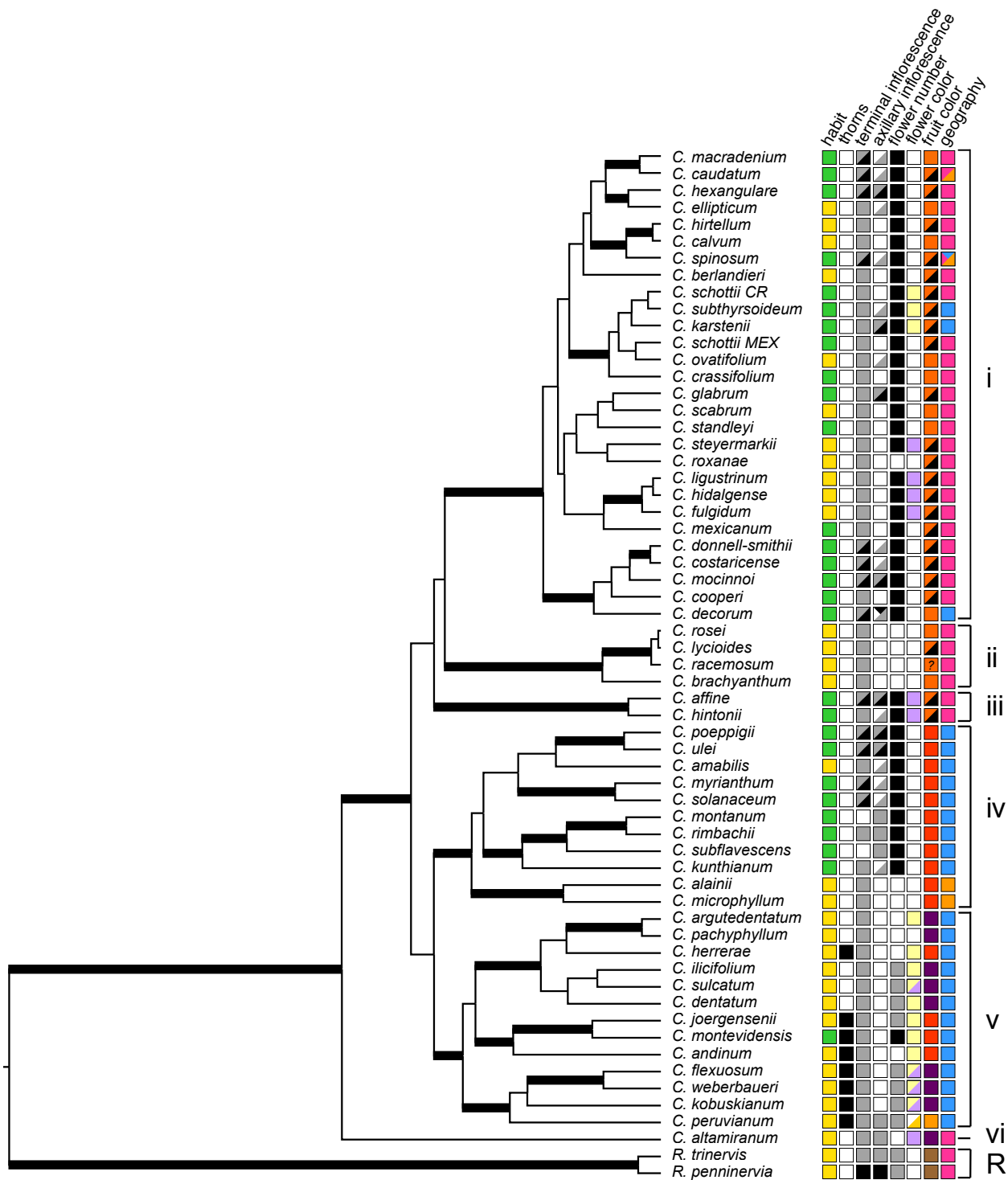
Fig. 2. Gene tree cartoons for cp, nr, lowcopy nuclear combined, and individual lowcopy nuclear datasets showing topological differences among gene trees. Roman numerals on branches correspond to clades of the tree recognized in the text; R marks the genus *Rehdera*. For gene trees in which one clade nested within another, the numeral for that clade is placed within the inclusive clade (e.g. clade iii in PPR24 and PPR123). Data for species in clade iii were missing for PPR62, and for species in clade ii for PPR123. Solid lines on branches indicate clades; dashed lines indicate grades. Tip labels may be found in Fig. 3.

Fig. 3. Bayesian consensus tree for all data combined. Thickened branches indicate high support (≥ 70 bootstrap support from maximum likelihood (ML) analyses or ≥ 90 % posterior probability from Bayesian inference (BI)). Support for nodes are plotted as bootstrap/posterior probability (percent). Roman numerals, curved lines at the tips, and branch colors correspond to clades recognized in the text. R indicates the genus *Rehdera*.

Fig. 4. *BEAST multi-species coalescent tree. Thickened branches indicated nodes with high support (posterior probability ≥ 0.95). Colored boxes represent character states of species. First column from the left—habit: tree (green) or shrub (yellow); thorns: present (black) or absent (white); terminal inflorescence: compound (black), simple (gray), or absent (white); axillary inflorescence: compound (black), simple (gray), or absent (white); flower number: >20 (black), 10-20 (gray), or <10 (white); flower color: literal (white, pale yellow, purple, pale yellow with purple lobes (split yellow and purple boxes), white with orange lobes (split white and orange box)); mature fruit color: literal (red with no intermediate, black with no intermediate, black with red/orange intermediate (split orange and black boxes)), or dry fruits (brown); Geography: Central America (pink), Caribbean (orange), or South America (blue), boxes with multiple color inhabit multiple regions. Roman numerals correspond to clades identified in previous figures and the proposed subgenera of *Citharexylum*: (i) *C.* subg. *Citharexylum*, (ii) *C.* subg. *Mexicanum*, (iii) *C.* subg. *Affine*, (iv) *C.* subg. *Sylvaticum* (v) *C.* subg. *Andinum* (vi) *C.* subg. *Altamiranum*. R indicates the genus *Rehdera*.







Habit: tree (green), shrub (yellow)
 Thorns: present (black), absent (white)
 Inflorescence: compound (black), simple (grey), absent (white)
 Flower number: >20 (black), 10-20 (grey), <10 (white)
 Geography: Central America (pink), South America (blue), Caribbean (orange)

SUPPLEMENTAL FIGURES

Fig. S1. Gene trees for cpDNA. Right: maximum likelihood (ML) tree from RAxML; left: Bayesian consensus tree (BI) from MrBayes.

Fig. S2. Gene trees for nrDNA. Right: maximum likelihood (ML) tree from RAxML; left: Bayesian consensus tree (BI) from MrBayes.

Fig. S3. Gene trees for PPR24. Right: maximum likelihood (ML) tree from RAxML; left: Bayesian consensus tree (BI) from MrBayes.

Fig. S4. Gene trees for PPR62. Right: maximum likelihood (ML) tree from RAxML; left: Bayesian consensus tree (BI) from MrBayes.

Fig. S5. Gene trees for PPR70. Right: maximum likelihood (ML) tree from RAxML; left: Bayesian consensus tree (BI) from MrBayes.

Fig. S6. Gene trees for PPR123. Right: maximum likelihood (ML) tree from RAxML; left: Bayesian consensus tree (BI) from MrBayes.

Fig. S7. Gene trees for waxy haplotype 1. Right: maximum likelihood (ML) tree from RAxML; left: Bayesian consensus tree (BI) from MrBayes.

Fig. S8. Gene trees for waxy haplotype 2. Right: maximum likelihood (ML) tree from RAxML; left: Bayesian consensus tree (BI) from MrBayes.

Fig. S9. Ancestral character reconstructions for presence/absence of thorns. Pie charts at nodes indicate the probability of a given state at that node—present (black) or absent (white).

Fig. S10. Ancestral character reconstructions for terminal inflorescences. Pie charts at nodes indicate the probability of a given state at that node—compound (black), simple (gray) or absent (white).

Fig. S11. Ancestral character reconstructions for axillary inflorescences. Pie charts at nodes indicate the probability of a given state at that node—compound (black), simple (gray) or absent (white).

Fig. S12. Ancestral character reconstructions for flower number per raceme. Pie charts at nodes indicate the probability of a given state at that node—>20 (black), 10-20 (gray) or <10 (white).

Fig. S13. Ancestral character reconstructions for flower color. Pie charts at nodes indicate the probability of a given state at that node—literal (white, pale yellow, orange, or purple).

Fig. S14. Ancestral character reconstructions for fruit color. Pie charts at nodes indicate the probability of a given state at that node—red with no intermediate (red), black with no intermediate (black), red with black intermediate (blue), or dry fruits (brown).

Fig. S1. cpDNA



Fig. S2. nrDNA

ML



BI

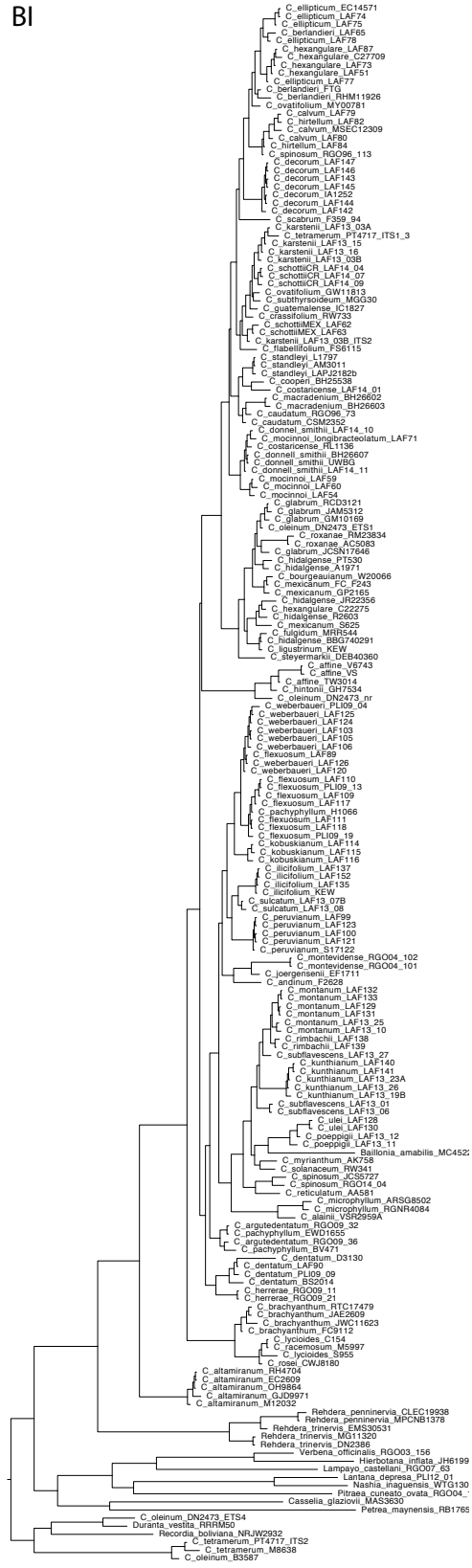


Fig. S3. PPR24

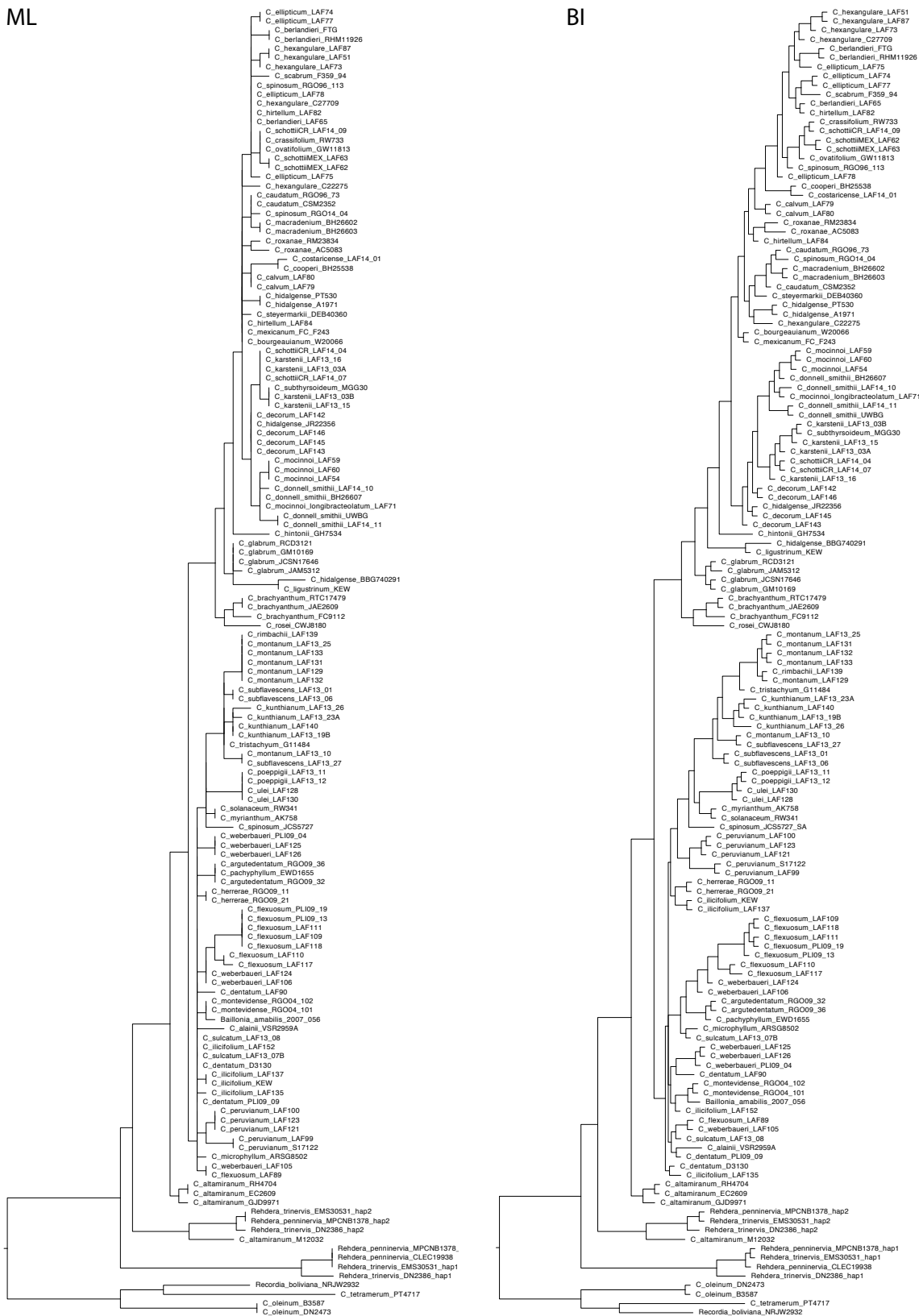
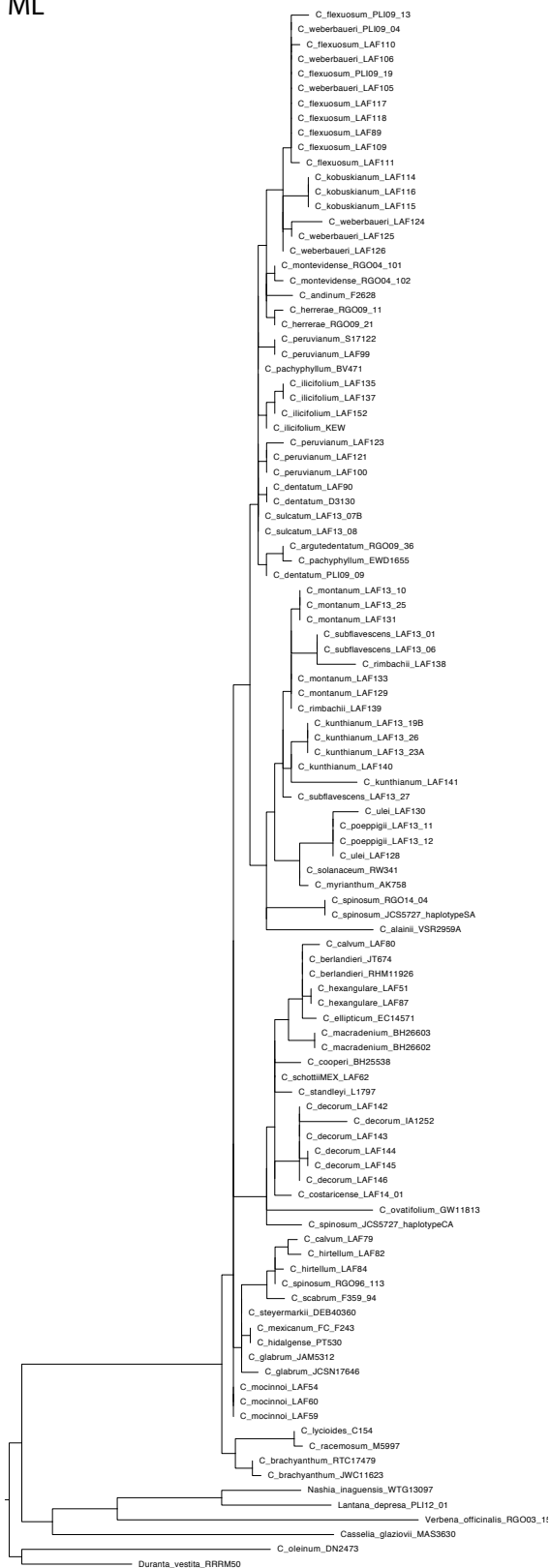


Fig. S4. PPR62

ML



BI

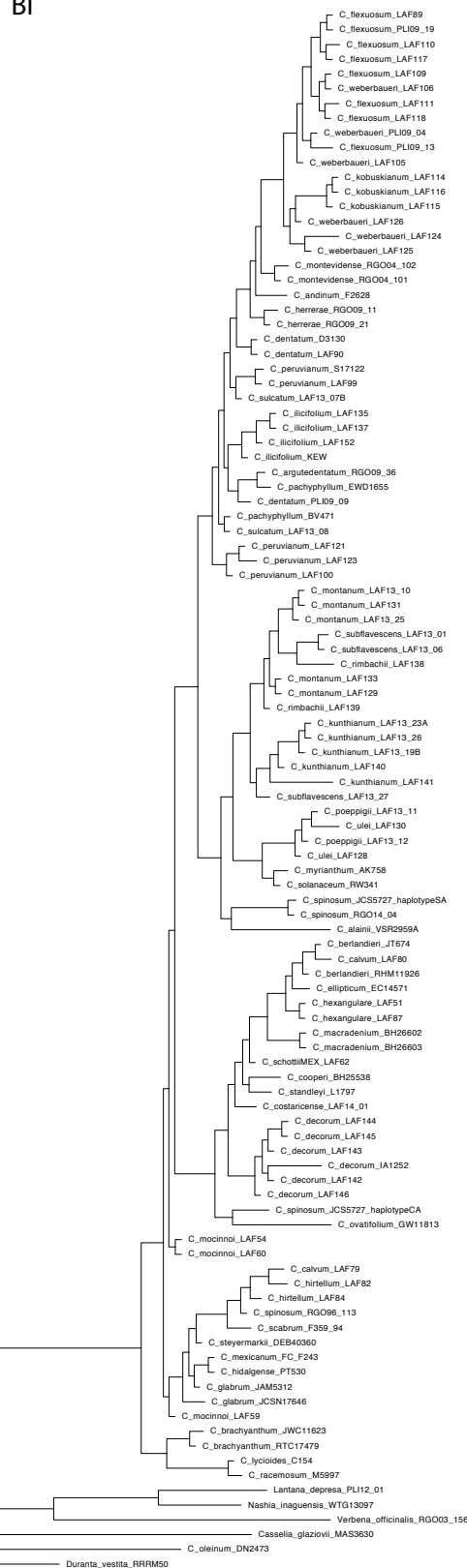


Fig. S5. PPR70

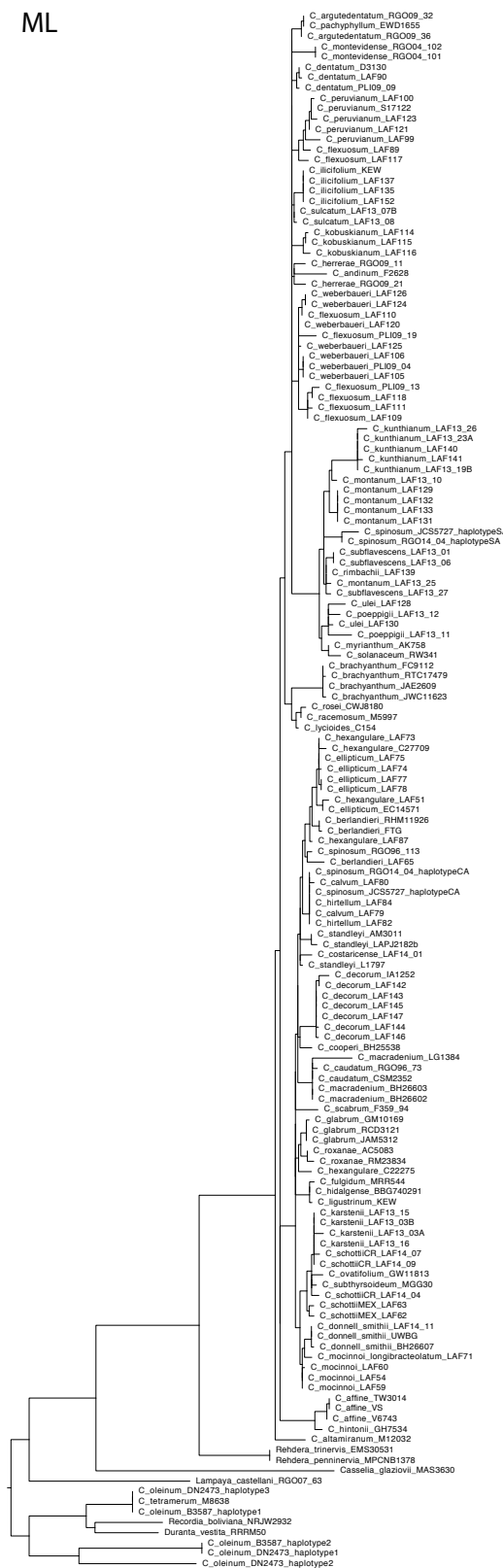


Fig. S6. PPR123



Fig. S7. waxy haplotype 1

ML



BI

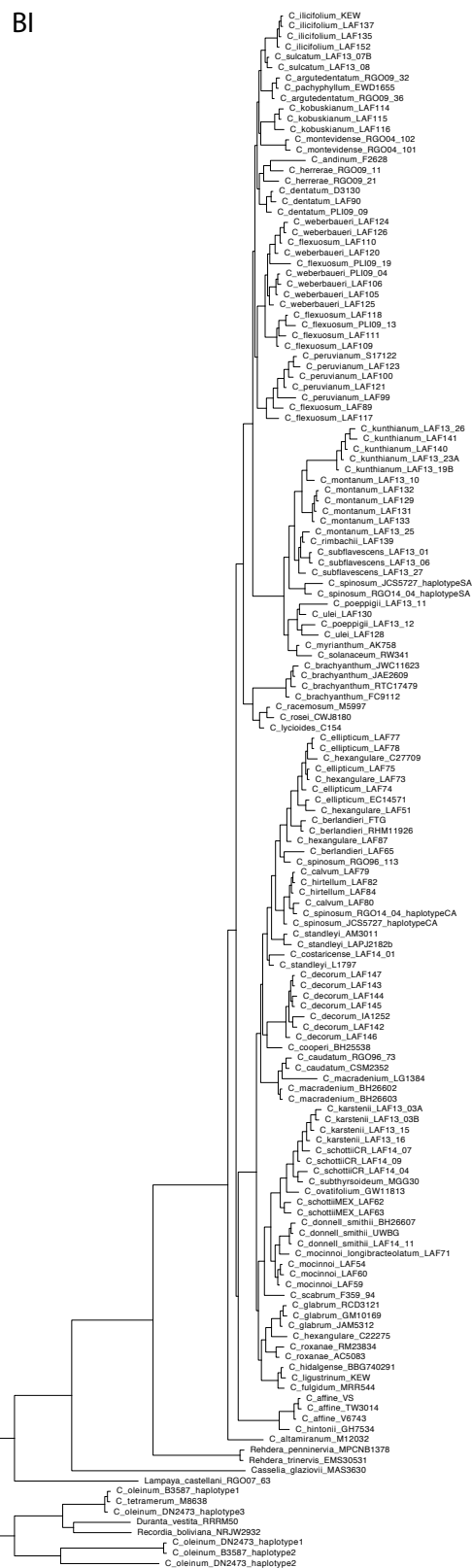
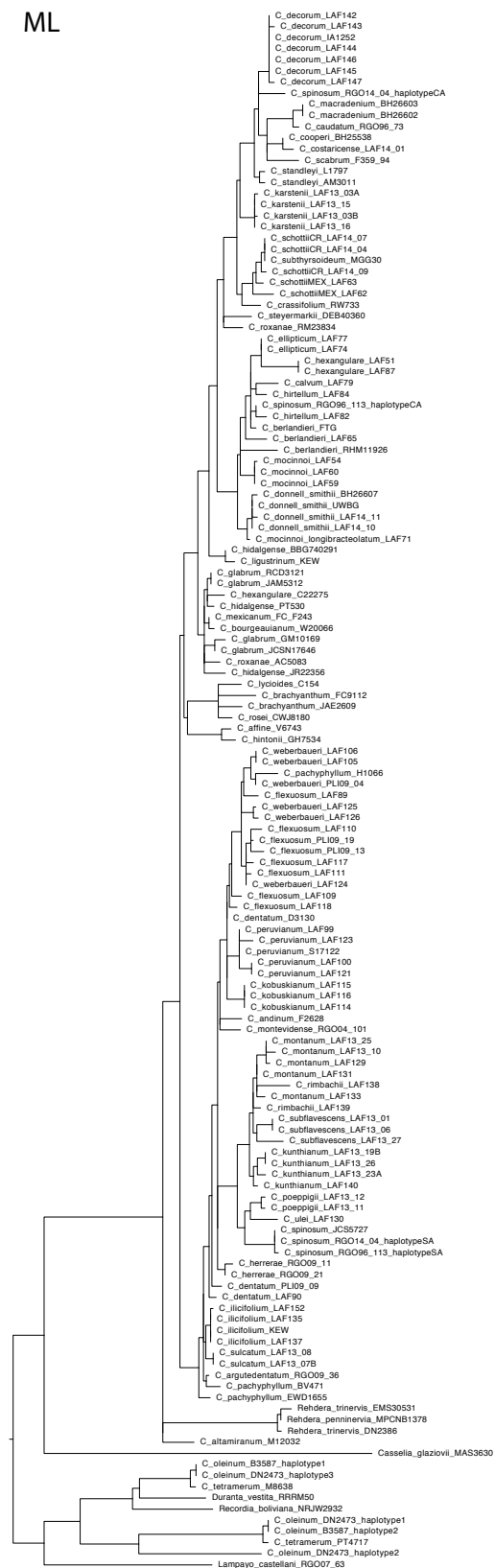


Fig. S8. waxy haplotype 2

ML



BI

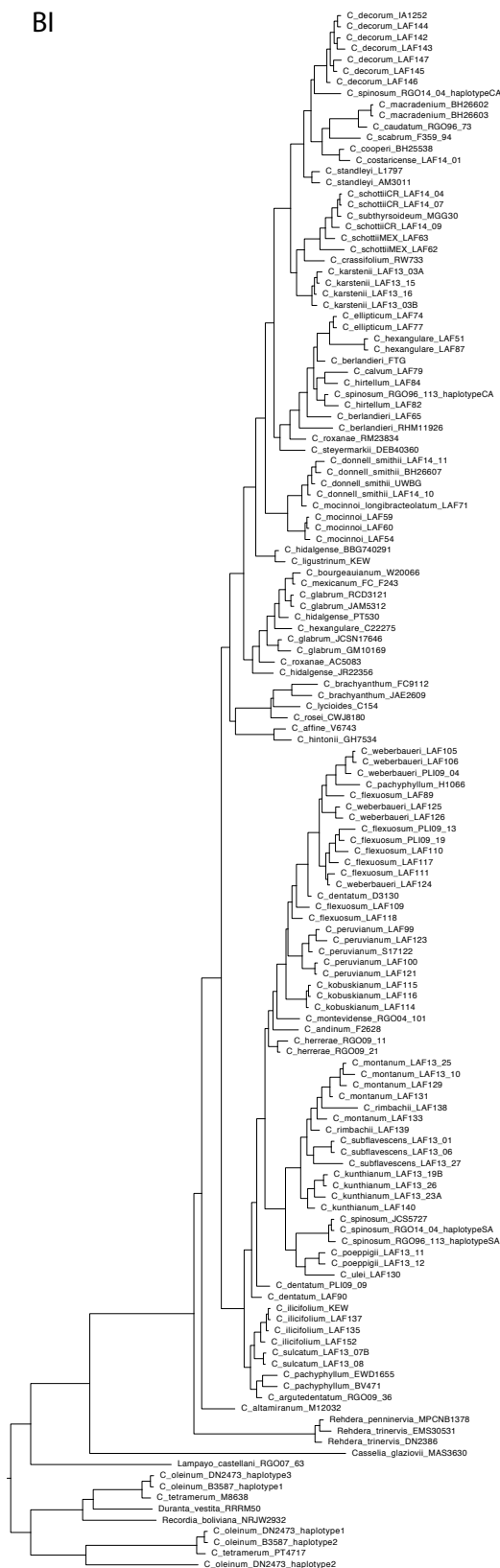


Fig. S9. Thorns

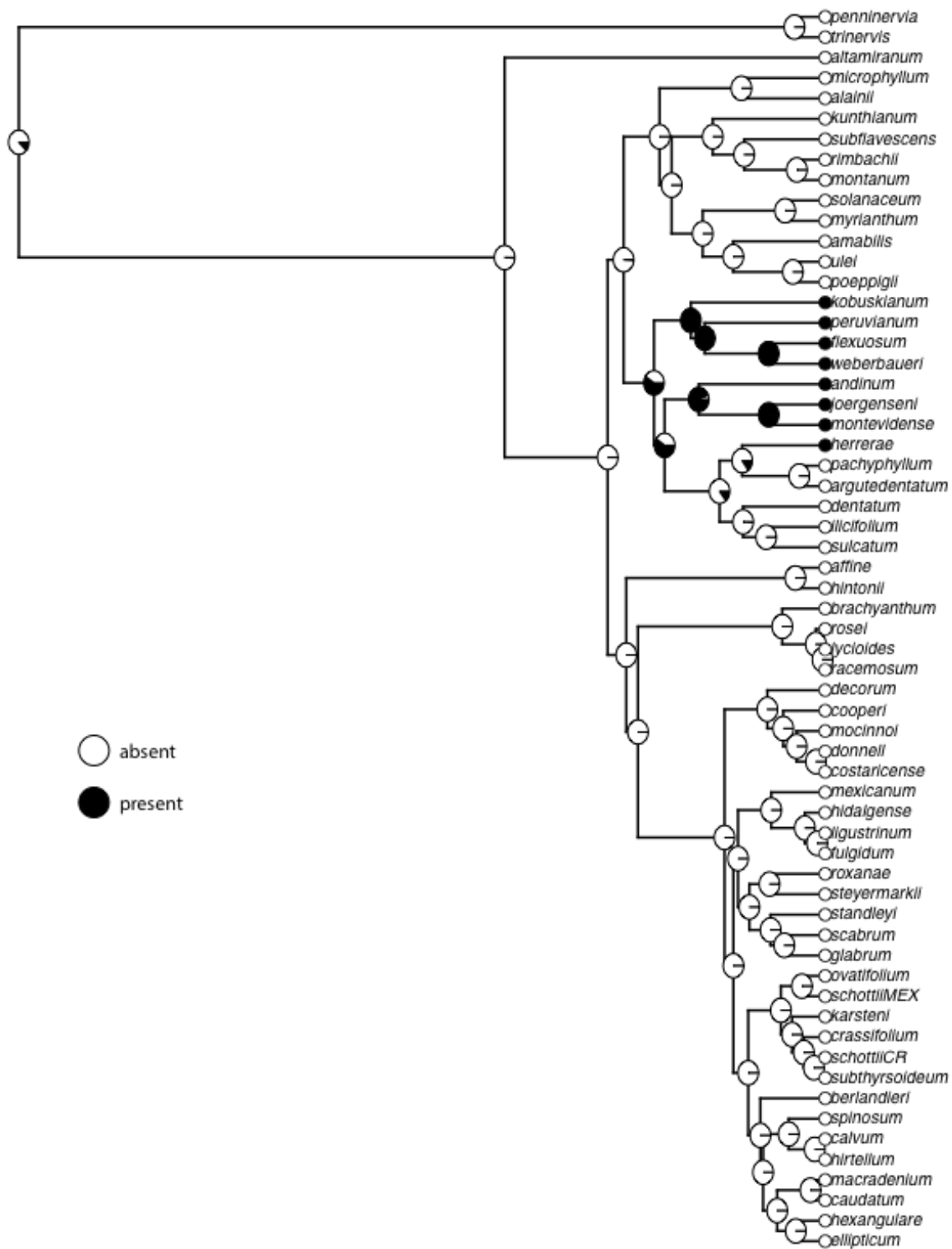


Fig. S10. Terminal inflorescences

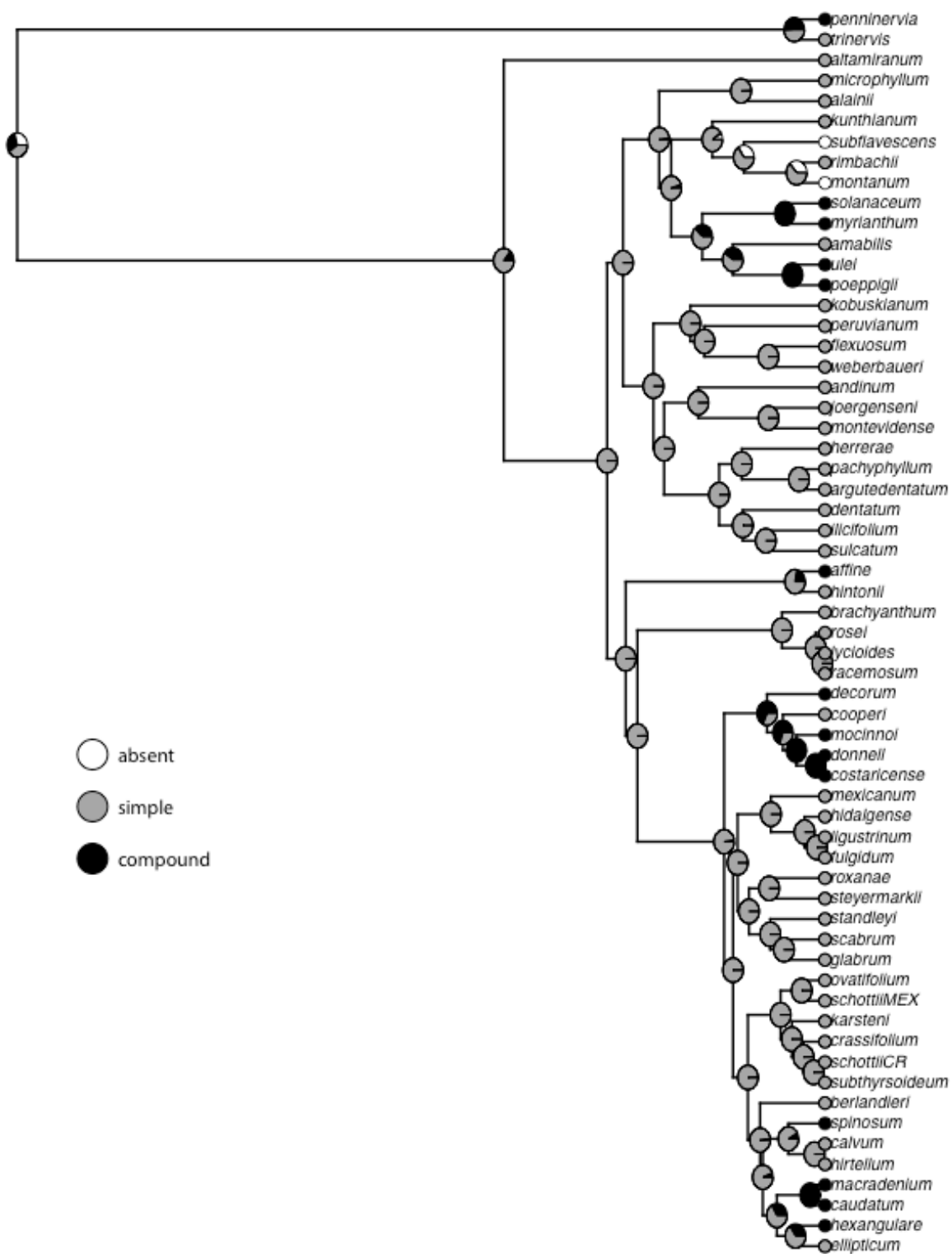


Fig. S11. Axillary inflorescences

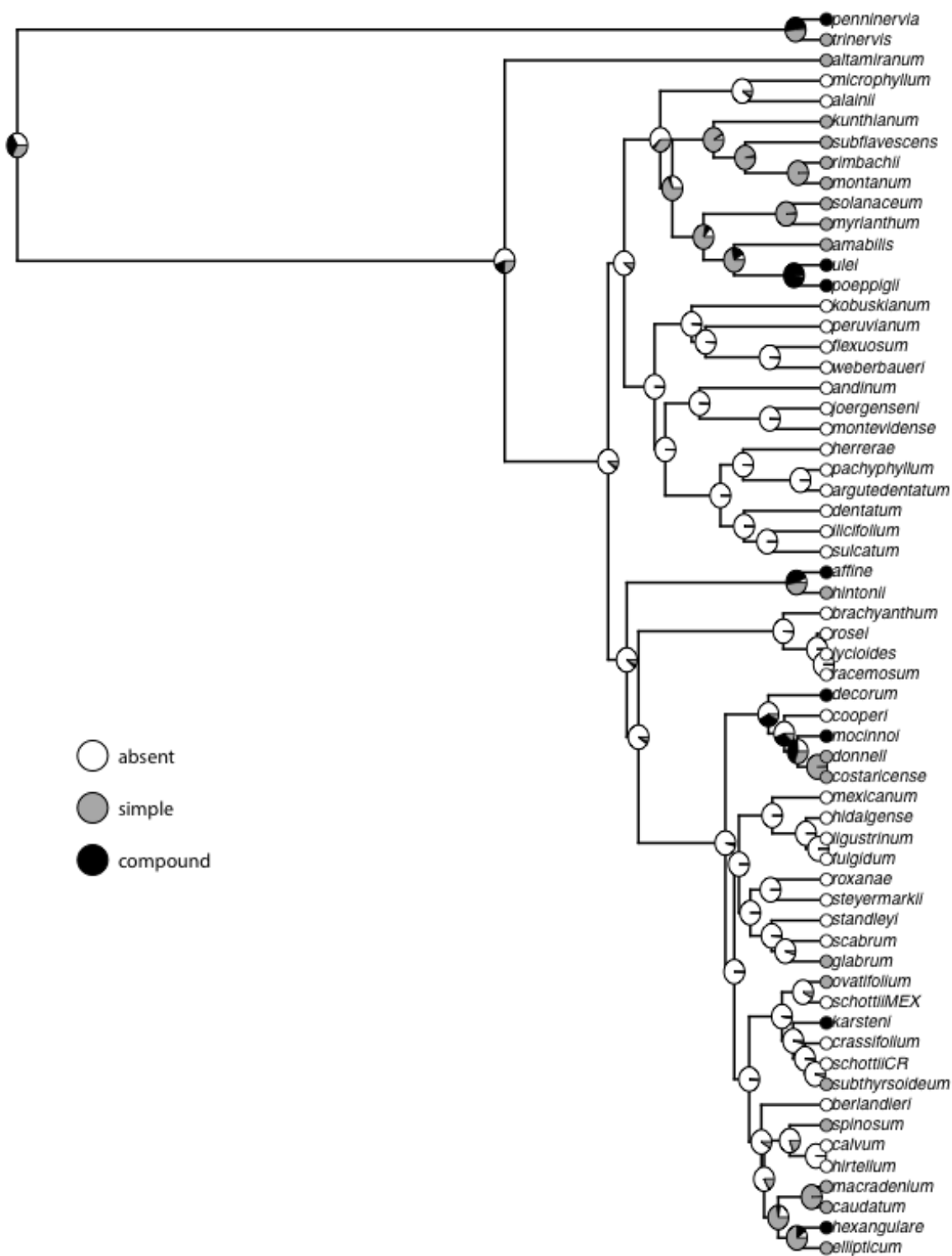


Fig. S12. Flower number

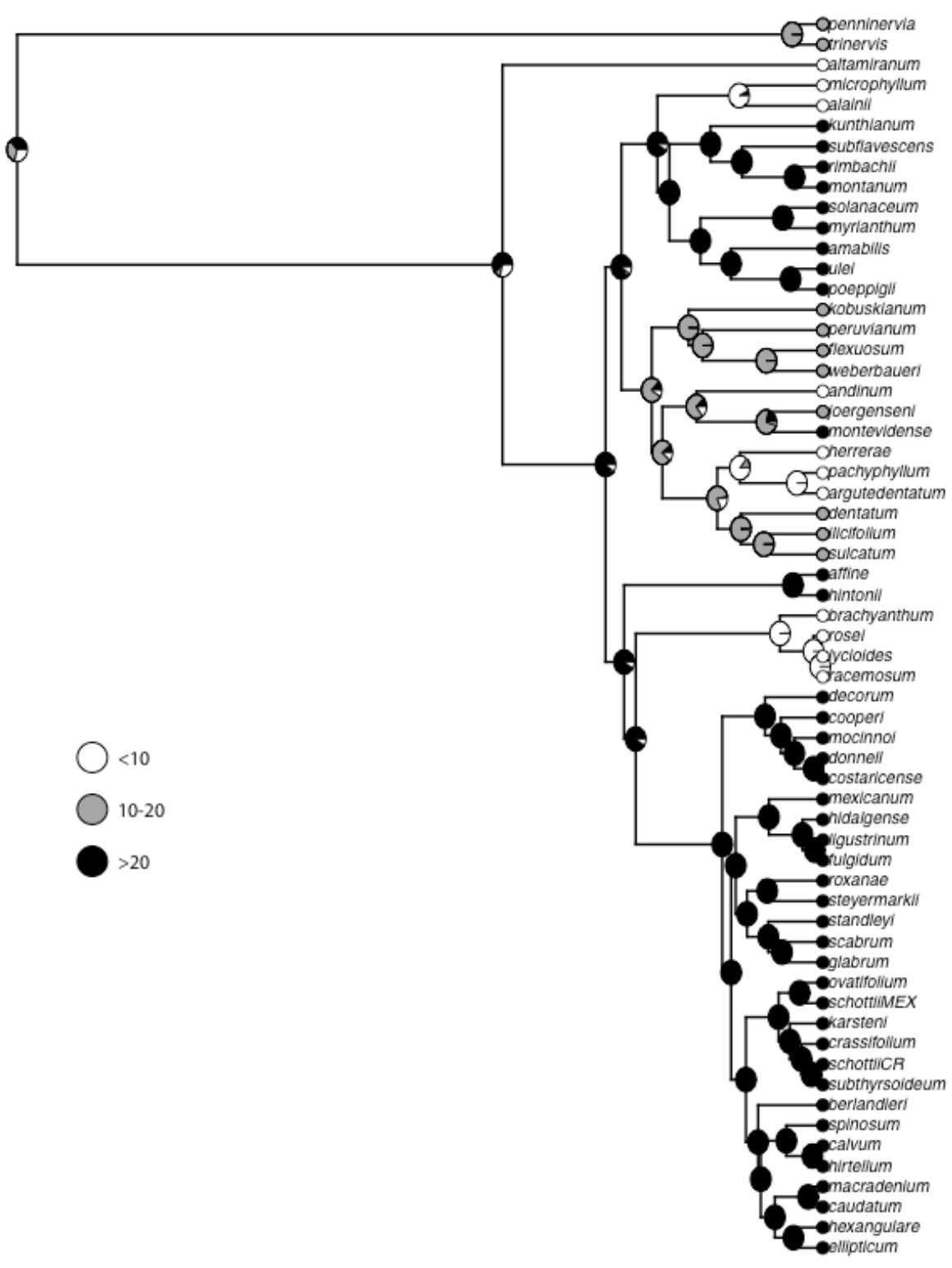


Fig. S13. Flower color

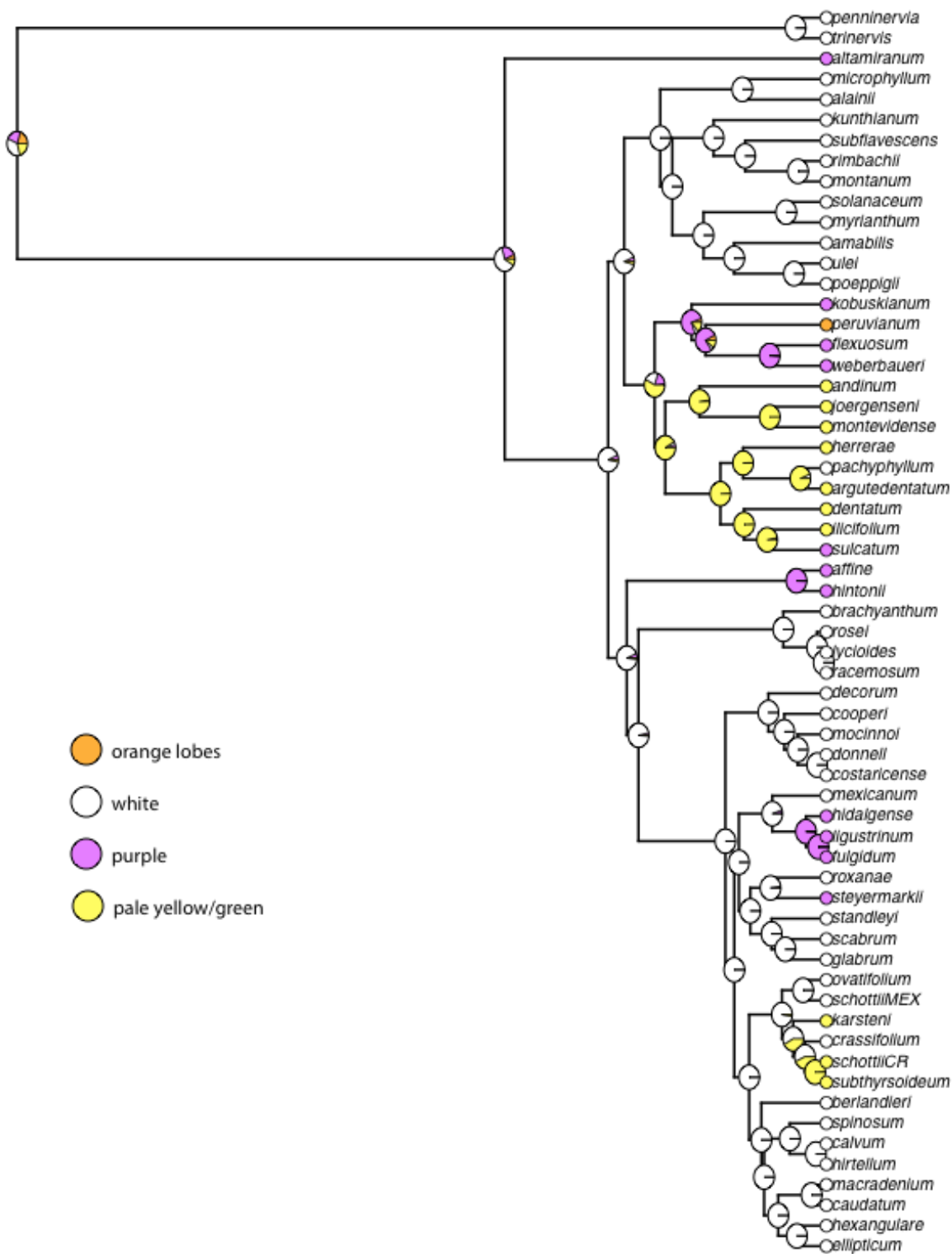
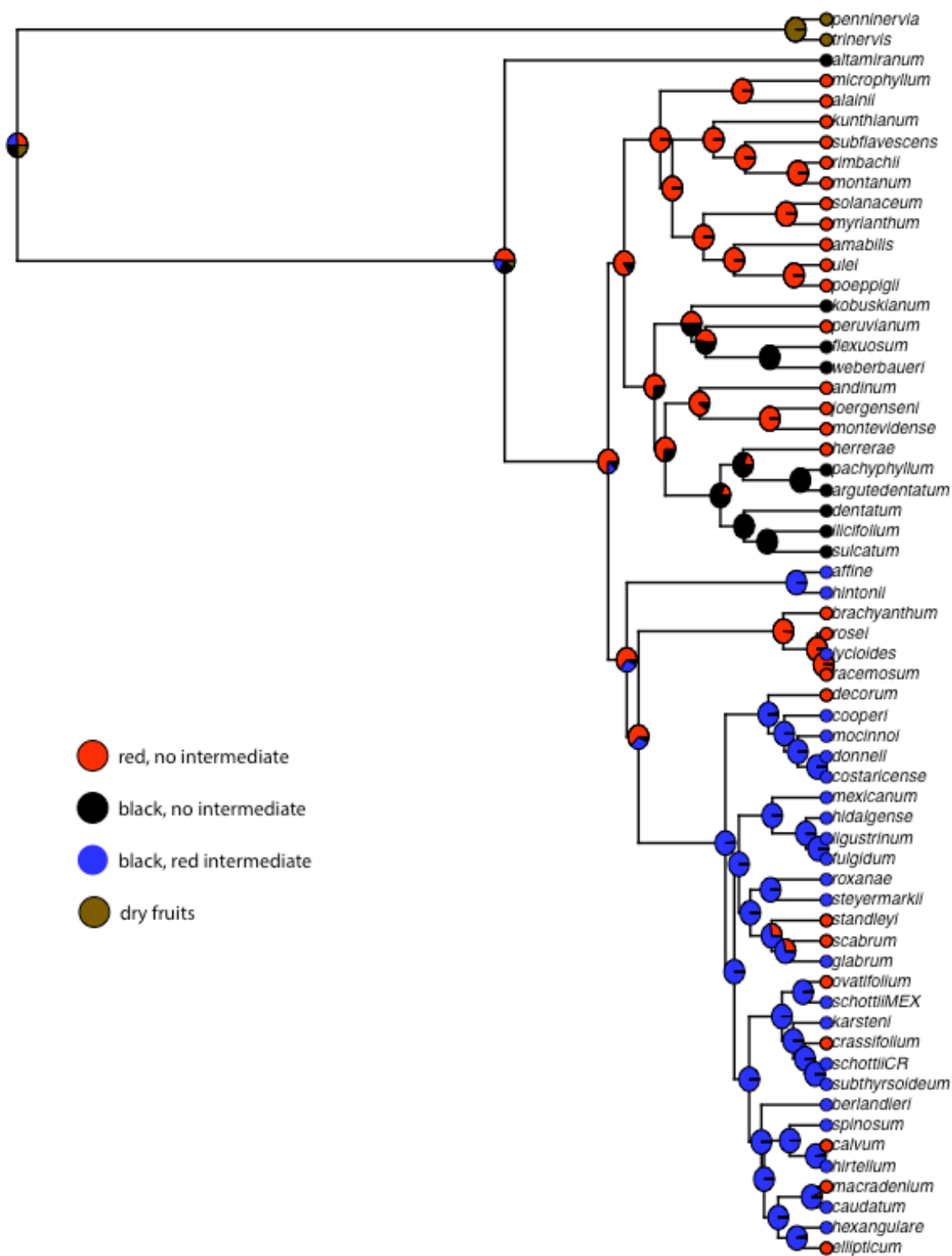


Fig. S14. Fruit color through maturation



CHAPTER 2:

Is it faster to move or evolve? Comparing effects of niche conservatism and niche evolution on diversification rate in the Neotropical plant genus *Citharexylum* (Verbenaceae)

ABSTRACT

Aim: Niche evolution has emerged as an important biogeographical pattern in plant lineages, but we are only beginning to understand how these events contribute to diversification. These patterns are poorly understood in the Neotropics, the area of highest plant diversity in the world. We use the fiddlewoods (*Citharexylum*) a flowering plant genus of Neotropical origin and with a broad distribution in multiple biomes through the Neotropics to assess the direction and frequency of biome shift and how radiation within a biome versus colonization of new biomes affects diversification.

Location: The New World tropics, from northern Mexico to southern Brazil and Argentina

Taxon: *Citharexylum* (Verbenaceae)

Methods: Phylogenetic relationships were reconstructed with near-complete taxonomic sampling of tribe Citharexyleae and representative sampling of the geographic range and biome diversity. Divergence times were estimated, and the dated phylogeny was used to infer biogeographical history through reconstruction of discrete ancestral areas in BioGeoBEARS and fitting of multi-optima Ornstein-Uhlenbeck models to climate variables.

Results: *Citharexylum* originated in Mesoamerica in the mid-Miocene, but the crown radiation occurred in the late Miocene to early Pliocene. Early diversification occurred in mid-elevation montane forests with some temperate elements. Dispersal to South America was followed by separate radiations in open, Andean biomes and low to mid-elevation forest. In Mesoamerica, species repeatedly colonized xeric, seasonally dry, and moist forest biomes. Diversification rates were highest in Mesoamerica and lowest in open biomes in South America.

Main Conclusions: Both niche conservatism and niche evolution have played important roles in the diversification of *Citharexylum*. The Mesoamerican clade exhibits a pattern of radiation within the ancestral biome with more recent, independent colonization events, whereas the South American clade exhibits a pattern of early colonization and radiation within biomes. Despite differences in biogeographic patterns and diversification rates, both clades have produced similar taxonomic diversity in the same amount of time.

1 INTRODUCTION

Understanding patterns of global biodiversity is a primary goal of historical biogeography. The disparity in plant species richness between New World and Old World tropics has fueled interest in how plant lineages diversify in the Neotropics (Antonelli and Sanmartín, 2011). Biogeographic studies at global scales have often revealed patterns of phylogenetic niche conservatism (PNC), the tendency for descendants to occupy similar climatic environments as their ancestors due to evolutionary constraints (Peterson et al. 1999, Prinzing et al. 2001, Wiens and Graham, 2005; Edwards and Donoghue 2006, Qian and Ricklefs 2004; Crisp et al. 2009; Kerkhoff et al. 2014). Early case studies of diversification in Neotropical groups found patterns consistent with phylogenetic niche conservatism (Hughes and Eastwood, 2006; Pennington et al., 2009, 2010; others about niche conservatism), lending support to the idea that physiological adaptations may be difficult to acquire and, therefore, uncommon. Overall, it might be easier to move than to evolve (Moore & Donoghue, 2007; Donoghue, 2008).

However, support for PNC may be biased by the fact that many case studies of Neotropical diversification have focused on large radiations within a single biome including rain forest (Richardson et al., 2001; Davis et al. 2004; mid-elevation), montane forest (Ornelas and González, 2014; Schwery et al., 2015; Lagomarsino et al., 2016), seasonally dry tropical forest (Pennington et al., 2004; Pennington et al., 2010; Werneck et al. 2011; Särkinen et al., 2012), paramo (Hughes and Eastwood, 2006; Madriñan et al., 2013; Nürk et al., 2013; Hughes and Atchison, 2015; Nürk et al., 2015; but see Nürk et al., 2018). With an increased body of literature and improved phylogenetic resolution, niche evolution (also called biome shift), the

ability of descendants to adapt to climatic environments different from that of their ancestors, has emerged as a prominent pattern in plant lineages (Spriggs et al., 2015, Givnish et al., 2014, Weeks et al., 2014; Cardillo et al., 2017).

Seemingly difficult evolutionary events are common in some lineages (e.g., evolution of C4 photosynthesis in PACMAD grasses; Edwards and Smith, 2010), leading to a revision of Donoghue's earlier statement: it is easy both to move and to evolve (Edwards and Donoghue, 2013). Edwards and Donoghue (2013) hypothesize that niche evolution may serve as a driver of speciation and niche conservatism is a deeper phylogenetic pattern. It seems that niche evolution could impact diversification in two ways: (1) high diversification rates in a colonized biome leading to a single, large radiation within an otherwise niche-conserved lineage, or (2) speciation through repeated and frequent colonization of different biomes—but possibly with high extinction—so that the majority of shifts occur near the tips, from ancestors inhabiting the original niche. Donoghue and Edwards (2014) go on to develop hypotheses of niche evolution based on emergent patterns: (1) biome shifts will occur more frequently into/out of the larger biomes and less frequently into/out of smaller ones; (2) more shifts will take place between adjacent and broadly connected biome than between geographically disjunct or narrowly connected biomes; (3) older, once more expansive biomes will more often be donors (e.g., tropical rainforest), and younger, once more restricted biomes will more often be receivers (e.g. deserts, savannas, alpine habitats); (4) if a lineage has shifted between a pair of biomes, it has likely done so multiple times.

Indeed, repeated biome shifts within many tropical lineages have been documented, including multiple colonizations of savannas within tropical moist forest lineages (Simon et al.,

2009; Bouchenak-Khelladi et al. 2010; Edwards and Smith, 2010; Lohmann et al., 2013), tropical dry forest within tropical moist forest lineages (Crayn et al., 2006; Weeks et al., 2014), arid biomes within mesic lineages (Arrigo et al. 2013), Andean-alpine, or paramo, within mid-elevation montane forest lineages (Sklenar et al., 2010), and alpine biomes within arid-adapted lineages (Heibl & Renner, 2012). Beyond the repeated colonization of one biome, studies have found shifts into/out of multiple different biomes within a lineage (Cardillo et al., 2017; Weeks et al. 2014; De-Nova et al. 2012; Heibl and Renner, 2012; Schrire et al., 2009; Olmstead, 2013; Arrigo et al., 2013; Holstein and Renner, 2011; Tölpel et al., 2012). While niche evolution has been documented in many lineages, few studies have investigated how frequency of niche evolution impacts diversification (Cardillo et al., 2017; Kozak and Weins, 2010; Weeks et al., 2014) or the effects shift directionality/occupation of different biomes has on diversification rates within lineages (Cardillo et al., 2017). Even fewer have investigated this in a Neotropical lineage (Weeks et al., 2014).

The verbena family (Verbenaceae) is a family of ca. 800 species that originated in the Neotropics during the Paleogene (Marx et al., 2010; Magallón et al., 2015; Tank and Olmstead, unpublished). Centers of diversity are in arid to semi-arid habitats, but some groups are abundant in more mesic habitats. The fiddlewoods (*Citharexylum*) is a genus of about 70 spp. of trees and shrubs with a generalist insect pollination syndrome and colorful, fleshy fruits (Frost et al., in prep.). The genus is distributed throughout the Neotropics from northern Mexico to southern Brazil and Argentina. Species inhabit moist broadleaf forest, seasonally dry tropical forests, savannas, midelevation montane forest, montane grasslands and shrublands (subparamo), and xeric shrublands in both Mesoamerica and South America (Fig. 1). A previous phylogenetic

study of *Citharexylum* (Frost et al., in prep.) revealed that the early diverging lineages of *Citharexylum* are distributed in Mesoamerica and that most of the diversity is evenly divided between two clades defined by geography: a Mesoamerican (MA) clade and South American (SA) clade. *Citharexylum* is well-suited for the study of the impact of biome shift on diversification, because it occupies multiple biomes on two continents, it includes clades of equal age and diversity in Mesoamerica and South America, and it has no obvious morphological traits or innovations that might otherwise influence diversification rates within the genus (e.g. pollinator specialization, changes in fruit type, etc.). With *Citharexylum* we will address the following questions:

1. What are the crown and stem ages of *Citharexylum*? When did dispersals between continents and colonizations of different biomes occur and how do those events relate to geologic history (e.g. closure of the Isthmus of Panama or Andean orogeny)?
2. Which biome did the most recent common ancestor of *Citharexylum* occupy?
3. What is frequency and directionality of biome shift? How do inferred patterns compare to hypotheses of niche evolution?
4. Do some biomes incur higher or lower diversification rates than others?
5. Is one pattern—niche conservatism or niche evolution—associated with higher diversification rates: Is it faster to move or evolve?

To do this, we used the multi-locus, 61-species dataset for tribe Citharexyleae from Frost et al. (in prep.) to infer a dated phylogeny for the group. We analyzed niche evolution by assigning species to biomes and performing ancestral area reconstructions and by locating shifts in climatic optima for species/clades through fitting a multi-optima Ornstein-Uhlenbeck process

to individual climate variables and climate scores. The second approach provides some indication of how climatically distinct some biomes are from the ancestral, and that shifts inferred from discrete ancestral area reconstructions are, in fact, climatically significant. Finally, the number and location of diversification rate shifts were inferred.

2 METHODS

2.1 Divergence Time Estimation

Bayesian multi-species coalescent (MSC) analyses were performed in BEAST v1.8.4 (Drummond et al., 2012) using the Citharexyleae dataset and partitioning scheme from Frost et al. (in prep.). Four species from the broader Verbenaceae were added to provide nodes for secondary calibration: *Verbena officinalis*, *Stachytarpheta cayennensis*, *Duranta vestita*, and *Petra volubis* (*Stachytarpheta* and *Duranta* will be referred to as a group by the name of the inclusive tribe Duranteae). Inclusion of these species follows sampling of a fossil-calibrated phylogeny of the Lamiales (Tank and Olmstead, unpublished). Species sets for all taxa, Citharexyleae + *Verbena* + Duranteae, and Citharexyleae + *Verbena* were constrained as monophyletic and normal priors with SD +/- 1 were set at 43.1 (44.8-41.4), 33.8 (35.4-32.2), and 28.7 (30.3-27.06) Ma, respectively (Tank and Olmstead, unpublished). Three independent chains of mcmc were run for 500 million generations, sampling every 50,000 generations. Results were visualized in Tracer v1.6 (Rambaut et al., 2014) to determine appropriate burn-in and to verify that effect sample size (ESS) values were adequate (> 200), individual runs had reached stationarity, and separate runs had converged. The runs were combined with LogCombiner v1.8.4 (Drummond et al., 2012), and a maximum clade credibility tree was summarized and annotated with

TreeAnnotator v1.8.4 (Drummond et al., 2012). Output was visualized in FigTree v1.4.3 (<http://tree.bio.ed.ac.uk/software/figtree/>).

2.2 Climate Data

Climatic variables were used to approximate niche/biome. Data for the 19 BioClim variables were extracted from WorldClim global climate layers (Fick and Hijmans, 2017) for species of Citharexyleae. Data were extracted for each species using the R packages raster (Hijmans, 2017) and dismo (Hijmans et al., 2017) with GPS coordinates obtained from geo-referenced, databased specimens in GBIF (gbif.org, 27-29 March 2108) and voucher specimens (Supplementary table). Individuals were manually geo-referenced if coordinates for databased specimens were not available (Supplementary table). Elevation data were also collected for each species from those records. Coordinates were processed so that only unique occurrence points were retained. Additionally, points outside of the natural range (e.g. collections of individuals in botanical gardens or invasives) as well as specimens with georeferencing errors (e.g. points that mapped in the ocean or the center of a country when locality data was limited to the country level) were removed from analyses. For each species the average of extracted data was taken for all 19 climate variables and elevation (from now on referred to as the average dataset). The range (max - min) of extracted data for each species was also taken for all 19 climate variables as a proxy for niche breadth (from now on referred to as the range dataset). A phylogenetic principal component analysis (pPCA) was performed on the average datasets using the R package phytools (Revell, 2012) to obtain climatic niche scores for species for subsequent analyses and to determine which climatic variables were important to niche.

2.3 Ancestral Reconstruction

Ancestral area reconstructions were performed for geographic area and biome with the BioGeoBEARS (Matzke, 2013; Matzke, 2014; Massana et al., 2015) package implemented in RASP v4.0 (Yu et al., 2015). To more accurately reconstruct early nodes, analyses were performed using the Citharexyleae portion of the MSC tree plus one branch representing the sister lineage Casselleae. Geographic areas were defined as Mesoamerica, the Caribbean, and South America. The DIVAlite + j model (Matzke, 2014) was selected from six models as the best fitting model.

For ancestral biome reconstructions, species were assigned to one of the following biomes: moist broadleaf forest, seasonally dry tropical forest, mid-elevation montane forest (1000-2500 m elevation), xeric shrublands, or montane grasslands and shrublands (subparamo; >2500 m elevation). Biomes were adapted from Olson et al. (2001). Some terrestrial ecoregions were combined to better detect broad patterns: seasonally dry forest encompassed tropical/subtropical dry broadleaf forest and tropical/subtropical grasslands, savannas and shrublands; montane forest included tropical coniferous forest and moist broadleaf forest between 1000-2500 m. Maximum likelihood estimations of ancestral characters were performed for all climate variables in the average and range datasets using the R package phytools (Revell, 2012). Reconstructions for continuous data were performed using the MSC tree topology for Citharexyleae. Outgroup taxa were trimmed using the R package ape (Paradis et al., 2004)

2.4 Niche evolution

To detect major shifts in climatic optima within lineages of *Citharexylum*, PC scores and individual climate variables from the average dataset were treated as continuous characters and analyzed using the R package bayou (Uyeda et al., 2013; Uyeda & Harmon, 2014). Because bayou fits multi-optima OU models to the data, the R package geiger (Pennell et al., 2014) was used to ensure that an OU model was the best fit compared to Brownian motion or white noise. Precipitation variables were log normalized to correct for edge effects. PC scores for the first two principal components and individual variables were analyzed with a standard error of 0.5. The maximum number of shifts per branch was limited to one with equal probability of a shift occurring across all branches. A half-cauchy distribution was set as the prior for rate of adaptation (α) and magnitude of uncorrelated diffusion (σ^2), a normal prior was set for the optimum (θ), and a conditional Poisson was set for the number of shifts (k) [make.prior(tree, dists = list(dalpha="dhalfcauchy", dsig2="dhalfcauchy", dsb="dsb", dk="cdpois", dtheta="dnorm"), param = list(dalpha=list(scale=1), dsig2=list(scale=1), dk=list(lambda=8, kmax=120), dsb=list(bmax=1, prob=1), dtheta=list(mean=mean(dat), sd=2*sd(dat)))]]. The mcmc was run for 1 million generations and the first 30% of samples were discarded as burn-in.

2.5 Diversification rate analysis

The number and location of rate shifts were estimated using BAMM (bayesian analysis of macroevolutionary mixtures; Rabosky et al., 2013; Rabosky, 2014). Analyses were performed on the Citharexyleae portion of the MSC. To account for incomplete and biased sampling, a sampling fraction was applied to each of the six subgenera of *Citharexylum* and to *Rehdera*. The

lambda initial prior, lambda shift prior, mu initial prior, and the prior for expected number of shifts were set using the `setBAMMpriors()` function in the R package `BAMMtools` (Rabosky et al., 2014). One analysis was run with default settings for the remaining priors and another was run with a “MEDUSA-like” model (`updateRateLambdaShift=0`). The mcmc was run for 5 million generations, sampling every 2,000 generations. The first 10% of samples were discarded as burnin. The R package `coda` (Plummer et al., 2006) was used to verify that the run had converged and ESS values were adequate. Results were summarized and visualized with `BAMMtools`.

3 RESULTS

3.1 Divergence Time Estimation

Topology and support for major clades in the dated tree were concordant with previous studies of Citharexyleae. Divergence time estimations for calibrated nodes were 41.3 (45.3-37.8), 32.7 (35.9-29.4), and 30.1 (33.3-26.3) Ma for all taxa, Citharexyleae + Verbena + Duranteae, and Citharexyleae + Verbena, respectively (Fig. 1). These estimates are congruent with clade ages from the fossil-calibrated phylogeny of the Lamiales. The crown age for the Citharexyleae was estimated as 14.8 (19.2-11.4) Ma and the crown age for *Citharexylum* 5.9 (8.4-3.5) Ma. The divergence of MA and SA clades was estimated to be 4.0 (5.2-3.4) Ma, and the crown ages of the MA clade and the SA clade 3.7 (4.5-2.8) Ma and 3.7 (4.4-2.4) Ma, respectively. See Table 1 for divergence times of subgenera.

3.2 Climate Data

The number of unique occurrences for species ranged from three (*C. fulgidum*) to 439 (*C. caudatum*). In total, 3,679 unique occurrence points were used. For the average dataset, the first three principal components explained 84.8% of the variation (PC1: 41.5%, PC2: 31.8%, and PC3: 11.5%). Variables that retained most variance in PC1 were minimum temperature of coldest month (bio 6), mean temperature of coldest quarter (bio 11), and mean temperature of driest quarter (bio 9). Twelve of the 20 variables contributed more than average to the variability of the first principal component (Table ?). Variables that retained most variance in PC2 were maximum temperature of warmest month (bio 5), mean temperature of wettest quarter (bio 8), and mean temperature of warmest quarter (bio 10). Eight of the 20 variables contributed more than average to the variability of the second principal component.

3.3 Ancestral Reconstructions

3.3.1 Geographic area

Mesoamerica was reconstructed as the ancestral area of the MRCA for both Citharexyleae and *Citharexylum* (Fig. 2). Dispersal to South America occurred five times. The first dispersal, establishing the SA clade, was estimated to have occurred 4.0 (5.2-3.4) to 3.7 (4.4-2.4) Ma. Four subsequent dispersals to South America have occurred within the last million years, each resulting in a single South American species. Three species (*C. decorum*, *C. karstenii*, and *C. subthyrsoideum*) have ancestors in Mesoamerica; *C. spinosum* is found in the Caribbean and northern South America from ancestors in Mesoamerica. *Citharexylum caudatum* has extended its range from Mesoamerica to include the Caribbean.

3.3.2 Biome

Montane forest was reconstructed as the ancestral biome of the most recent common ancestor (MRCA) of *Citharexylum* (Fig. 3). This was also the most probable ancestral biome for early nodes of the MA clade and the ancestor of the SA clade. In *Citharexylum*, eleven shifts from montane forest to other biomes were inferred (six to broadleaf moist forest, two to seasonally dry forest, and three to xeric shrublands; Fig. 2; Table 2). Three shifts back to montane forest were inferred (two from broadleaf moist forest and one from seasonally dry forest), but two of them with low support. Six additional shifts between colonized biomes were inferred: four from moist broadleaf forest to seasonally dry forest, one from xeric shrublands to seasonally dry forest, and one from seasonally dry forest to montane grasslands and shrublands (Fig. 2; Table 2).

Climate variables—Results for ancestral character estimations of both averages and ranges of individual climate variables are available in Supplementary #-#. Precipitation variables (annual precipitation, precipitation of driest quarter, and precipitation of wettest quarter), reconstruct values for the MRCA of the SA clade (Table 3) more similar to the MRCA of MA and SA clades, which was reconstructed to be montane forest in discrete character analyses, than the MRCA of *C. subg. Andinum*, which was reconstructed to be xeric shrubland in discrete character analyses.

3.4 Niche evolution

Eleven shifts within *Citharexylum* were detected by the bayou analysis of climate scores (PC1) from the PCA (Fig. 3a; Fig. S1). Shifts were detected along branches leading to five of the six subgenera. A shift was not detected at the base of *C. subg. Citharexylum*, but four shifts were found within the subgenus. An additional shift was found in *C. subg. Andinum* leading to *C.*

montevidense, and another in *C.* subg. *Sylvaticum* on the branch leading to *C. poeppigii* and *C. ulei*. Five of the shift locations found by analyses of climate scores were concordant with biome shifts inferred by the BioGeoBEARS analysis (Fig. 4a,c), Nine shifts were detected in the analysis of PC2: six in subg. *Citharexylum*, one in subg. *Andinum*, and two in subg. *Sylvaticum*. Six of the shift locations for PC2 corresponded with shifts inferred by the BioGeoBEARS analysis (Fig. 4a,c; Fig. S2).

Analyses of individual climate variables detected shifts in 30 locations on the tree (Fig. 4b; Figs. S3-S21). Shifts in multiple variables were found on the branches leading to subg. *Mexicanum*, subg. *Andinum*, and subg. *Sylvaticum* (Fig. 4b). Eight subsequent shifts were found in subg. *Andinum*, five by multiple variables and three by a single climate variable. Four more shift locations were recovered in subg. *Sylvaticum*, three by multiple and one by a single variable. In subg. *Citharexylum*, shifts were found in twelve locations, four by multiple variables and eight by a single variable. Six of the shift locations found by analyses of individual variables corresponded with the analysis of climate scores (Fig. 4a,b) and ten were concordant with biome shifts inferred by the BioGEOBEARS analysis (Fig. 4b,c).

3.5 Diversification rate analysis

In both the default-setting and the MEDUSA-like model, one shift on the branch leading to the ancestor of the MA and SA clades was detected with strong support (Fig. S21-S22). A second shift on the branch leading to subg. *Citharexylum* was also detected in both with weak support (Figs. S21-S22). Rates varied throughout the tree at intermediate levels.

DISCUSSION

The stem age for *Citharexylum* is about 15 (19.2-11.4) Ma; the crown age is 6 (8.4-3.5) Ma. Dispersals to South America occurred within the last 4 Ma, when the Isthmus of Panama had more or less reached its current conformation (Montes et al., 2012). Similarly, biomes that are currently occupied by *Citharexylum* would have been present at the time of radiation (i.e., species were not colonizing biomes when the niche space was new/uninhabited) with the possible exceptions of mid-elevation montane biomes and montane grasslands in the northern Andes, which only reached their full height in the last 3 Ma. The MRCA of *Citharexylum* was reconstructed as inhabiting mid-elevation montane forests of Mesoamerica. Repeated colonizations of other biomes from the ancestral biome were reconstructed, the most frequent from mid-elevation montane forest to moist broadleaf forest. Multiple shifts from mid-elevation montane forest to xeric shrublands and from mid-elevation montane forest to seasonally dry forests and savannas were also found. Re-entry into mid-elevation montane forest occurred at least once from moist broadleaf forest (*C. macradenium*), possibly a second time in subg. *Sylvaticum*, though support is weak for moist broadleaf forest as the ancestral biome in this case. Another possible re-entry to mid-elevation montane forest from seasonally dry forest was found for *C. glabrum*, again, with weak support.

Following initial colonization of alternate biomes, shifts occurred multiple times from moist broadleaf forest to seasonally dry forest, in fact, more shifts than occurred from mid-elevation montane forest to seasonally dry forest. Single shifts from xeric shrublands to seasonally dry forest and from xeric shrublands to montane grasslands and shrublands were recovered. Shifts did not occur between moist broadleaf forest and montane grasslands and

shrublands, moist broadleaf forest and xeric shrublands, mid-elevation montane forest and montane grasslands and shrublands, or from seasonally dry forest to moist broadleaf forest, seasonally dry forest to xeric shrublands, montane grasslands and shrublands to xeric shrublands, xeric shrublands to mid-elevation montane forest.

A single shift in diversification rate with high support was placed near the base of *Citharexylum*, but rate variation along the branches revealed higher rates in the MA clade and overall lower rates in the SA clade. The lowest rates were found in subg. *Andinum*, which inhabits inter-Andean dry valleys and subparamo. The most shifts in climate optima were inferred at the base of this clade. Diversification rates were highest in subg. *Citharexylum*, which has repeatedly colonized multiple, adjacent biomes, but these colonizations did not show marked differences in many aspects of climate.

4.1 Origin and early-diverging lineages of *Citharexylum*

The ancestor of Citharexyleae originated in Mesoamerica ca. 15 (19.2-11.4) Ma, around the mid-Miocene climatic optimum. The crown group radiation started ca. 6 (8.4-3.5) Ma. The ancestral biome is inferred to be montane forest, which included coniferous, oak, and pine-oak forests of Mexico and mesic mid-elevation forest in this study. The origin in Mesoamerica and the distribution of early-diverging Mesoamerican lineages (*C. altamiranum* and subg. *Affine*) in pine-oak forest of Mexico, suggests that this is likely the ancestral biome for *Citharexylum*. Pollen collected from the upper Miocene Paraje Solo formation in Veracruz, Mexico reflect temperate coniferous and deciduous elements in the flora (Graham, 1976), elements that remain present in contemporary coniferous-oak forests of Mexico. Other elements of this late Miocene

flora suggest that temperatures would have been slightly cooler and precipitation more evenly distributed throughout the year than at present (Graham, 1976). There is no direct evidence of *Citharexylum* in this flora, but it does establish paleocommunities similar to the reconstructed ancestral biome concurrent with the crown age of the genus and a precursor to modern biomes in which species are distributed.

Except for a single, early-diverging species, *Citharexylum* comprises two major clades, one distributed primarily in Mesoamerica and one distributed primarily in South America. The dispersal to South America establishing the SA clade is estimated to have occurred approximately 4.0 (5.2-2.3) Ma, within younger, Pliocene estimates of the closure of the Isthmus of Panama (Keigwin, 1978; Coates et al., 2004). The ancestral biome of the SA clade is unresolved; both xeric grassland and montane forest biomes were reconstructed with similar probabilities in the discrete character analysis. Continuous character analyses on individual climate variables estimated values more similar to species inhabiting mid-elevation montane forest than xeric grasslands. Additionally, multi-optima fitting analyses for climate scores and individual variables located shifts along the daughter branches of the MRCA of the SA clade rather than the branch leading to it, suggesting that shifts in climatic optima occurred after establishment in South America.

4.2 The Mesoamerican clade

Mid-elevation montane forest is confidently reconstructed along the backbone of the MA clade. The clade exhibits the second of the two hypothesized patterns for niche evolution and niche conservatism when it is easy to move and to evolve: the ancestral biome for the genus is

conserved at deeper nodes and shifts to novel biomes occur more frequently near the tips. Additionally, shifts in fewer climate variables per shift location on the phylogeny are found in the MA clade compared to shift events in the SA clade (i.e., more elements of the ancestral biome are retained). Two radiations within a colonized biome are inferred in the MA clade: one in xeric shrublands bordering the Chihuahuan Desert of Central Mexico (*C. subg. Mexicanum*) and one in broadleaf mesic forests along the Gulf Coast and Yucatan Peninsula (*C. ellipticum-C. spinosum*). Tropical wet forests often act as a source biome, but transitions into them are relatively rare (Donoghue and Edwards, 2014; Antonelli et al., 2018). However, in Mesoamerica, wet tropical forests were restricted during late Miocene and Pliocene, and tropical elements are poorly represented in paleofloras near the Gulf Coast during the Pliocene (Graham and Dilcher, 1998). If cool-temperate forests like those of the Paraje Solo formation were widespread, this would fit the hypothesis that shifts occur from a more expansive source biome (e.g., mid-elevation montane forest) into a more restricted biome (e.g., moist broadleaf forest).

The Gulf Coast/Caribbean clade of subg. *Citharexylum* is the only radiation within BMF in Mesoamerica, but the species have repeatedly colonized broadleaf moist forest in Mesoamerica. Four additional colonizations of broadleaf moist forest from mid-elevation montane forest by single species are found, two from mid-elevation, pine-oak forest by *C. schottii* (Costa Rica and Mexico populations, which are not each other's closest relative) and two from cloud forests in Costa Rica by *C. cooperi* and *C. costaricense*. Repeated colonizations of open biomes have also occurred. Two of these shifts also correspond with dispersals to South America: one by *C. decorum*, which is distributed in Ecuadorian dry forests west of the Andes, and one by *C. subthyrsoideum*, which has a narrow distribution in the Lower Catuche wood and

shrublands near Caracas, Venezuela. Colonization of xeric biomes has occurred three times in the MA clade: by subg. *Mexicanum*, distributed in shrublands bordering the Chihuahuan desert, and separately by *C. roxanae* and *C. flabellifolium* (not sampled in this study but see Frost et al., 2017 and Frost et al., in prep. for discussion of this species), distributed in Baja California Sur and Sonora.

The divergence of xeric-adapted subg. *Mexicanum* occurred ca. 3.5 (4.3-2.5) Ma, within the timeframe that the ancestor of subg. *Andinum* colonized inter-Andean dry valleys (4.3-1.9). However, extant diversity in subg. *Mexicanum* radiated within the last million years, whereas divergence times in subg. *Andinum* are older. Each of the subgenera in the MA clade was established in the Pliocene, but did not radiate until the Pleistocene. Species diversity in some plant groups has been attributed to recent periods of unstable climate during Pleistocene glaciation cycles promoting allopatric speciation through fractured populations in refugia. These cycles may have promoted speciation within biomes, such as within xeric biomes in subg. *Mexicanum*, but may have also promoted shifts between biomes. Mesoamerica is hypothesized to have fluctuated between dry and wet cycles during Pleistocene (cite), these different cycles could have altered the connectivity of different biomes at different times, making shifts between them more probable.

4.3 The South American clade

In South America, biome shifts occurred early in lineages, and shifts were followed by radiation within those biomes. The two daughter lineages of the MRCA of the SA clade, subg. *Andinum* and subg. *Sylvaticum*, exhibit shifts in climatic optima in opposite directions. subg.

Andinum represents a radiation in cooler, drier, and higher biomes in the Andes. Species diversified in inter-Andean dry valleys of Peru (*C. flexuosum*, *C. weberbaueri*, *C. peruvianum*, and *C. kobuskianum*) and seasonally dry forest of Bolivia and northern Argentina (*C. andinum* and *C. joergensenii*) before colonizing montane grasslands and shrublands, or subparamo (>3,000 m a.s.l.). In the present distribution of Neotropical biomes, montane grasslands and shrublands have their greatest expanse in southern Peru, Bolivia, and northern Argentina. Seasonally dry forests flank the eastern slopes of the Andes in Bolivia and northern Argentina where xeric grasslands flank the western slopes in Peru and northern Chile. Both xeric shrublands and seasonally dry biomes are present in inter-Andean valleys in these countries and have persisted since the late Miocene, so there is potentially a history of connectivity between these biomes. This is the only region in which an exchange between xeric grasslands and seasonally dry tropical forest was found, and the only colonization of high-elevation montane grassland and shrublands. High alpine species show a history of northward dispersal in the Andes and allopatric speciation: *C. herrerae*, *C. argutedentatum*, and *C. pachyphyllum* are endemic to southern Peru, *C. dentatum* to central Peru, *C. illicifolium* to northern Peru and Ecuador, and *C. sulcatum* to Colombia.

Subgenus *Sylvaticum*, radiated in warmer, wetter, lower elevation biomes. The subgenus includes the only dispersal out of South America to the Caribbean, resulting a small clade of seasonal to humid-forest-adapted shrubs. Most of the diversity in subg. *Sylvaticum* is distributed in a clade of Amazonian and Atlantic forest trees and a clade of mid-elevation, cloud forest trees in the Northern Andes. One shift occurred in the Amazonian clade from moist broadleaf forest to tropical savanna in *C. amabilis*. This species, which was previously classified in a different

genus (*Baillonia*), is the only species of *Citharexylum* distributed in the Cerrado. *Citharexylum montevidense*, is distributed in the adjacent humid chaco and Uruguayan savanna. Aside from a couple of recent colonizations by single species, South American groups show a history of early colonization followed by a period of diversification within that biome.

4.4 Diversification

The MA and SA clades of *Citharexylum* provide a natural experiment for patterns of niche evolution and diversification on separate continents in the Neotropics. They are the same age and comprise similar species diversity, but exhibit distinct patterns. The only well-supported shift in diversification rate was located near the MRCA of the MA and SA clades. Variation of rates among branches reveals higher rates in the MA clade and lower rates in the SA clade; a weakly supported shift toward higher rates was found at the base of subg. *Citharexylum*. Frequent biome shifts were found in subg. *Citharexylum* by the analysis of discrete biomes, but these shifts corresponded to shifts in few climate variables, often only one variable.

In the SA clade, rates are lower in subg. *Andinum* and higher in subg. *Sylvaticum*. Both clades are preceded by shifts in optima for multiple climatic variables, but rates seem marginally higher in cloud forest species (*C. montanum*, *C. subflavescens*, *C. rimbachii*, and *C. kunthianum*) and Atlantic forest species (*C. myrianthum* and *C. solanaceum*) of subg. *Sylvaticum*. In each of these groups, elements of ancestral environment are restored. The cloud forest species reenter mid-elevation montane forest and the Atlantic coast forest, though characterized as moist broadleaf forest, is not as warm and wet as the Amazon forest occupied by other members of this clade. The Pleistocene glaciation and refugia model has also been invoked for speciation in

Atlantic forest (cite) and the northern Andean biomes (van der Hammen, 1974, Gentry 1982); this could explain higher rates of diversification in those environments. It could also explain lower rates in inter-Andean dry valleys and seasonally dry forests in subg. *Andinum*. Pennington et al. (2004) found that Pleistocene glaciation cycles did not influence speciation in woody, South American plants inhabiting those biomes.

Another interpretation of lower diversification rates in subg. *Andinum* is that properties of biomes themselves influence rates in lineages. Hypotheses for Neotropical biomes are most developed for Andean habitats. Species poor and slowly diversifying, but highly endemic groups are characteristic of inter-Andean valley/seasonally dry forest biomes (Pennington et al., 2010; Särkinen et al., 2012). Somewhat more recent and rapid diversification is characteristic of mid-elevation montane forest (Lagomarsino et al., 2016; Givnish et al., 2014). Some of the highest diversification rates in plants have been reported from high-elevation, Andean grasslands, or paramo. Lowest rates would be expected in seasonally dry forest and xeric shrublands and higher rates in mid-elevation montane forest; both of these patterns are observed in *Citharexylum*. The highest rates would be expected in montane grasslands and shrublands, which is not observed. This could be due to the fact that *Citharexylum* does not reach the paramo, but only the subparamo, and perhaps there is a marked difference in speciation between the two.

Subgenus *Andinum* also exhibited the greatest climatic divergence of any clade of *Citharexylum*. The colonization of xeric shrublands inferred at the base of subg. *Andinum* corresponded to shifts in 11 out of 20 climate variables assessed. To give perspective, shifts to xeric grasslands in Mesoamerica corresponded with shifts in 6 variables for subg. *Mexicanum* and 5 variables for *C. roxannae*. The lowest diversification rates were found in the group that is

most distinct from the ancestor. Likewise, the highest rates were found in sugb. *Citharexylum* in which shifts were common, but only in one or two variables. Retention of elements of the ancestral niche combined with some lability could promote parapatric speciation. If colonized biomes are climatically more similar to the ancestral biome, this may also reduce extinction rate in those biomes versus colonization of more dissimilar biomes.

Ultimately, the Mesoamerican and South American radiations have produced similar species diversity in the same amount of time. In Mesoamerica, lineages did not radiate until the Pleistocene; there is a lag between when the Mesoamerican subgenera diverge and when they radiate. South American lineages have older, steadier speciation events. Though each clade displays different biogeographic patterns and different patterns of diversification, the result are, more or less, the same.

Conclusions

Niche evolution has occurred frequently in the evolutionary history of *Citharexylum*. Both repeated colonizations of biomes and radiations within biomes have occurred. Shifts occurred most commonly to and from the largest biomes and in areas of high connectivity between biomes, which is consistent with hypothesized patterns of biome shift. Lowest diversification rates were recovered for open biomes in South America, with rates somewhat higher in forested biomes of South America and higher overall in Mesoamerica. Observed patterns of diversification may be the result of Pleistocene glaciation, slower speciation rates in general in open biomes of South America, or how much of the ancestral niche is retained in a

colonization event. Overall, there is not an observable difference in the effect of niche conservatism or niche evolution on species diversity in this group.

Acknowledgements

The authors thank the curators of the following herbaria for permitting us to sample specimens:

F, HUH, MEX, MO, SI, TEX, USM, WTU; the following people for assistance in the field:

Carlos Burelo-Ramos, Warren Cardinal-McTeague, Itzue Caviedes-Solis, Ross Furbush, David

Garcia, Johan Home, Diego Morales-Briones, Lenis Prado, Sarah Tyson, and Simon Uribe-

Convers; and anonymous reviewers. Data collection and analyses performed by the IBEST

Genomics Resources Core at the University of Idaho were supported in part by NIH COBRE

grant P30GM103324. Field research was supported by the Garden Club of America, American

Society of Plant Taxonomists, Society of Systematic Biologist, and University of Washington

Biology Department. This study was supported by NSF grants DEB 0542493, DEB 0710026, and DEB 1020369 to RGO and DEB 1500919 to LAF and RGO.

REFERENCES

Antonelli, A., & Sanmartin, I. (2011) Why are there so many plant species in the Neotropics? *Taxon*, 60 (2), 403-414.

Arrigo, N., Therrien, J., Anderson, C.L., Windham, M.D., Haufler, C.H., Barker, M.S. (2013) A total evidence approach to understanding phylogenetic relationships and ecological diversity in *Selaginella* subg. *Tetragonostachys*. *American Journal of Botany*, 100(8), 1672-1682.

Bouchenak-Khelladi, Y., Maurin, O., Hurter, J., van der Bank, M. (2010) The evolutionary history and biogeography of Mimosoideae (Leguminosae); an emphasis on African acacias. *Molecular Phylogenetics and Evolution*, 57, 495-508.

Coates, A.G., Collins, L.S., Aubry, M.-P., and Berggren, W.A. 2004. The geology of the Darien, Panama, and the late Miocene–Pliocene collision of the Panama arc with northwestern South America: *Geological Society of America Bulletin*, 116, 1327–1344. doi:10.1130/B25275.1

Crayn, D.M., Rossetto, M., Maynard, D.J. (2006) Molecular phylogeny and dating reveals an Oligo-Miocene radiation of dry-adapted shrubs (former Tremandraceae) from rainforest tree progenitors (Elaeocarpaceae) in Australia. *American Journal of Botany*, 93(9), 1328-1342.

Crisp, M.D., Arroyo, M.T.K., Cook, L.G., Gandolfo, M.A., Jordan, G.J., et al. (2009) Phylogenetic biome conservatism on a global scale. *Nature*, 458, 754-756.

Davis, C.C., Webb, C.O., Wurdack, K.J., Jaramillo, C.A., Donoghue, M.J. (2005) Explosive radiation of Malpighiales supports a mid-Cretaceous origin of modern tropical rain forests. *American Naturalist*, 165, E36-E65

De-Nova, J.A., Medina, R., Montero, J.C., Weeks, A., Rosell, J.A. et al. (2012) Insights into the historical construction of species-rich Mesoamerican seasonally dry tropical forest: the diversification of *Bursera* (Buseraceae, Sapindales). *New Phytologist*, 193(1), 276-287

Donoghue, M.J. (2008) A phylogenetic perspective on the distribution of plant diversity. *Proceedings of the National Academy of Sciences*, 105, 11549-11555

Donoghue, M.J., & Edwards, E.J. (2104) Biome shifts and niche evolution in plants. *Annual Review of Ecology, Evolution, and Systematics*, 45, 547-572.

Drummond, A.J., Suchard, M.A., Dong Xie & Rambaut, A. (2012) Bayesian phylogenetics with BEAUti and the BEAST 1.7. *Molecular Biology and Evolution*, 29, 1969-1973.

Edwards, E.J., & Donoghue, M.J. (2006) *Pereskia* and the origin of the cactus life-form. *American Naturalist*, 167(6), 777-793

Edwards, E.J., & Donoghue, M.J. (2013) Is it easy to move and easy to evolve? Evolutionary accessibility and adaptation. *Journal of Experimental Botany*, 64, 4047-4052

Edwards, E.J., & Smith, S.A. (2010) Phylogenetic analyses reveal the shady history of C4 grasses. *Proceedings of the National Academy of Sciences*, 107(6), 2532-2538

Fick, S.E., and Hijmans, R.J. (2017) Worldclim 2: New 1-km spatial resolution climate surfaces for global land areas. *International Journal of Climatology*. DOI: 10.1002/joc.5086

Frost, L. A., Tyson, S. M., Lu-Irving, P., O'Leary, N., & Olmstead, R. G. (2017). Origins of North American arid-land Verbenaceae: More than one way to skin a cat. *American Journal of Botany*, 104(11), 1708-1716.

GBIF.org (2018), GBIF Home Page. Available from: <http://gbif.org> [27-29 March 2018].

GBIF.org (27th March 2018) GBIF Occurrence Download. <https://doi.org/10.15468/dl.lidyuv1>

GBIF.org (28th March 2018) GBIF Occurrence Download. <https://doi.org/10.15468/dl.pjcdof>

GBIF.org (29th March 2018) GBIF Occurrence Download. <https://doi.org/10.15468/dl.7ahgxl>

Gentry, A.H. (1982) Neotropical Floristic Diversity: Phytogeographical Connections Between Central and South America, Pleistocene Climatic Fluctuations, or an Accident of the Andean Orogeny? *Annals of the Missouri Botanical Garden*, 69 (3), 557-593.

Givnish, T.J., Barfuss, M.H.J., Van Es, B., Riina, R., Schulte, K., Horres, R. ... Sytsma, K.J.

(2014) Adaptive radiations, correlated and contingent evolution, and net species diversification in Bromeliaceae. *Molecular Phylogenetics and Evolution*, 71, 55-78. doi: 10.1016/j.ympev.

2013.10.010

Graham, A. (1976) Studies in Neotropical Paleobotany. II. The Miocene Communities of Veracruz, Mexico. *Missouri Botanical Garden Press*, 63 (4), 787-842.

Graham, A., & Dilcher, D.A. (1998) Studies in Neotropical paleobotany. XII. A palynoflora from the Pliocene Rio Banano Formation of Costa Rica and the Neogene vegetation of Mesoamerica. *American Journal of Botany*, 85(10), 1426-1438.

Hiebl, C., Renner, S.S. (2011) Distribution models and a dated phylogeny for Chilean *Oxalis* species reveal occupation of new habitats by different lineages, not rapid adaptive radiation. *Systematic Biology*, 61(5), 823-834

Hijmans, R.J. (2017) raster: Geographic Data Analysis and Modeling. R package version 2.6-7. <https://CRAN.R-project.org/package=raster>

Hijmans, R.J., Phillips, S., Leathwick, J., and Elith, J. (2017) dismo: Species Distribution Modeling. R package version 1.1-4. <https://CRAN.R-project.org/package=dismo>

Holstein, N., Renner, S.S. (2011) A dated phylogeny and collection records reveal repeated biome shifts in the African genus *Coccinia* (Cucurbitaceae). *BMC Evolution*, 11, 28.

Hughes, C., & Eastwood, R. (2006) Island radiation on a continental scale: Exceptional rates of plant diversification after uplift of the Andes. *Proceedings of the National Academy of Sciences*, 103 (27), 10334-10339.

Hughes, C.E., Atchison, G.W. (2015) The ubiquity of alpine plant radiations: from the Andes to the Hengduan Mountains. *New Phytologist*, 207, 275–282.

Keigwin, L.D. 1978. Pliocene closing of the Isthmus of Panama, based on biostratigraphic evidence from nearby Pacific Ocean and Caribbean Sea cores: *Geology*, 6(10), 630–634.

Kozak, K.H., and Wiens, J.J. (2010) Accelerated rates of climatic-niche evolution underlie rapid species diversification. *Ecology Letters*, 13, 1378-1389. doi: 10.1111/j.1461-0248.2010.01530.x

Lagomarsino, L.P., Condamine, F.L., Antonelli, A., Mulch, A., Davis, C.C. (2016) The abiotic and biotic drivers of rapid diversification in Andean bellflowers (Campanulaceae). *New Phytologist*, 210, 1430–1442.

Lohmann, L. G., Bell, C. D., Calió, M. F., & Winkworth, R. C. (2013) Pattern and timing of biogeographical history in the Neotropical tribe Bignonieae (Bignoniaceae). *Botanical Journal of the Linnean Society*, 171(1), 154-170.

Madriñán, S., Cortés, A. J., & Richardson, J. E. (2013) Páramo is the world's fastest evolving and coolest biodiversity hotspot. *Frontiers in genetics*, 4, 192.

Marx, H. E., O'Leary, N., Yuan, Y. W., Lu–Irving, P., Tank, D. C., Múlgura, M. E., & Olmstead, R. G. (2010). A molecular phylogeny and classification of Verbenaceae. *American journal of Botany*, 97(10), 1647-1663.

Magallón, S., Gómez–Acevedo, S., Sánchez–Reyes, L. L., & Hernández–Hernández, T. (2015). A metacalibrated time–tree documents the early rise of flowering plant phylogenetic diversity. *New Phytologist*, 207(2), 437-453.

Matzke N.J. (2013) BioGeoBEARS: BioGeography with Bayesian (and likelihood) evolutionary analysis in R Scripts, CRAN: The Comprehensive R Archive Network, Vienna, Austria. <http://cran.r-project.org/package=BioGeoBEARS>

Matzke, N.J. (2014). "Model Selection in Historical Biogeography Reveals that Founder-event Speciation is a Crucial Process in Island Clades." *Systematic Biology*. 63(6): 951-970. <http://dx.doi.org/10.1093/sysbio/syu056>

Montes, C., Cardona, A., McFadden, R., Morón, S. E., Silva, C. A., Restrepo-Moreno, S., ... & Bayona, G. A. 2012. Evidence for middle Eocene and younger land emergence in central Panama: implications for Isthmus closure. *Bulletin*, 124(5-6), 780-799.

Moore, B. R., & Donoghue, M. J. (2007) Correlates of diversification in the plant clade Dipsacales: geographic movement and evolutionary innovations. *the american naturalist*, 170(S2), S28-S55.

Nürk, N., Scheriau, & C., Madriñán S. (2013) Explosive radiation in high Andean *Hypericum*—rates of diversification among New World lineages. *Frontiers in Genetics*, 4, 175. doi:10.3389/fgene.2013.00175

Nürk, N., Uribe-Convers, S., Gehrke, B., Tank, D.C., & Blattner, F.R. (2015) Oligocene niche shift, Miocene diversification – cold tolerance and accelerated speciation rates in the St. John's Worts (*Hypericum*, *Hypericaceae*). *BMC Evolutionary Biology*, 15, 80. doi: 10.1186/s12862-015-0359-4

Nürk, N.M., Michling, F., & Linder, H.P. (2018) Are the radiations of temperate lineages in tropical alpine ecosystems pre-adapted? *Global Ecology and Biogeography*, 27, 334–345. <https://doi.org/10.1111/geb.12699>

Olmstead, R. G. (2013). Phylogeny and biogeography in Solanaceae, Verbenaceae and Bignoniaceae: a comparison of continental and intercontinental diversification patterns. *Botanical Journal of the Linnean Society*, 171(1), 80-102.

Ornelas, J. F. & González, C. (2014) Interglacial genetic diversification of *Moussonia deppeana* (Gesneriaceae), a hummingbird-pollinated, cloud forest shrub in northern Mesoamerica. *Molecular Ecology*, 23, 4119-4136. doi:10.1111/mec.12841

Paradis E., Claude J. & Strimmer K. (2004) APE: analyses of phylogenetics and evolution in R language. *Bioinformatics*, 20, 289-290.

Pennington, R.T., Lavin, M., Prado, D.E., Pendry, C.A., Pell, S.K. & Butterworth, C.A. (2004) Historical climate change and speciation: Neotropical seasonally dry forest plants show patterns of both Tertiary and Quaternary diversification. *Philosophical Transactions of the Royal Society B: Biological Sciences*, 359, 515-537. DOI: 10.1098/rstb.2003.1435

Pennington, R.T., Lavin, M., Särkinen, T., Lewis, G.P., Klitgaard, B.B., & Hughes, C.E. (2010) Contrasting plant diversification histories within the Andean biodiversity hotspot. *Proceedings of the National Academy of Sciences*, 107 (31), 13783-13787. DOI: 10.1073/pnas.1001317107

Peterson, A.T., Soberon, J., Sanchez-Cordero, V. (1999) Conservatism of Ecological Niches in Evolutionary Time. *Science*, 285, 1265-1267. DOI: 10.1126/science.285.5431.1265

Plummer, M., Best, N., Cowles, K., & Vines, K. (2006) CODA: Convergence Diagnosis and Output Analysis for MCMC. *R News*, 6, 7-11.

Rabosky, D.L., Santini, F., Eastman, J.M., Smith, S.A., Sidlauskas, B., Chang, J. & Alfaro, M.E. (2013) Rates of speciation and morphological evolution are correlated across the largest vertebrate radiation. *Nature Communications*, 4, 1958. doi:10.1038/ncomms2958.

Rabosky, D.L. (2014) Automatic detection of key innovations, rate shifts, and diversity-dependence on phylogenetic trees. *PLoS One*, 9, e89543.

Rabosky, D.L., Grudler, M.C., Anderson, C.J., Title, P.O., Shi, J.J., Brown, J.W., Huang, H., & Larson, J.G. (2014) BAMMtools: an R package for the analysis of evolutionary dynamics on phylogenetic trees. *Methods in Ecology and Evolution*, 5, 701-707.

Revell, L. J. (2012) phytools: An R package for phylogenetic comparative biology (and other things). *Methods in Ecology and Evolution*. 3 217-223. doi:10.1111/j.2041-210X.2011.00169.x

Richardson, J.E., Pennington, R.T., Pennington, T.D., Hollingsworth, P.M. (2001) Rapid Diversification of a species-rich genus of Neotropical rain forest trees. *Science*, 293, 2242-2245.

Ricklefs, R.E. (2004) A comprehensive framework for global patterns in biodiversity. *Ecology Letters*, 7(1):1-15

Särkinen, T., Pennington, R.T., Lavin, M., Simon, M.F., and Hughes, C.E. (2012) Evolutionary islands in the Andes: persistence and isolation explain high endemism in Andean dry tropical forests. *Journal of Biogeography*, 39, 884-900

Schnitzler, J., Graham, C.H., Dormann, C.F., Schiffers, K., Linder, H.P. (2012) Climatic niche evolution and species diversification in the Cape flora, South Africa. *Journal of Biogeography*, 39(12), 2201-2211

Schrire, B.D., Lavin, M., Barker, N.P., Forest, F. 2009. Phylogeny of the tribe Indigofereae (Leguminosae—Papilionoideae): geographically structured more in succulent-rich and temperate settings than in grass-rich environments. *American Journal of Botany*, 96(4), 816-852

Schwery, O., Onstein, R.E., Bouchenak-Khelladi, Y., Xing, Y., Carter, R.J., Linder, H.P. (2015) As old as the mountains: the radiations of the Ericaceae. *New Phytologist*, 207, 355-367. doi: 10.1111/nph.13234

Simon, M.F, Grether, R., de Queiroz, L.P., Skema, C., Pennington, R.T., Hughes, C.E. (2009) Recent assembly of the Cerrado, a neotropical plant diversity hotspot, by in situ evolution of adaptations to fire. *Proceeding son the National Academy of Sciences*, 106(48), 816-852

Sklenář, P., Dušková, E. & Balslev, H. (2011) Tropical and Temperate: Evolutionary History of Páramo Flora. *The Botanical Review*, 77(2): 71-108. <https://doi.org/10.1007/s12229-010-9061-9>

Spriggs, E. L., Clement, W. L., Sweeney, P. W., Madriñán, S., Edwards, E. J., & Donoghue, M. J. (2015) Temperate radiations and dying embers of a tropical past: the diversification of *Viburnum*. *New Phytologist*, 207(2), 340-354.

Tiede, Y., Homeier, J., Cumbicus, N., Peña, J., Albrecht, J., Ziegenhagen, B., . . . Farwig, N. (2016) Phylogenetic niche conservatism does not explain elevational patterns of species

richness, phylodiversity and family age of tree assemblages in Andean rainforest. *Erdkunde*, 70(1), 83-106.

Töpel, M., Antonelli, A. Yesson, C., Eriksen, B. (2012) Past climate change and plant evolution in western North America: a case study in Rosaceae. *PLOS ONE*, 7(12), e50358

Uyeda, J.C., Eastman, J., & Harmon, L. (2013) bayou: Bayesian fitting of Ornstein-Uhlenbeck models to phylogenies. R package version 1.0.

Uyeda, J.C., & Harmon, L. (2014) A Novel Bayesian Method for Inferring and Interpreting the Dynamics of Adaptive Landscapes from Phylogenetic Comparative Data. *Systematic Biology*, 63(6), 902-918. DOI:10.1093/sysbio/syu057

van der Hammen, T. (1974). The Pleistocene changes of vegetation and climate in tropical South America. *Journal of Biogeography*, 3-26.

Weeks, A., Zapata, F., Pell, S. K., Daly, D. C., Mitchell, J. D., & Fine, P. V. 2014. To move or to evolve: contrasting patterns of intercontinental connectivity and climatic niche evolution in “Terebinthaceae”(Anacardiaceae and Burseraceae). *Frontiers in Genetics*, 5, 409.

Werneck, F.P. (2011) The diversification of eastern South American open vegetation biomes: historical biogeography and perspectives. *Quaternary Science Reviews*, 30, 1630-1648. doi: 10.1016/j.quascirev.2011.03.2009

Wiens, J.J., & Graham, C.H. (2005) Niche conservatism: integrating evolution, ecology, and conservation biology. *Annual Review of Ecology, Evolution, and Systematics*, 36, 519-539.

Yu, Y., Harris, A.J., Blair, C., & He, X.J. (2015) RASP (Reconstruct Ancestral State in Phylogenies): a tool for historical biogeography. *Molecular Phylogenetics and Evolution*, 87, 46-49.

TABLES

Table 1. Divergence times for major clades of *Citharexylum*.

	Stem age (error)	Crown age (error)
Citharexylum	14.84 (19.25-11.44)	5.90 (8.42-3.54)
subg. Altamiranum	5.90 (8.42-3.54)	5.90 (8.42-3.54)
- SA clade	4.00 (5.21-3.39)	3.71 (4.38-2.35)
subg. Sylvaticum	3.71 (4.38-2.35)	3.05 (4.19-2.16)
subg. Andinum	3.71 (4.38-2.35)	3.15 (4.07-1.96)
- MA clade	4.00 (5.21-3.39)	3.66 (4.47-2.76)
subg. Affine	3.66 (4.47-2.76)	0.55 (1.63-0.0022)
subg. Mexicanum	3.45 (4.31-2.49)	0.79 (2.14-0.11)
sugb. Citharexylum	3.45 (4.31-2.49)	1.85 (3.16-1.33)

Table 2. Inferred biome shifts and their locations from discrete biome reconstructions in BioGeoBEARS and analysis of PC1 and PC2 scores and individual climate variables in bayou with support values and biological interpretation.

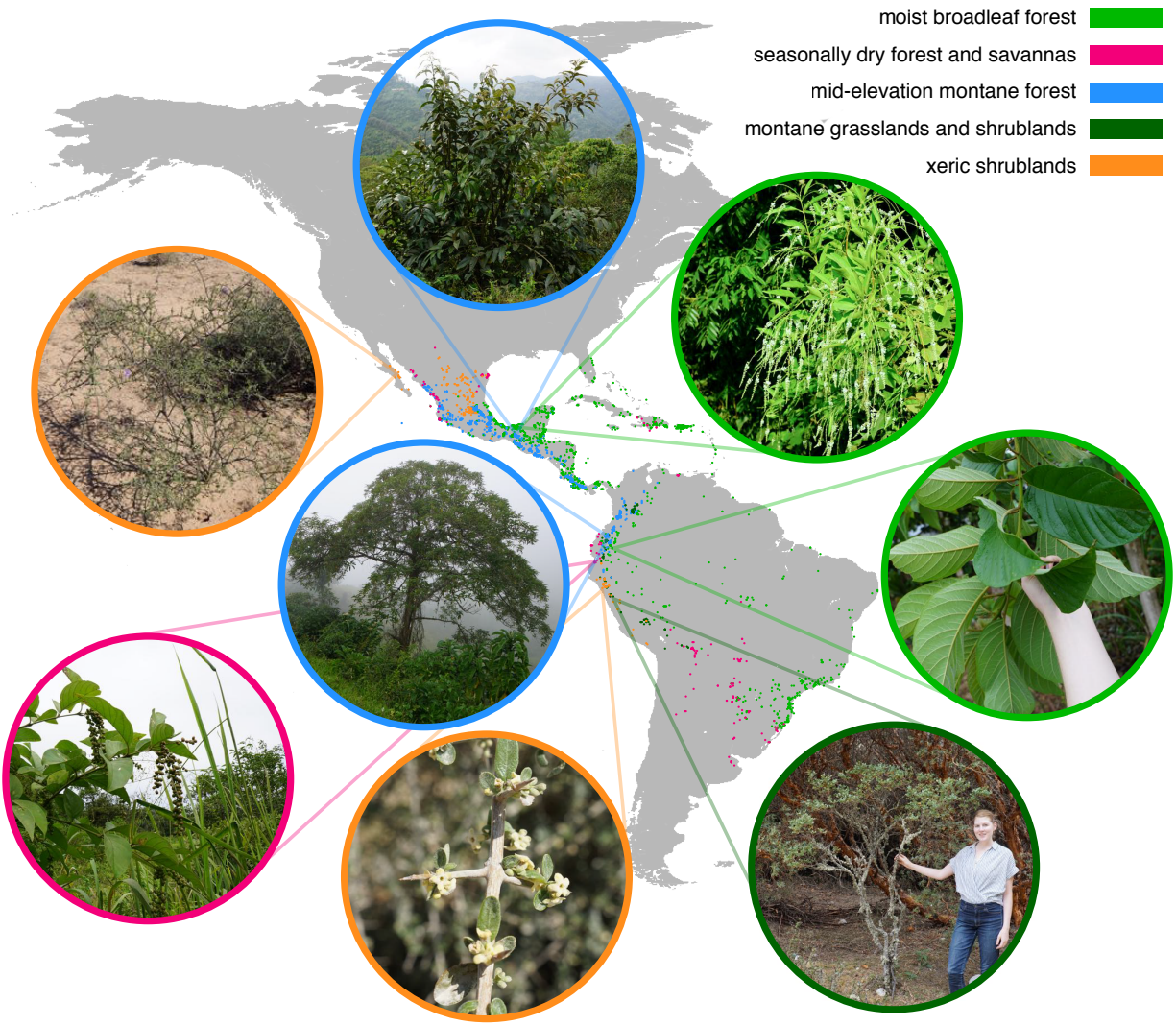
FIGURE LEGENDS

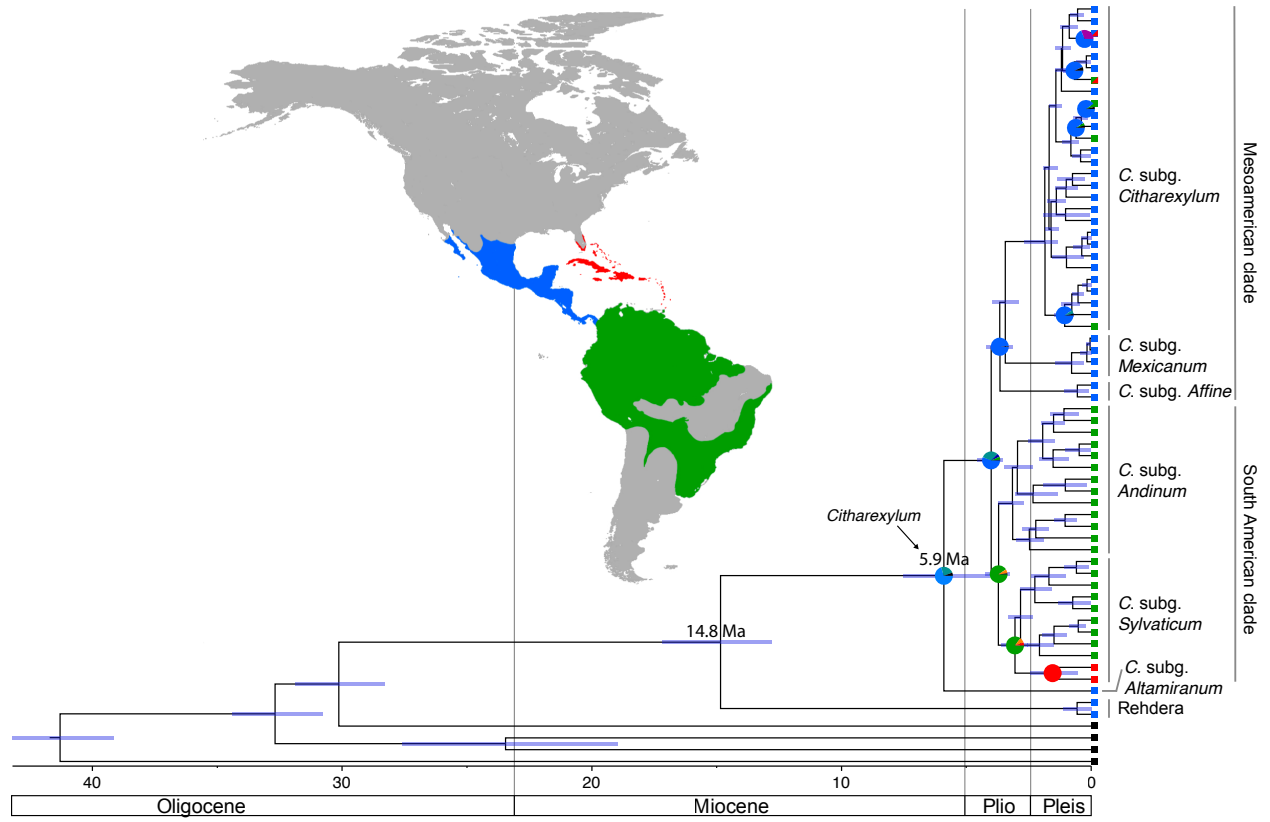
Fig. 1 Distribution map of *Citharexylum*. Points indicate individual occurrences, and points are colored according to the biome assignment for that given species. Photos of representative species for each biome include:

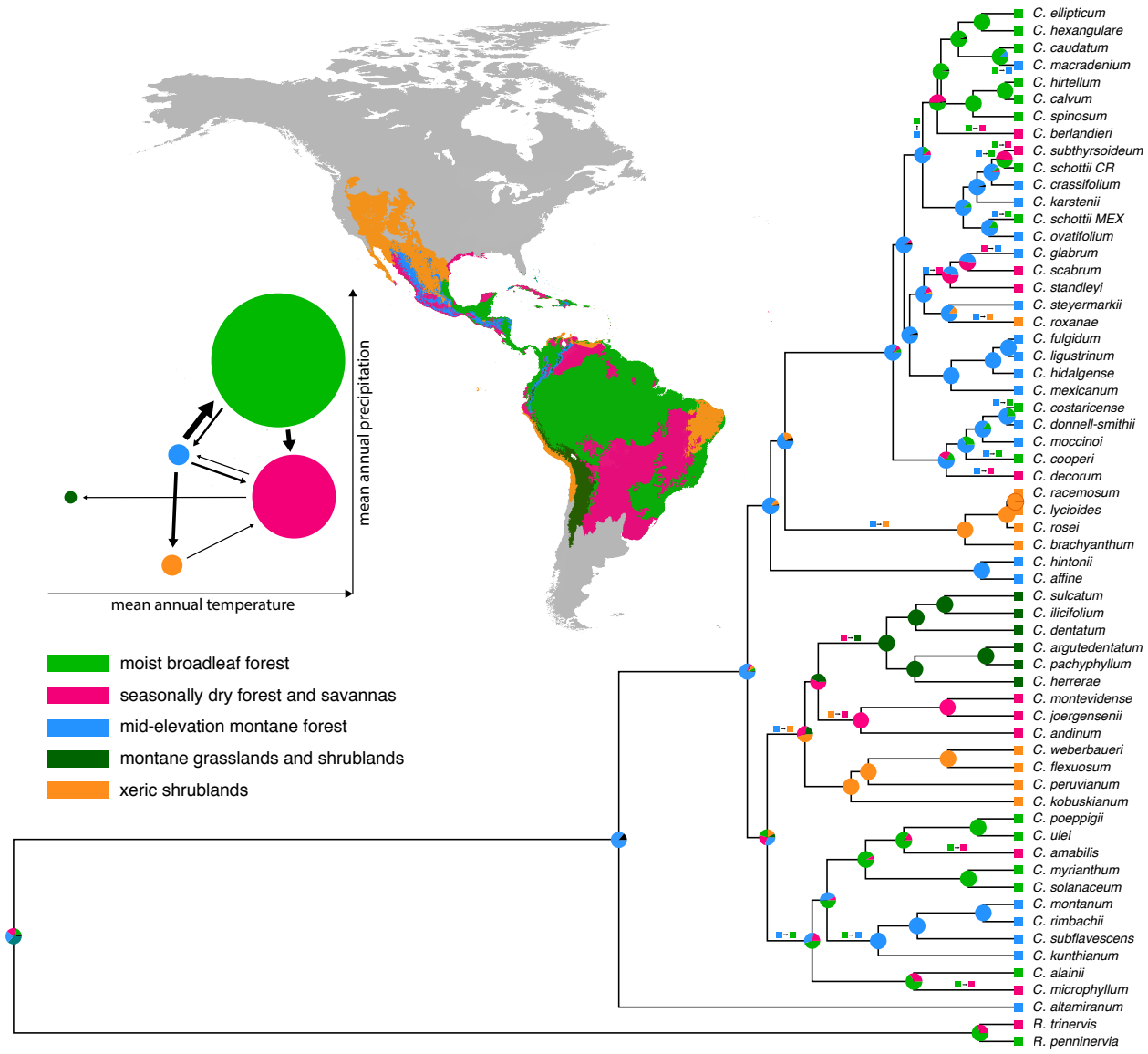
Fig. 2 Multispecies coalescent tree with divergence time estimations from *BEAST and ancestral area reconstructions for geographic area. Bars at nodes indicate error surrounding age estimates. Colored squares at branch tips indicate the current distribution of each species; colors and assignments correspond to the map in the top left corner. Pie charts on nodes display the probability of the reconstructed ancestral biome and indicate locations of dispersal events on the tree.

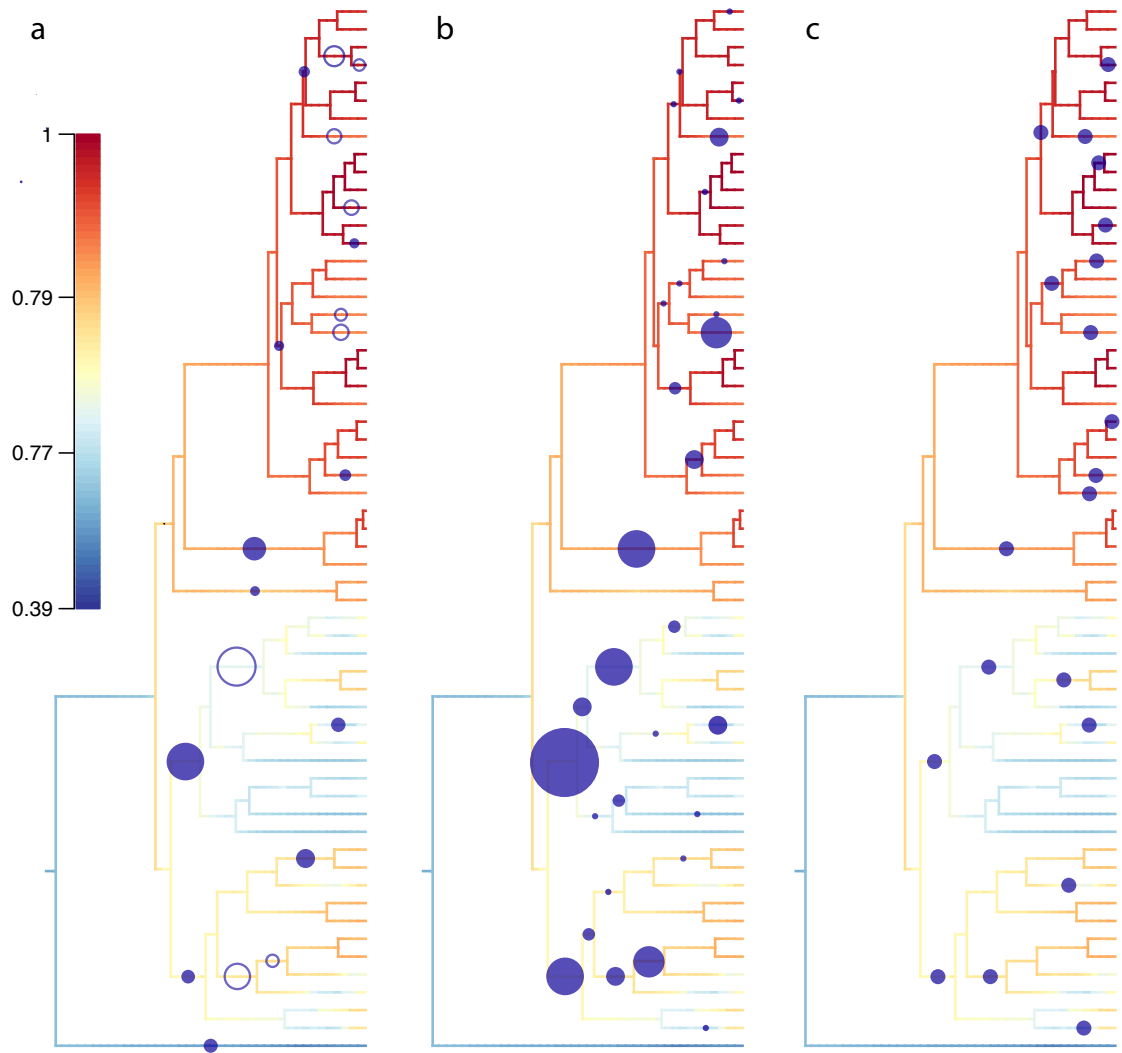
Fig. 3 Biome reconstructions mapped on the MSC tree, trimmed to tribe Citharexyleae. Pie charts on nodes indicate the probability of a given biome at that node. Colors correspond to biome assignments, noted by the legend in the lower left. The map in the center displays the extent of each Neotropical biome in the New World; it does not represent the distribution of *Citharexylum*. The graph on the left provides the relative size of biomes (km²) and relative placement of biomes in relation to annual temperature and annual precipitation. Arrows indicate the direction and number of shifts between biomes; heavier weighted arrows indicate more shifts from one biome to another.

Fig. 4 Niche evolution and diversification rate analysis results. Heated colors on branches represent relative rates inferred from the MEDUSA-like model depicted using quantile breaks to highlight variation between lineages. Circles mapped onto to trees represent: (a) shifts detected in PC scores for PC1 (closed circles) and PC2 (open circles), size represents the posterior probability of the shift; (b) summary results of individual climate variables, size of circles reflects the number of variables that recovered a shift on that branch (smallest circles represent a shift in one variable, the largest circle represents shifts in eleven variables); and (c) locations of shifts inferred in the discrete biome analysis for comparison, the size of the circles is arbitrary.









SUPPLEMENTARY FIGURES

Fig. S1. bayou output for analysis of PC1 scores (posterior probability cutoff = 0.##) including plots for (a) phylogenetic tree with posterior probabilities from the bayouMCMC chain (b) heat map of reconstructed parameter values on phylogeny (c) phenogram and posterior density for optima values (d) topology of input phylogeny.

Fig. S2. bayou output for analysis of PC2 scores (posterior probability cutoff = 0.12) including plots for (a) phylogenetic tree with posterior probabilities from the bayouMCMC chain (b) heat map of reconstructed parameter values on phylogeny (c) phenogram and posterior density for optima values (d) topology of input phylogeny.

Fig. S3. bayou output for analysis of mean annual temperature (WorldClim BioClim variable Bio 1; posterior probability cutoff = 0.1) including plots for (a) phylogenetic tree with posterior probabilities from the bayouMCMC chain (b) heat map of reconstructed parameter values on phylogeny (c) phenogram and posterior density for optima values (d) topology of input phylogeny.

Fig. S4. bayou output for analysis of mean diurnal range (WorldClim BioClim variable Bio 2; posterior probability cutoff = 0.14) including plots for (a) phylogenetic tree with posterior probabilities from the bayouMCMC chain (b) heat map of reconstructed parameter values on phylogeny (c) phenogram and posterior density for optima values (d) topology of input phylogeny.

Fig. S5. bayou output for analysis of isothermality (WorldClim BioClim variable Bio 3; posterior probability cutoff = 0.2) including plots for (a) phylogenetic tree with posterior probabilities from the bayouMCMC chain (b) heat map of reconstructed parameter values on phylogeny (c) phenogram and posterior density for optima values (d) topology of input phylogeny.

Fig. S6. bayou output for analysis of temperature seasonality (WorldClim BioClim variable Bio 4; posterior probability cutoff = 0.3) including plots for (a) phylogenetic tree with posterior probabilities from the bayouMCMC chain (b) heat map of reconstructed parameter values on

phylogeny (c) phenogram and posterior density for optima values (d) topology of input phylogeny.

Fig. S7. bayou output for analysis of maximum temperature of warmest month (WorldClim BioClim variable Bio 5; posterior probability cutoff = 0.2) including plots for (a) phylogenetic tree with posterior probabilities from the bayouMCMC chain (b) heat map of reconstructed parameter values on phylogeny (c) phenogram and posterior density for optima values (d) topology of input phylogeny.

Fig. S8. bayou output for analysis of minimum temperature of coldest month (WorldClim BioClim variable Bio 6; posterior probability cutoff = 0.11) including plots for (a) phylogenetic tree with posterior probabilities from the bayouMCMC chain (b) heat map of reconstructed parameter values on phylogeny (c) phenogram and posterior density for optima values (d) topology of input phylogeny.

Fig. S9. bayou output for analysis of annual temperature range (WorldClim BioClim variable Bio 7; posterior probability cutoff = 0.12) including plots for (a) phylogenetic tree with posterior probabilities from the bayouMCMC chain (b) heat map of reconstructed parameter values on phylogeny (c) phenogram and posterior density for optima values (d) topology of input phylogeny.

Fig. S10. bayou output for analysis of mean temperature of wettest quarter (WorldClim BioClim variable Bio 8; posterior probability cutoff = 0.15) including plots for (a) phylogenetic tree with posterior probabilities from the bayouMCMC chain (b) heat map of reconstructed parameter values on phylogeny (c) phenogram and posterior density for optima values (d) topology of input phylogeny.

Fig. S11. bayou output for analysis of mean temperature of driest quarter (WorldClim BioClim variable Bio 9; posterior probability cutoff = 0.12) including plots for (a) phylogenetic tree with posterior probabilities from the bayouMCMC chain (b) heat map of reconstructed parameter values on phylogeny (c) phenogram and posterior density for optima values (d) topology of input phylogeny.

Fig. S12. bayou output for analysis of mean temperature of warmest quarter (WorldClim BioClim variable Bio 10; posterior probability cutoff = 0.2) including plots for (a) phylogenetic tree with posterior probabilities from the bayouMCMC chain (b) heat map of reconstructed parameter values on phylogeny (c) phenogram and posterior density for optima values (d) topology of input phylogeny.

Fig. S13. bayou output for analysis of mean temperature of coldest quarter (WorldClim BioClim variable Bio 11; posterior probability cutoff = 0.13) including plots for (a) phylogenetic tree with posterior probabilities from the bayouMCMC chain (b) heat map of reconstructed parameter values on phylogeny (c) phenogram and posterior density for optima values (d) topology of input phylogeny.

Fig. S14. bayou output for analysis of mean annual precipitation (WorldClim BioClim variable Bio 12; posterior probability cutoff = 0.15) including plots for (a) phylogenetic tree with posterior probabilities from the bayouMCMC chain (b) heat map of reconstructed parameter values on phylogeny (c) phenogram and posterior density for optima values (d) topology of input phylogeny.

Fig. S15. bayou output for analysis of precipitation of wettest month (WorldClim BioClim variable Bio 13; posterior probability cutoff = 0.14) including plots for (a) phylogenetic tree with posterior probabilities from the bayouMCMC chain (b) heat map of reconstructed parameter values on phylogeny (c) phenogram and posterior density for optima values (d) topology of input phylogeny.

Fig. S16. bayou output for analysis of precipitation of driest month (WorldClim BioClim variable Bio 14; posterior probability cutoff = 0.3) including plots for (a) phylogenetic tree with posterior probabilities from the bayouMCMC chain (b) heat map of reconstructed parameter values on phylogeny (c) phenogram and posterior density for optima values (d) topology of input phylogeny.

Fig. S17. bayou output for analysis of precipitation seasonality (WorldClim BioClim variable Bio 15; posterior probability cutoff = 0.2) including plots for (a) phylogenetic tree with posterior

probabilities from the bayouMCMC chain (b) heat map of reconstructed parameter values on phylogeny (c) phenogram and posterior density for optima values (d) topology of input phylogeny.

Fig. S18. bayou output for analysis of precipitation of wettest quarter (WorldClim BioClim variable Bio 16; posterior probability cutoff = 0.13) including plots for (a) phylogenetic tree with posterior probabilities from the bayouMCMC chain (b) heat map of reconstructed parameter values on phylogeny (c) phenogram and posterior density for optima values (d) topology of input phylogeny.

Fig. S19. bayou output for analysis of precipitation of driest quarter (WorldClim BioClim variable Bio 17; posterior probability cutoff = 0.3) including plots for (a) phylogenetic tree with posterior probabilities from the bayouMCMC chain (b) heat map of reconstructed parameter values on phylogeny (c) phenogram and posterior density for optima values (d) topology of input phylogeny.

Fig. S20. bayou output for analysis of precipitation of warmest quarter (WorldClim BioClim variable Bio 18; posterior probability cutoff = 0.2) including plots for (a) phylogenetic tree with posterior probabilities from the bayouMCMC chain (b) heat map of reconstructed parameter values on phylogeny (c) phenogram and posterior density for optima values (d) topology of input phylogeny.

Fig. S21. bayou output for analysis of precipitation of coldest quarter (WorldClim BioClim variable Bio 19; posterior probability cutoff = 0.18) including plots for (a) phylogenetic tree with posterior probabilities from the bayouMCMC chain (b) heat map of reconstructed parameter values on phylogeny (c) phenogram and posterior density for optima values (d) topology of input phylogeny.

Fig. S22. 95% confidence set of diversification rate shift configurations inferred in BAMM using the default model.

Fig. S23. 95% confidence set of diversification rate shift configurations inferred in BAMM using the MEDUSA-like model.

Fig. S1. PC1

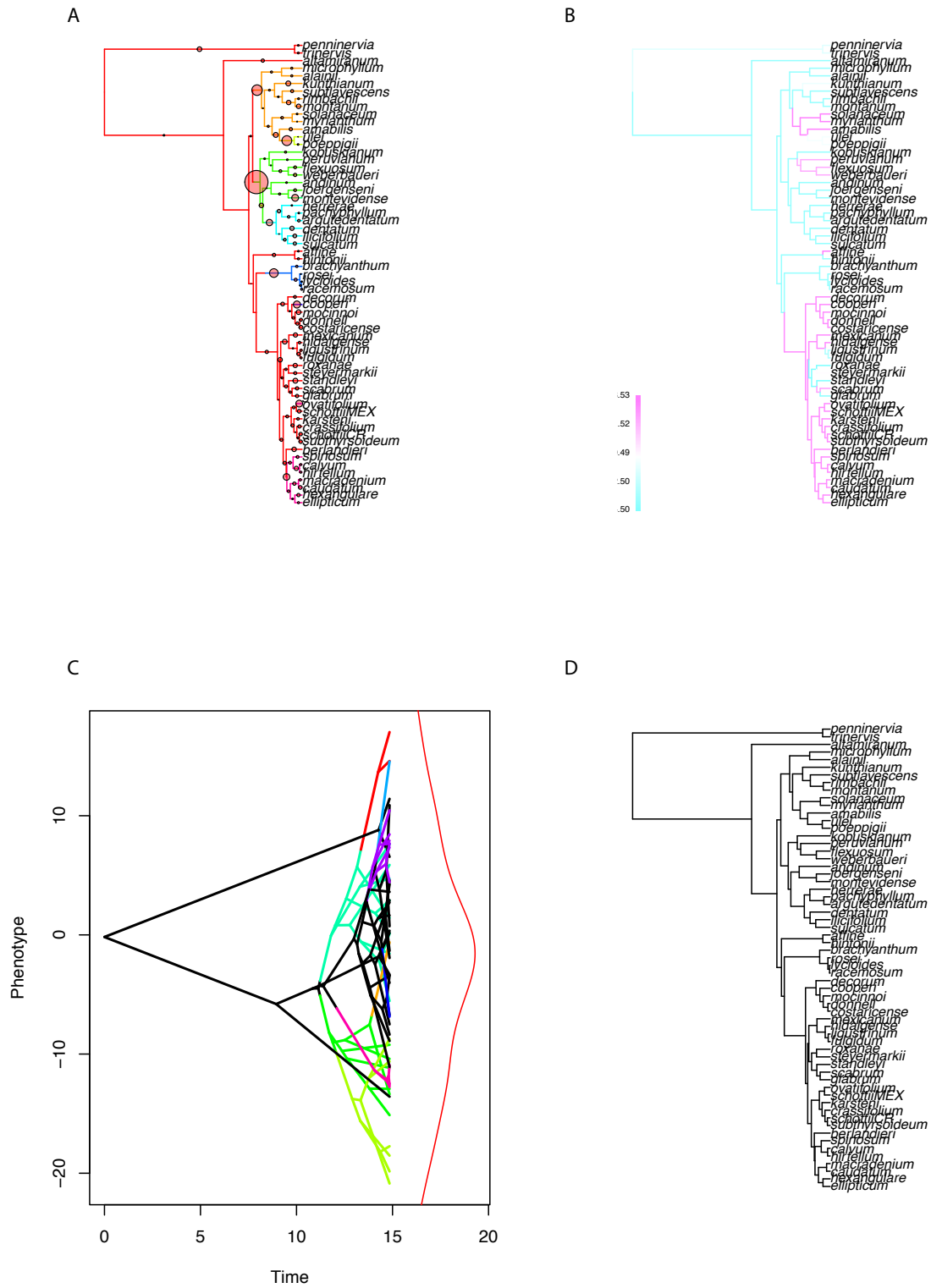


Fig. S2. PC2

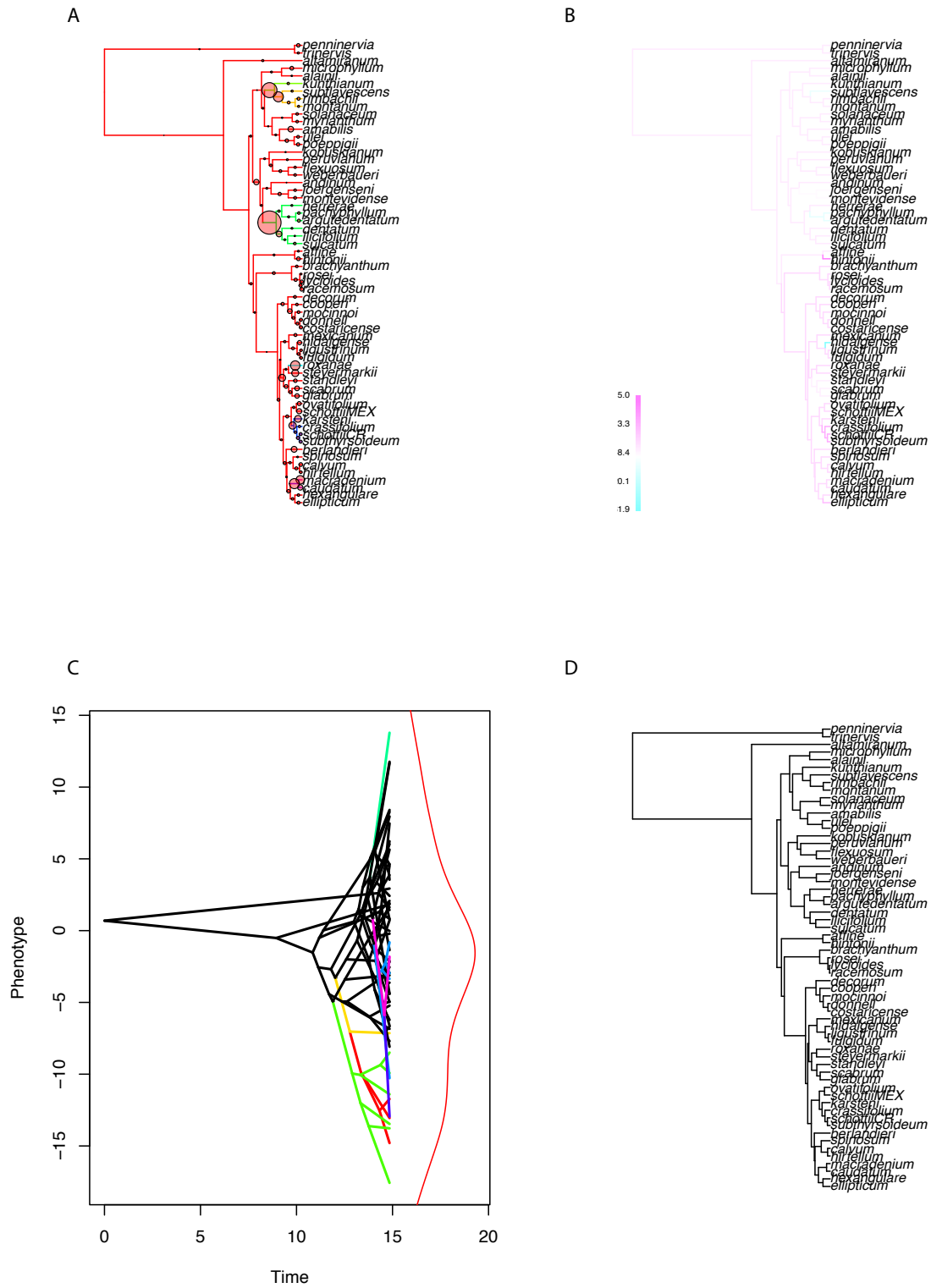


Fig. S3. Bio 1: mean annual temperature

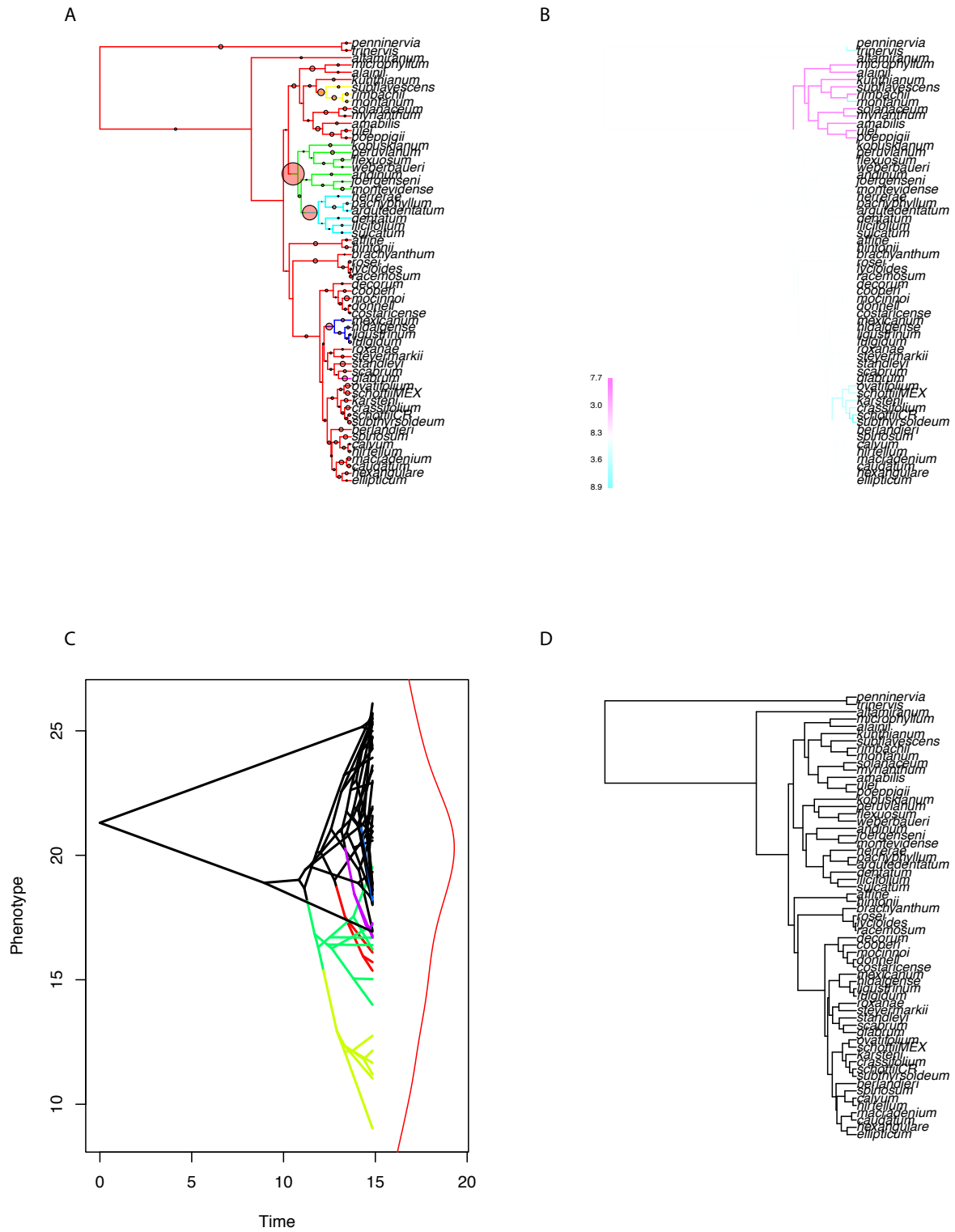


Fig. S4. Bio 2: mean diurnal range

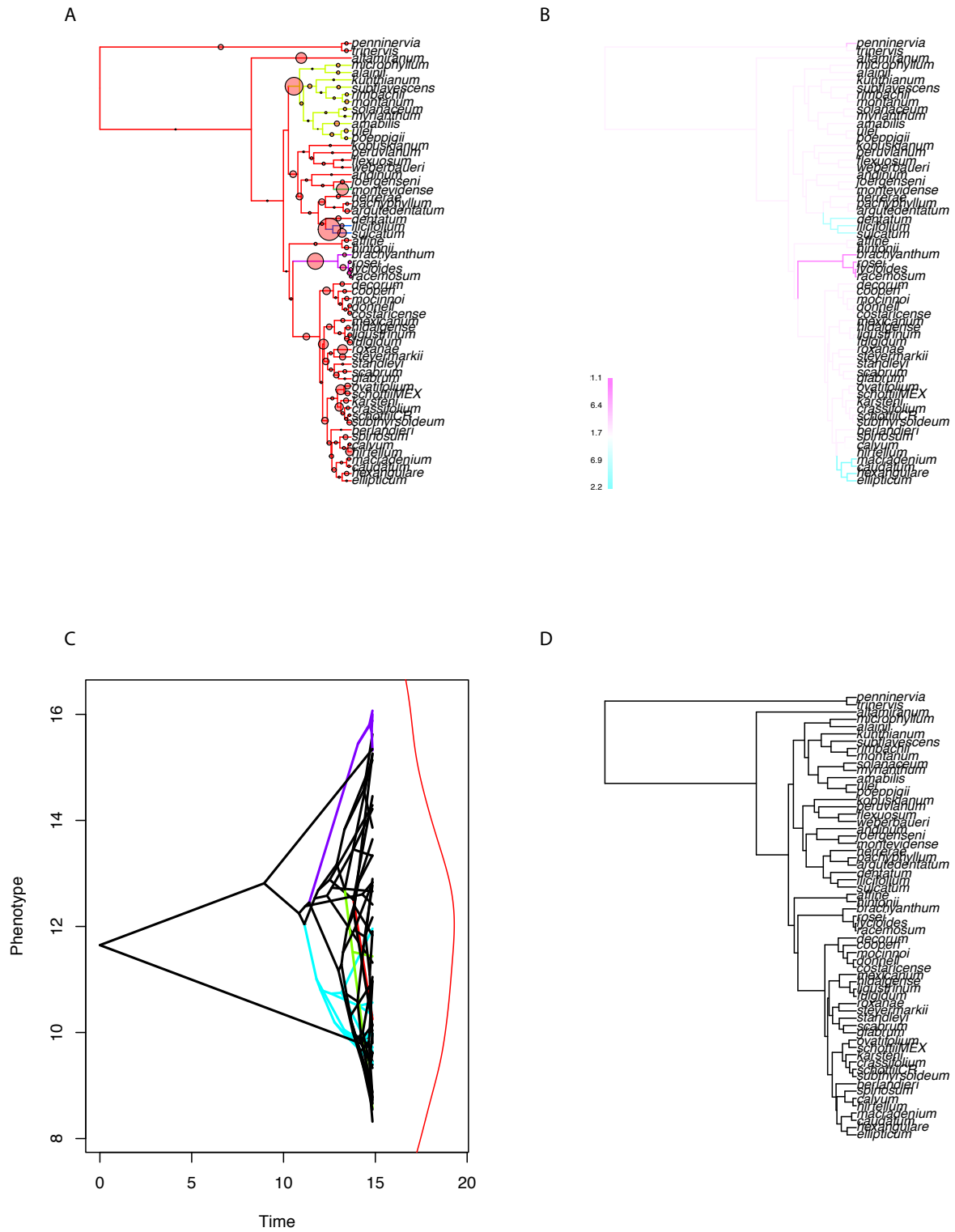


Fig. S5. Bio 3: isothermality

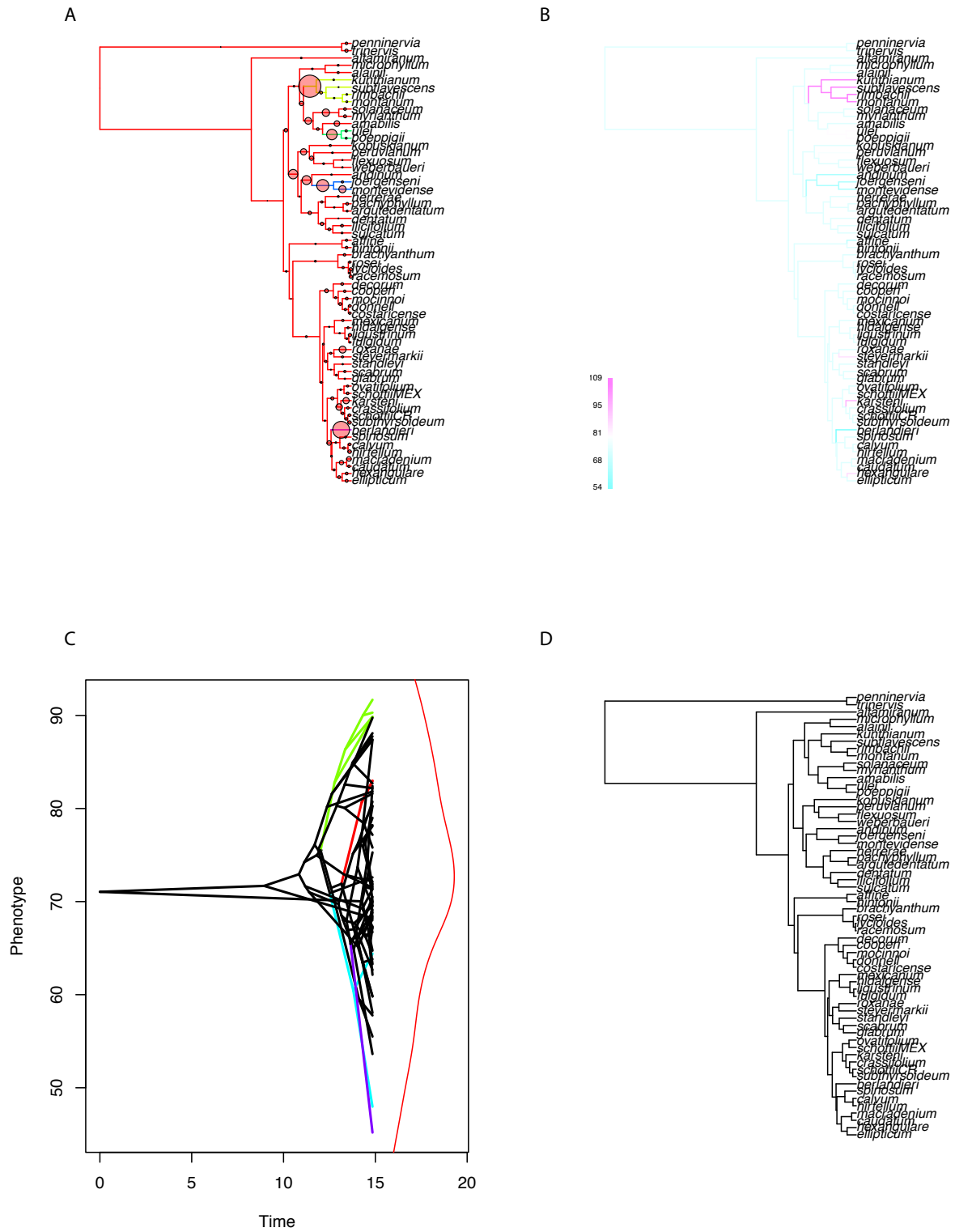


Fig. S6. Bio 4: temperature seasonality

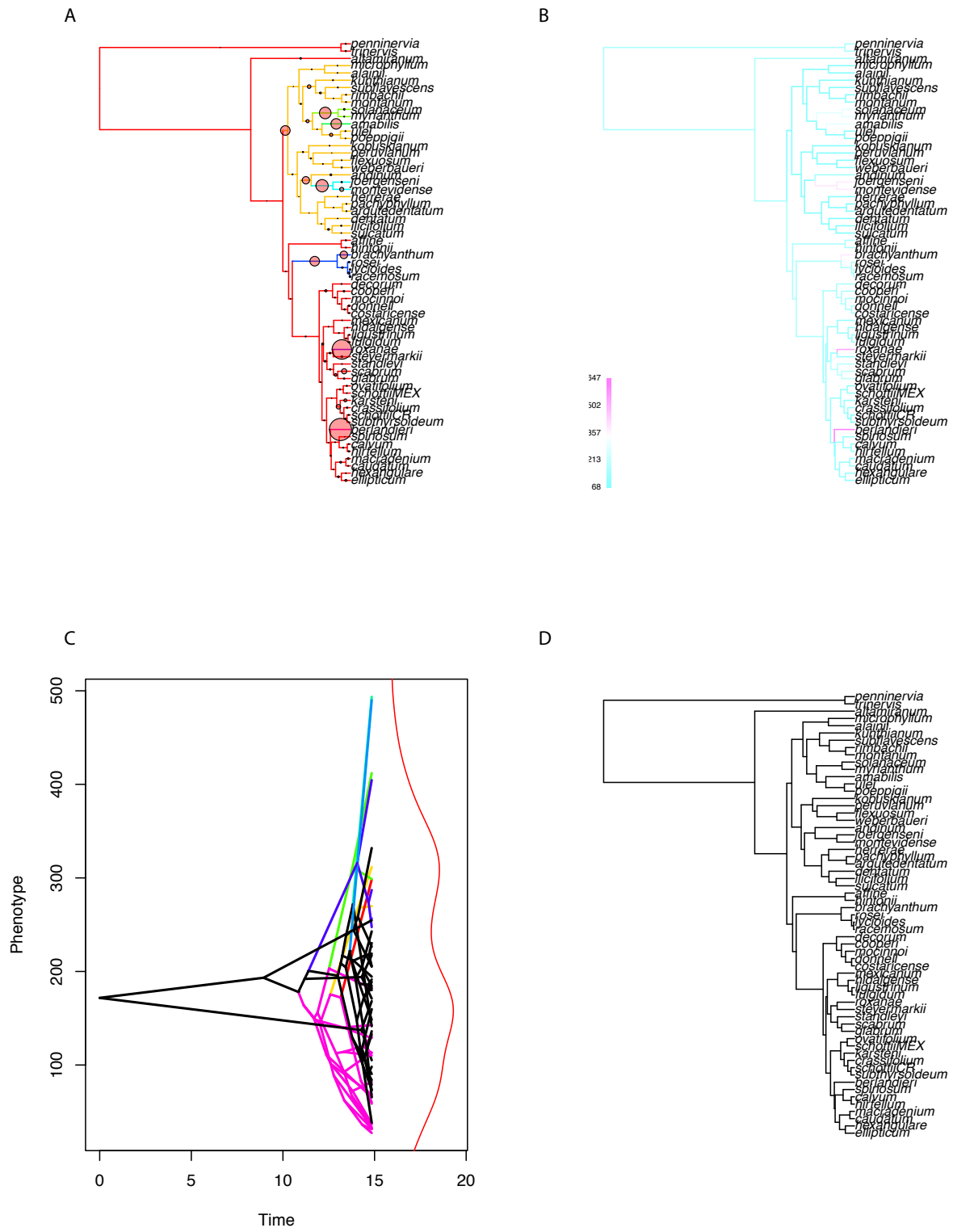


Fig. S7. Bio 5: maximum temperature of warmest month

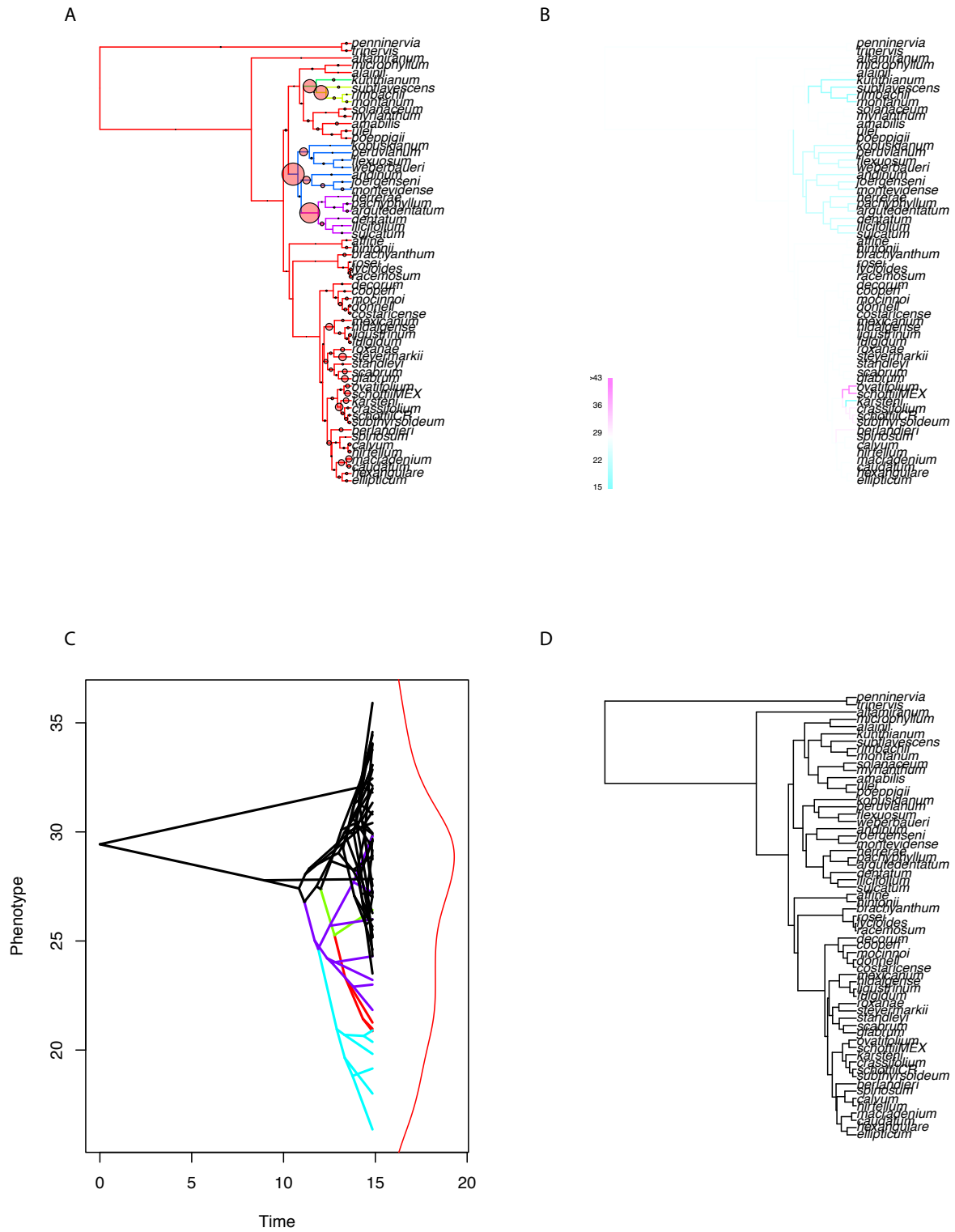


Fig. S9. Bio 7: temperature annual range

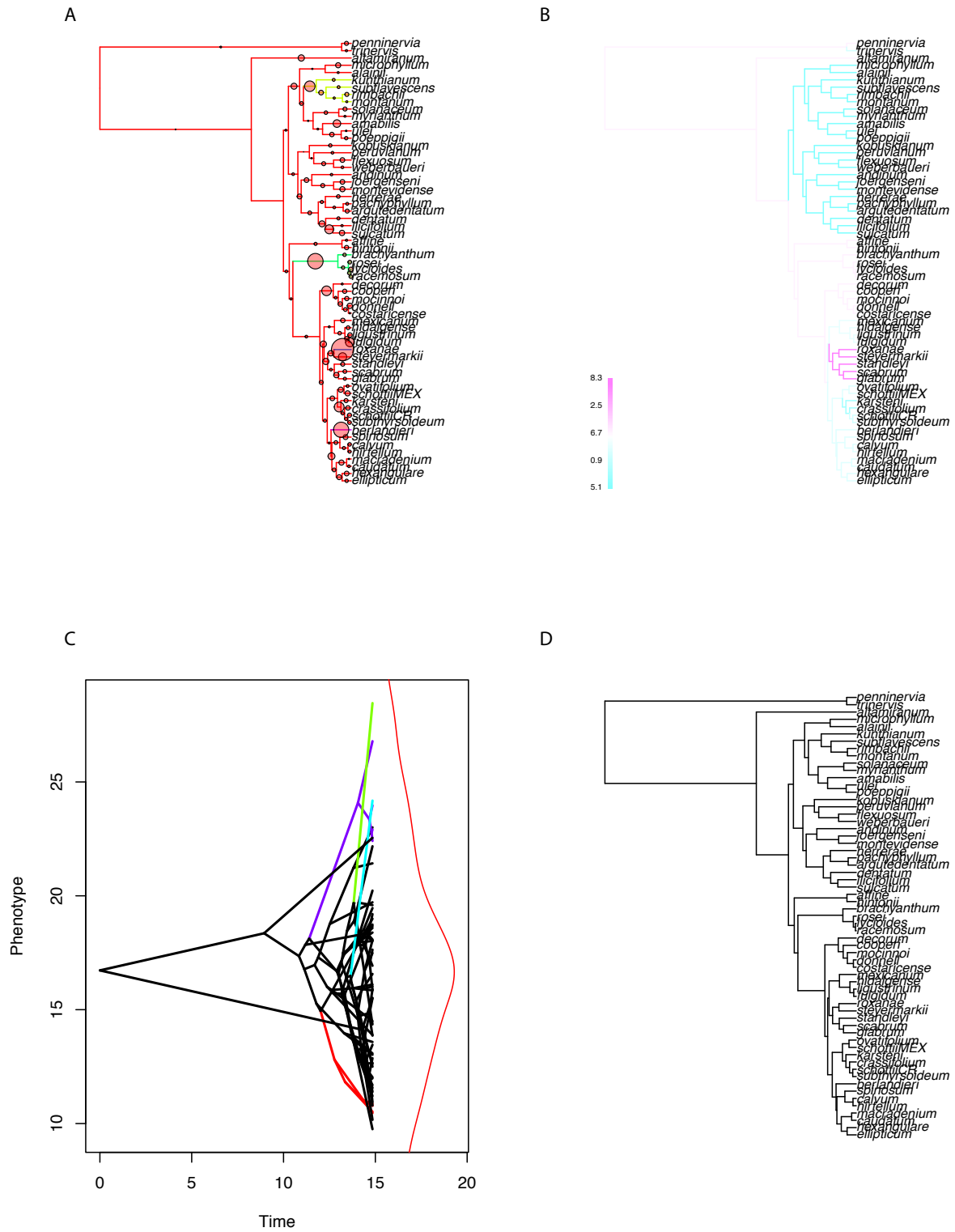


Fig. S10. Bio 8: mean temperature of wettest quarter

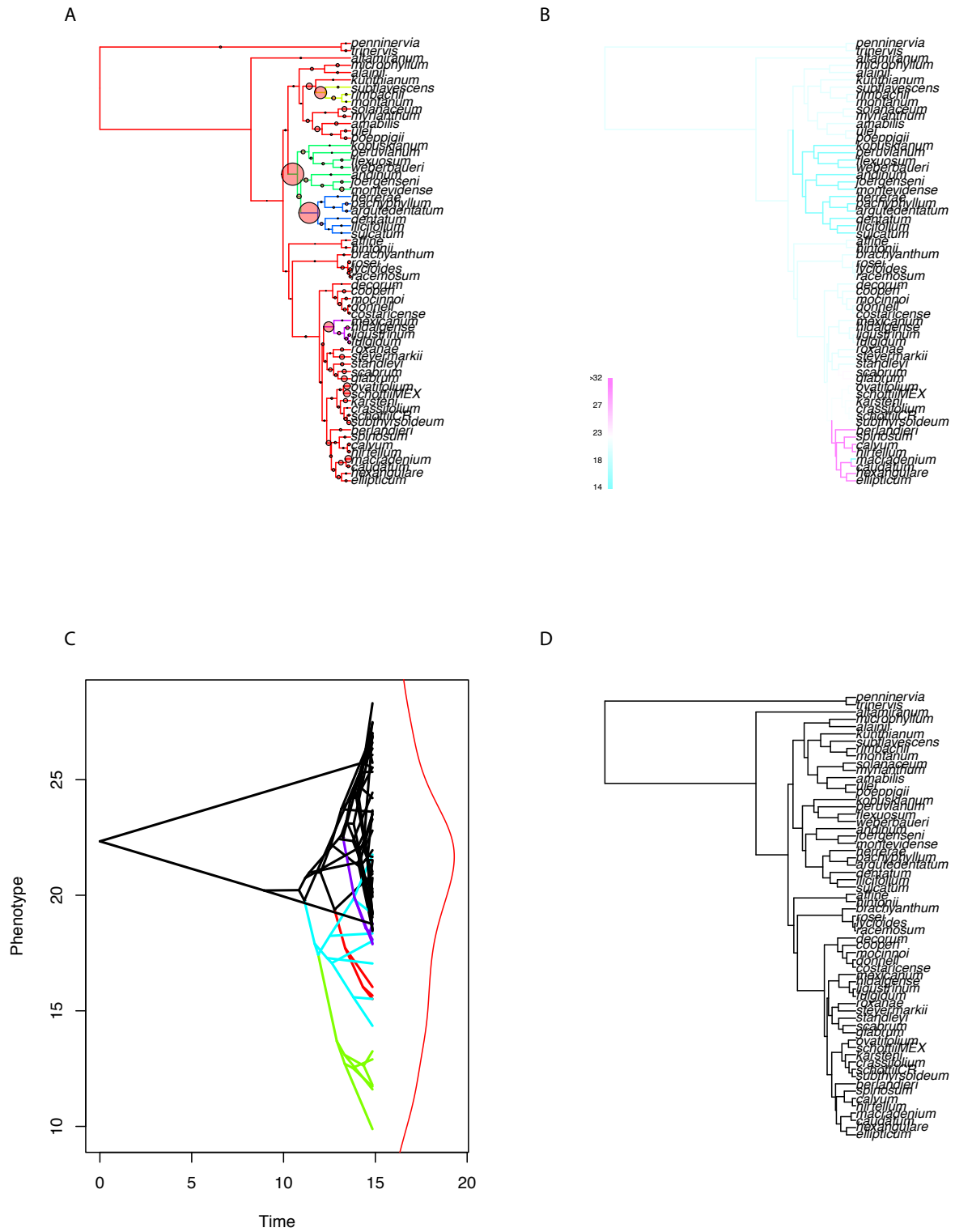


Fig. S11. Bio 9: mean temperature of driest quarter

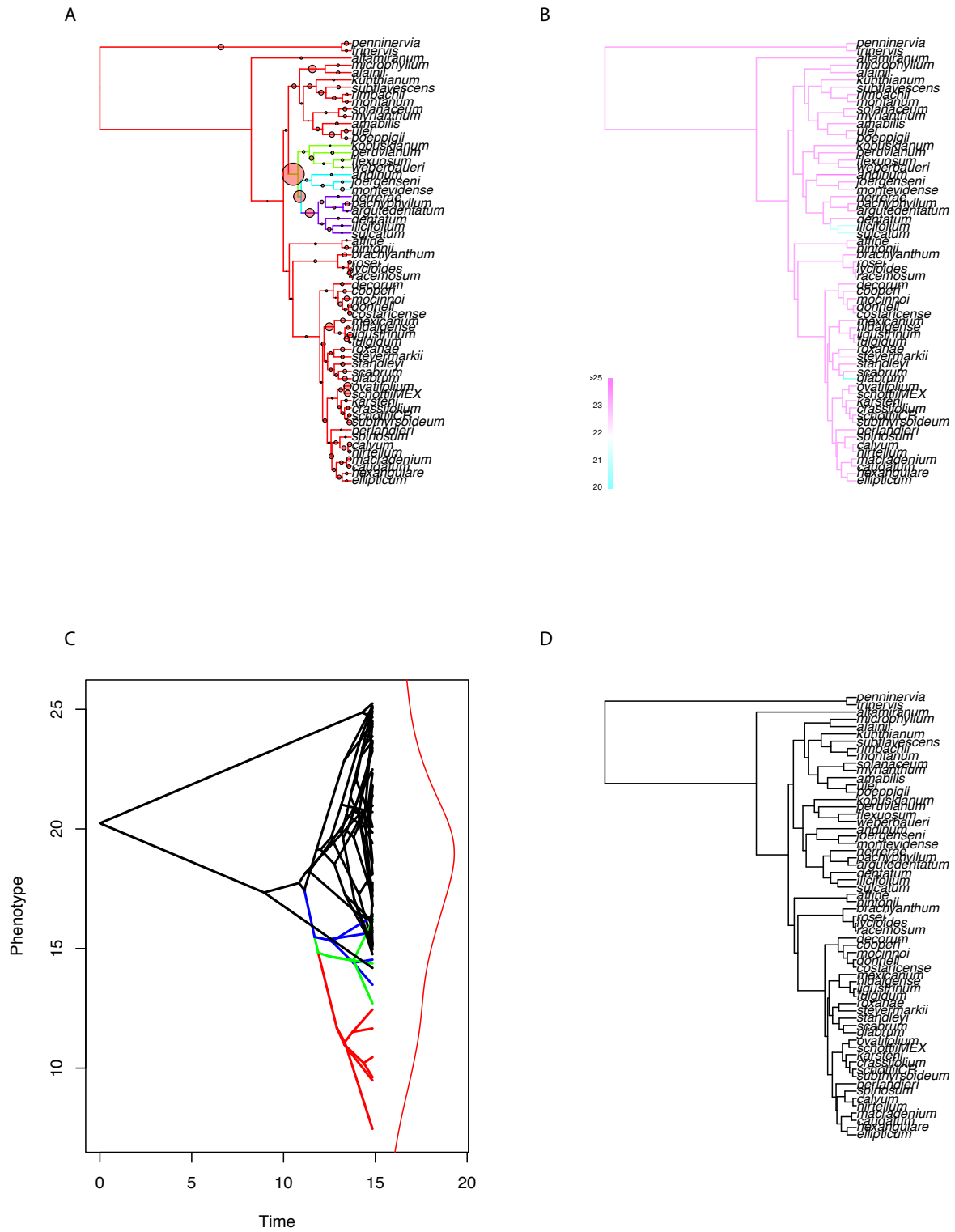


Fig. S12. Bio 10: mean temperature of warmest quarter

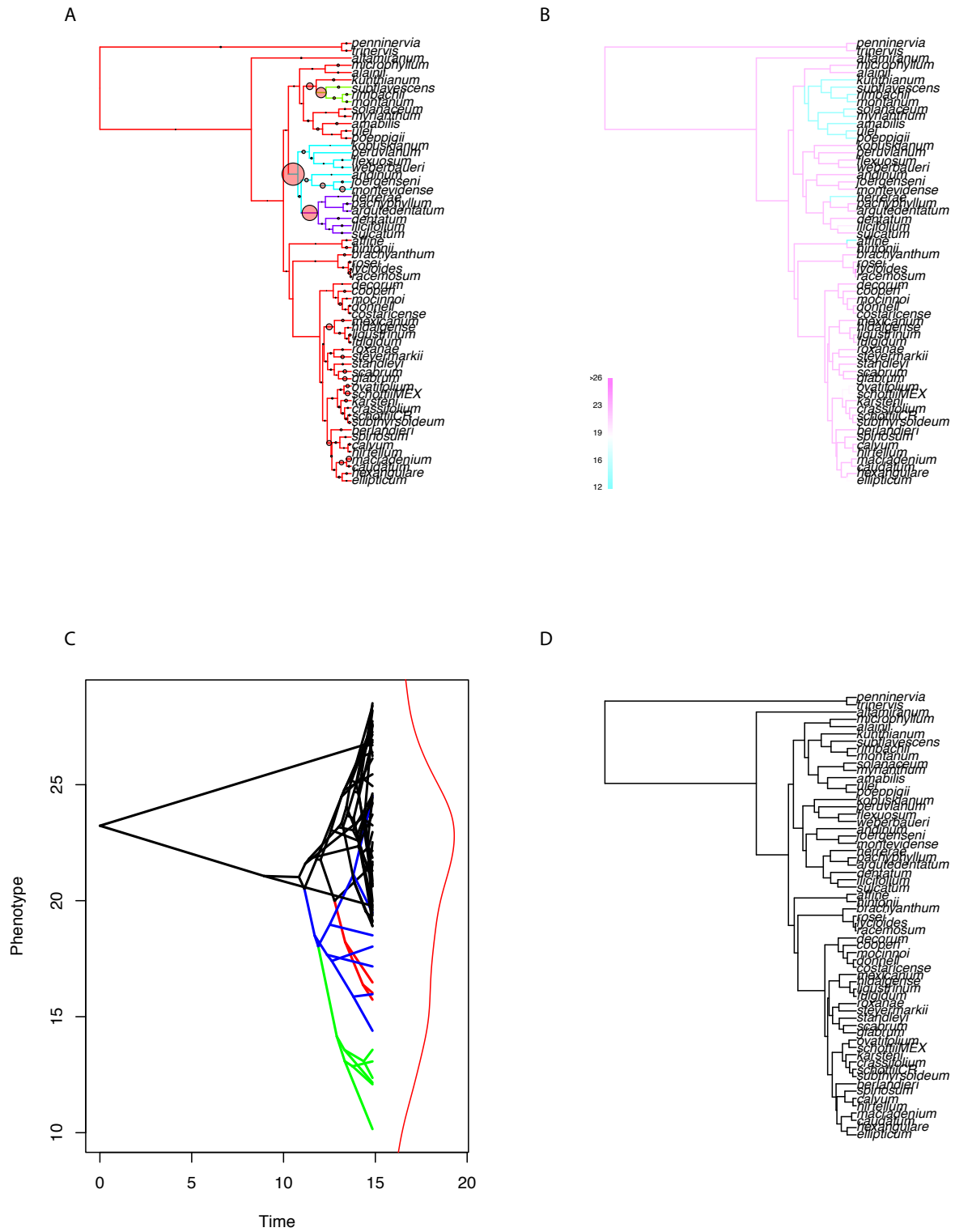


Fig. S13. Bio 11: mean temperature of coldest quarter

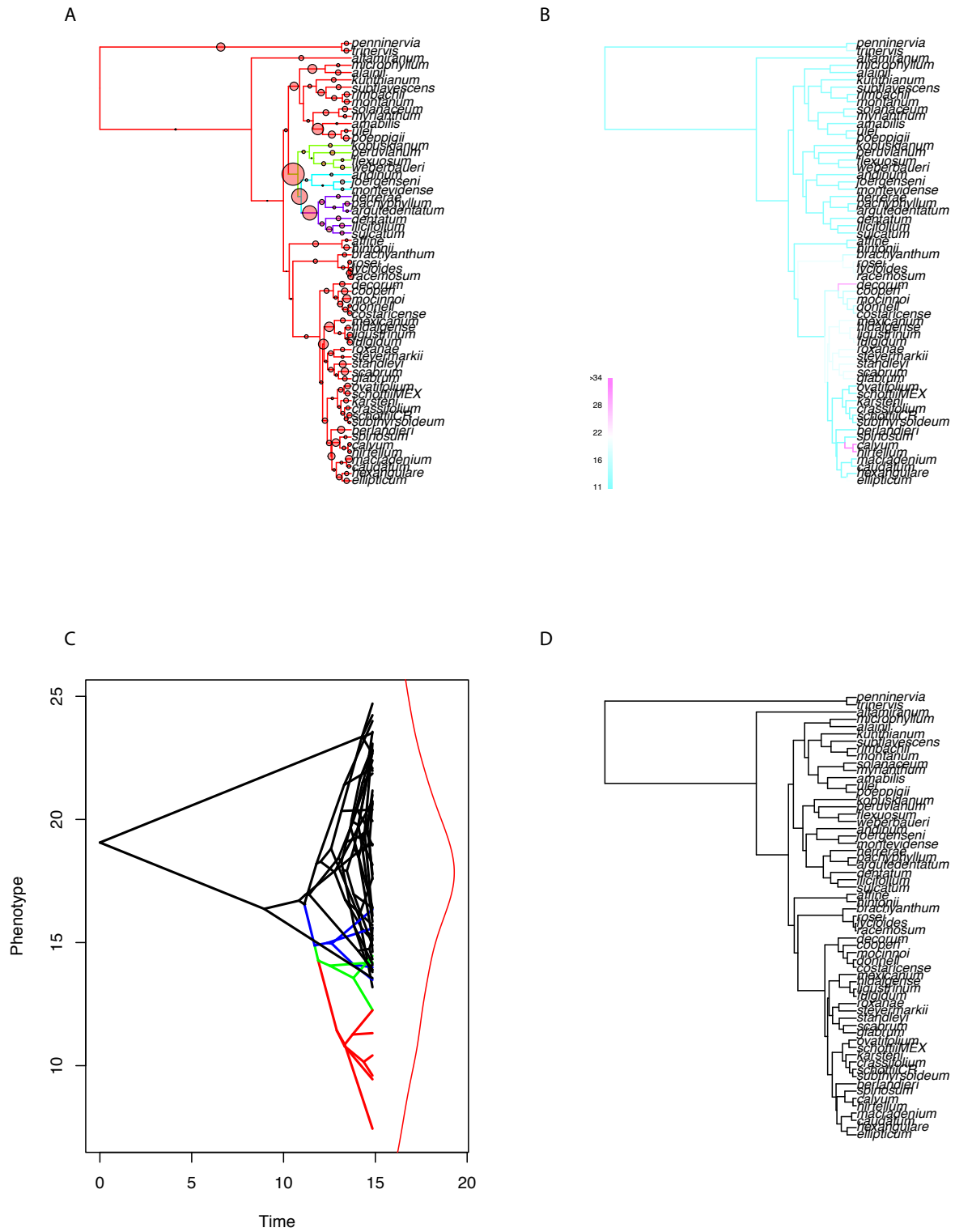


Fig. S15. Bio 13: precipitation of wettest month

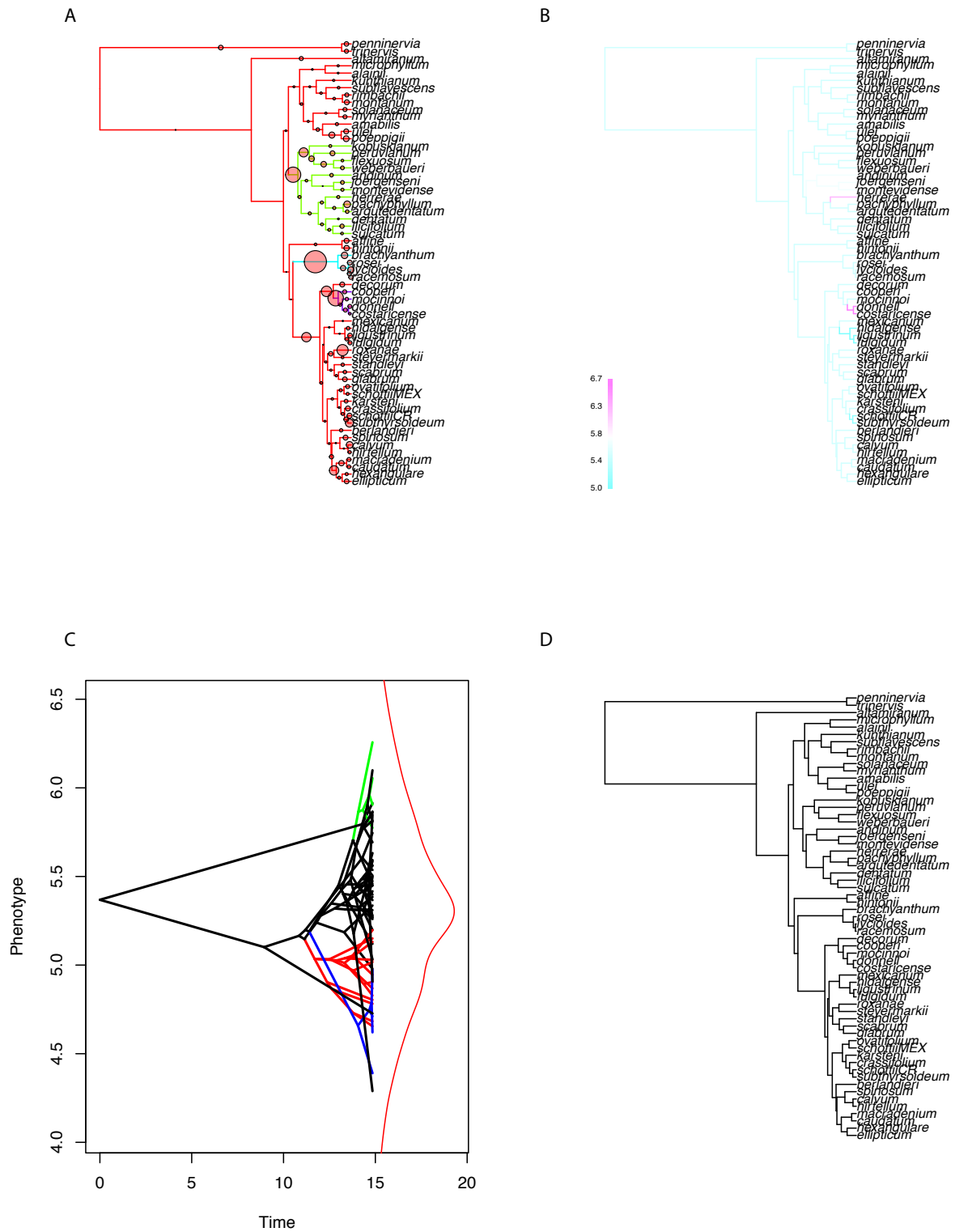


Fig. S16. Bio 14: precipitation of driest month

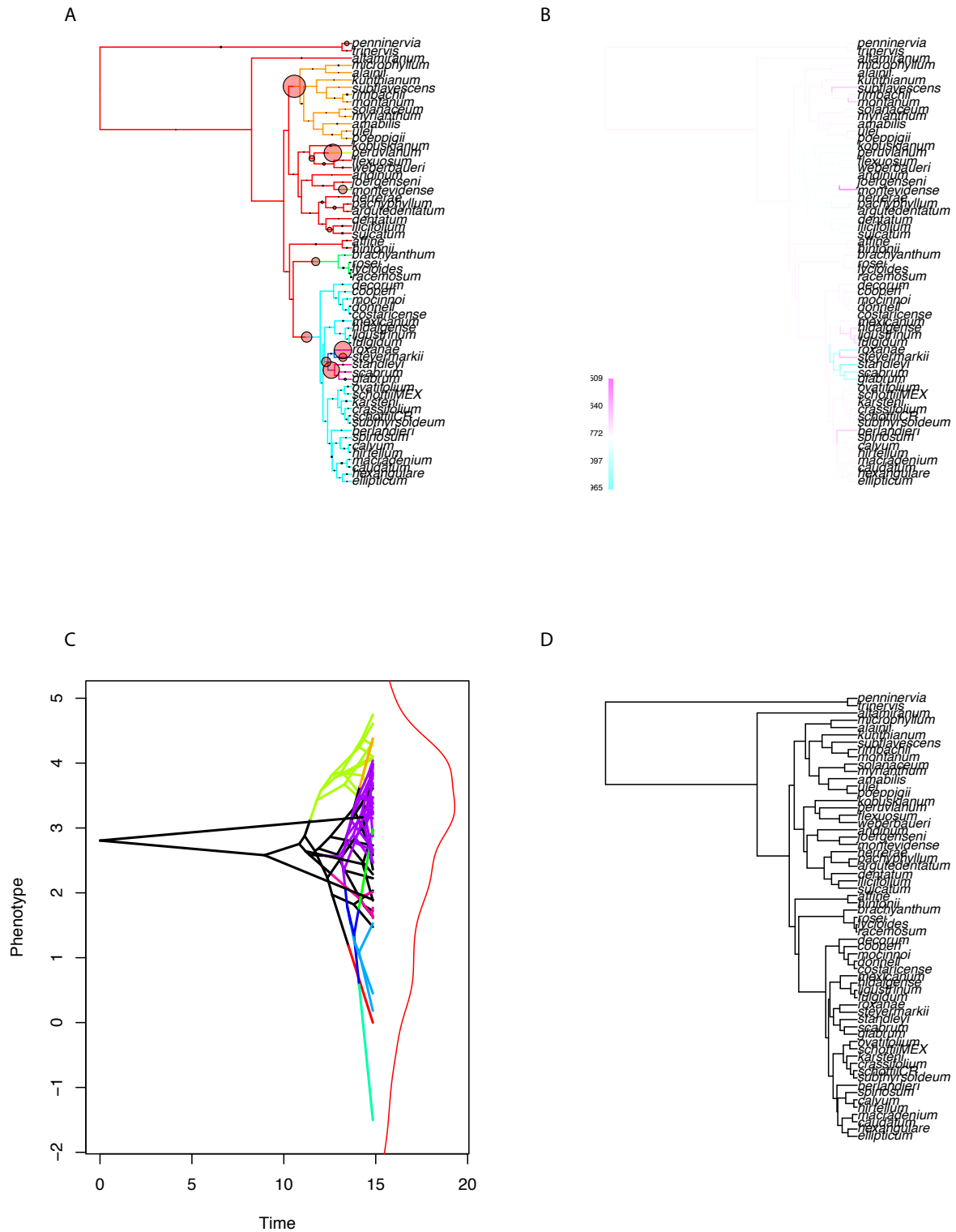


Fig. S17. Bio 15: precipitation seasonality

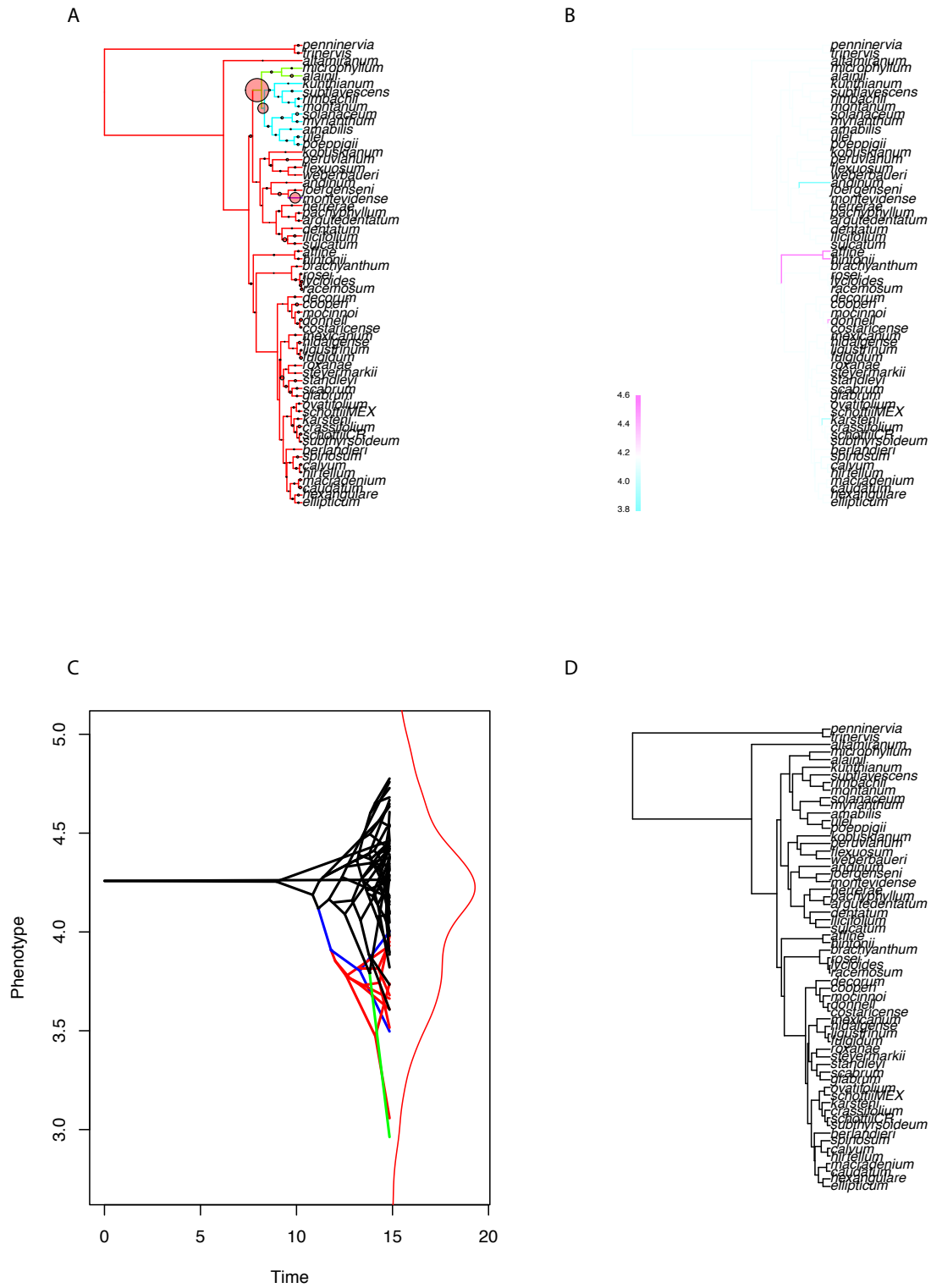


Fig. S19. Bio 17: precipitation of driest quarter

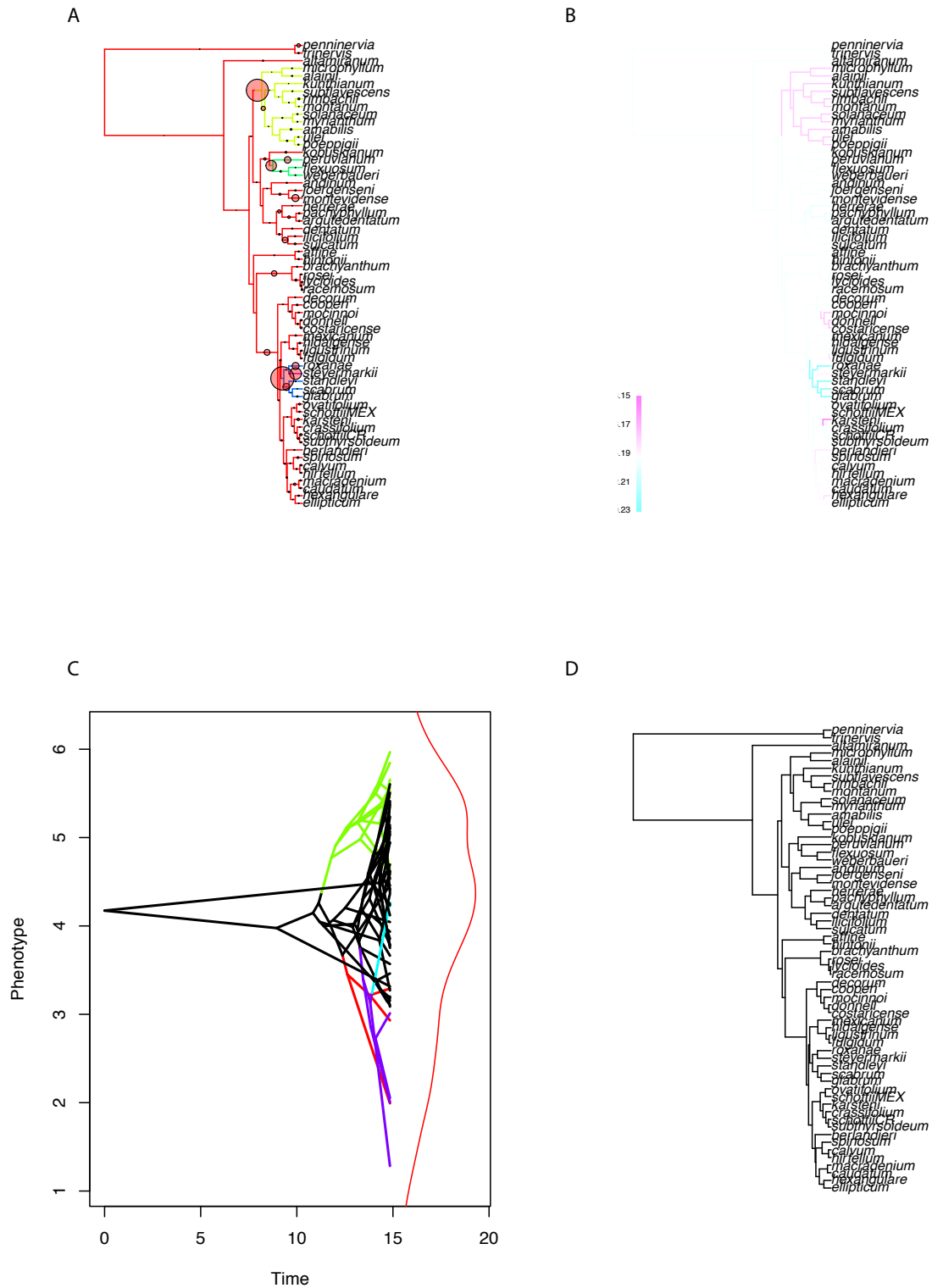


Fig. S20. Bio 18: precipitation of warmest quarter

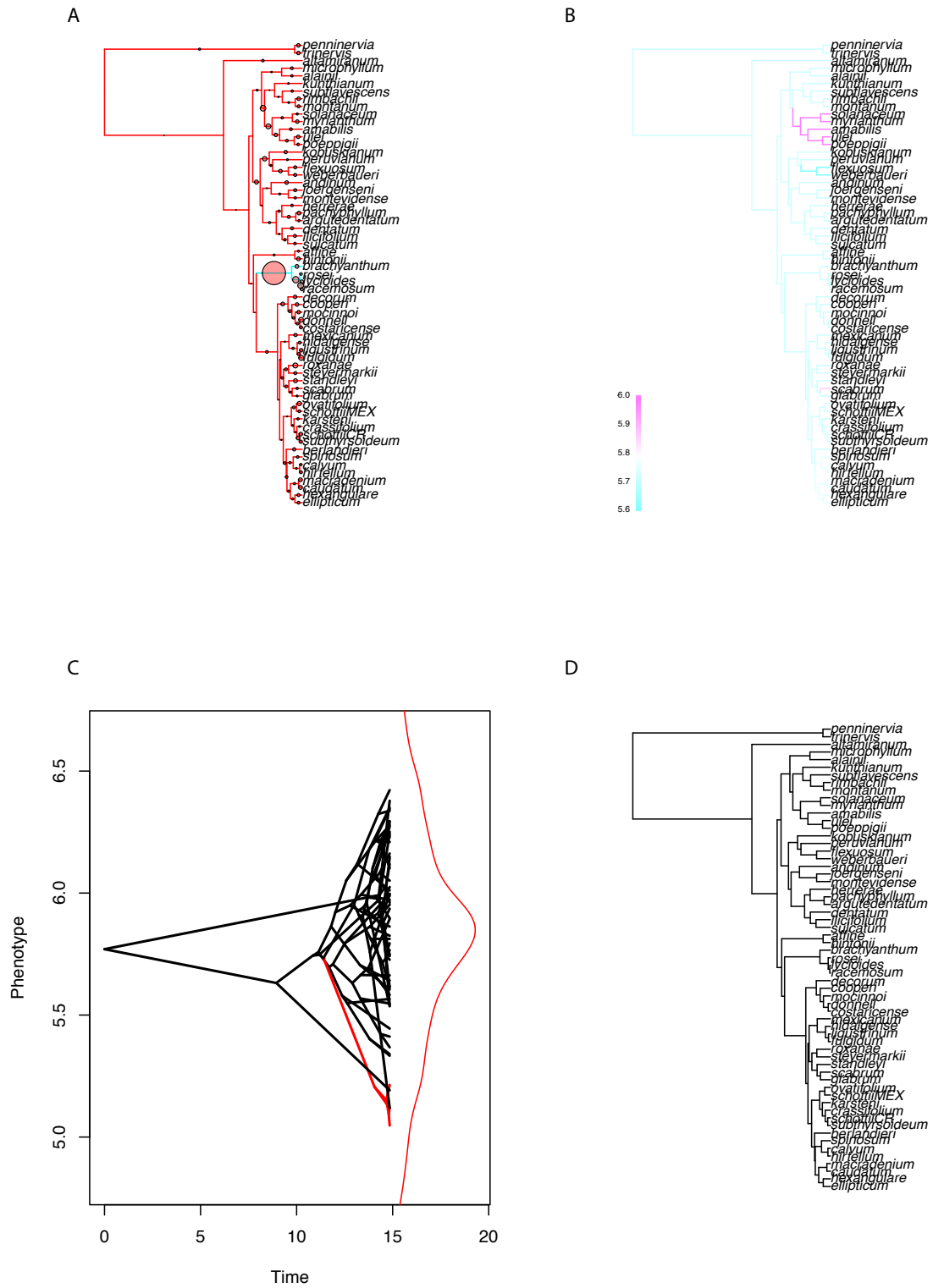


Fig. S22. 95% confidence set of diversification rate shift configurations inferred in BAMM using the default model.

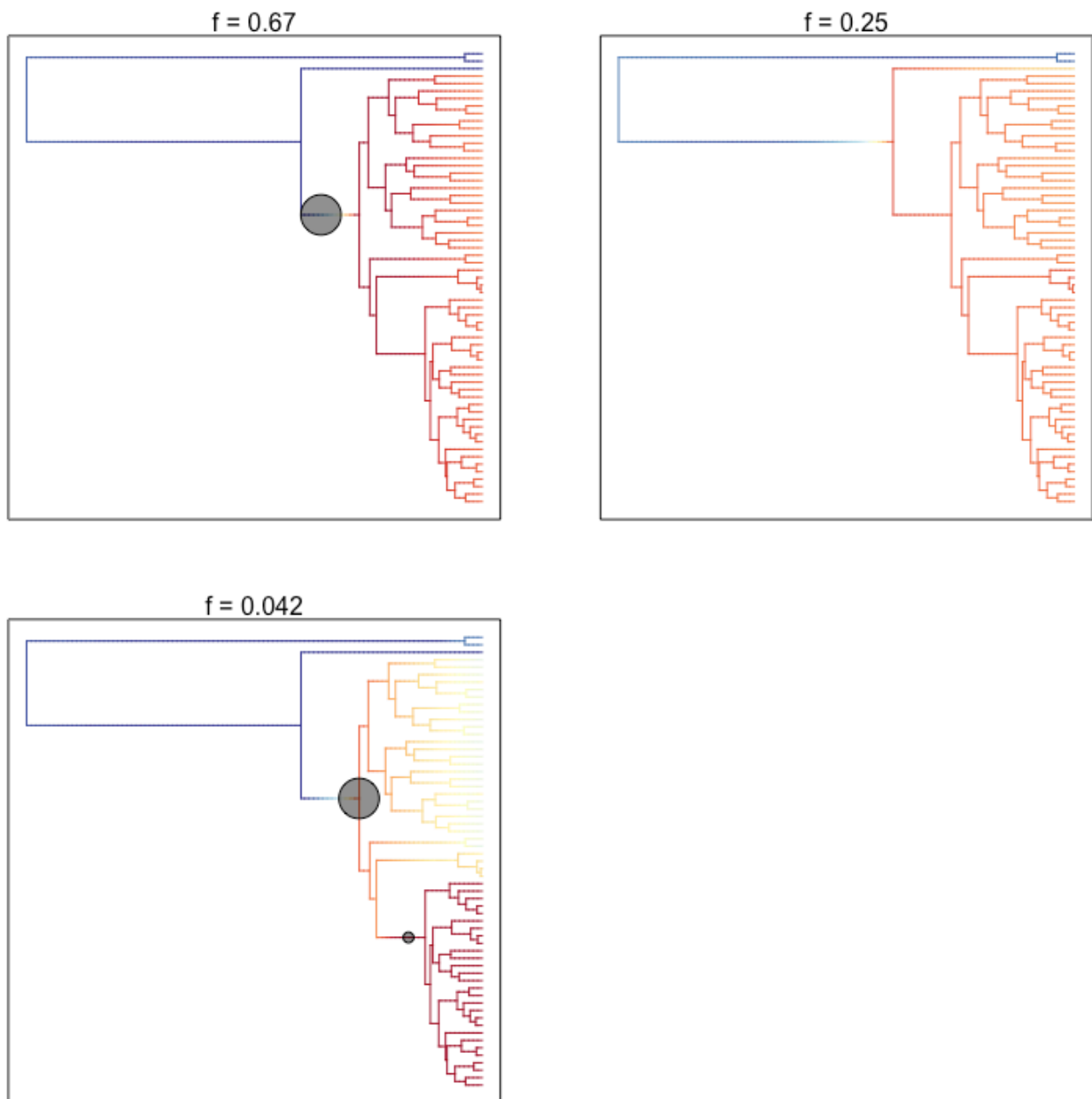
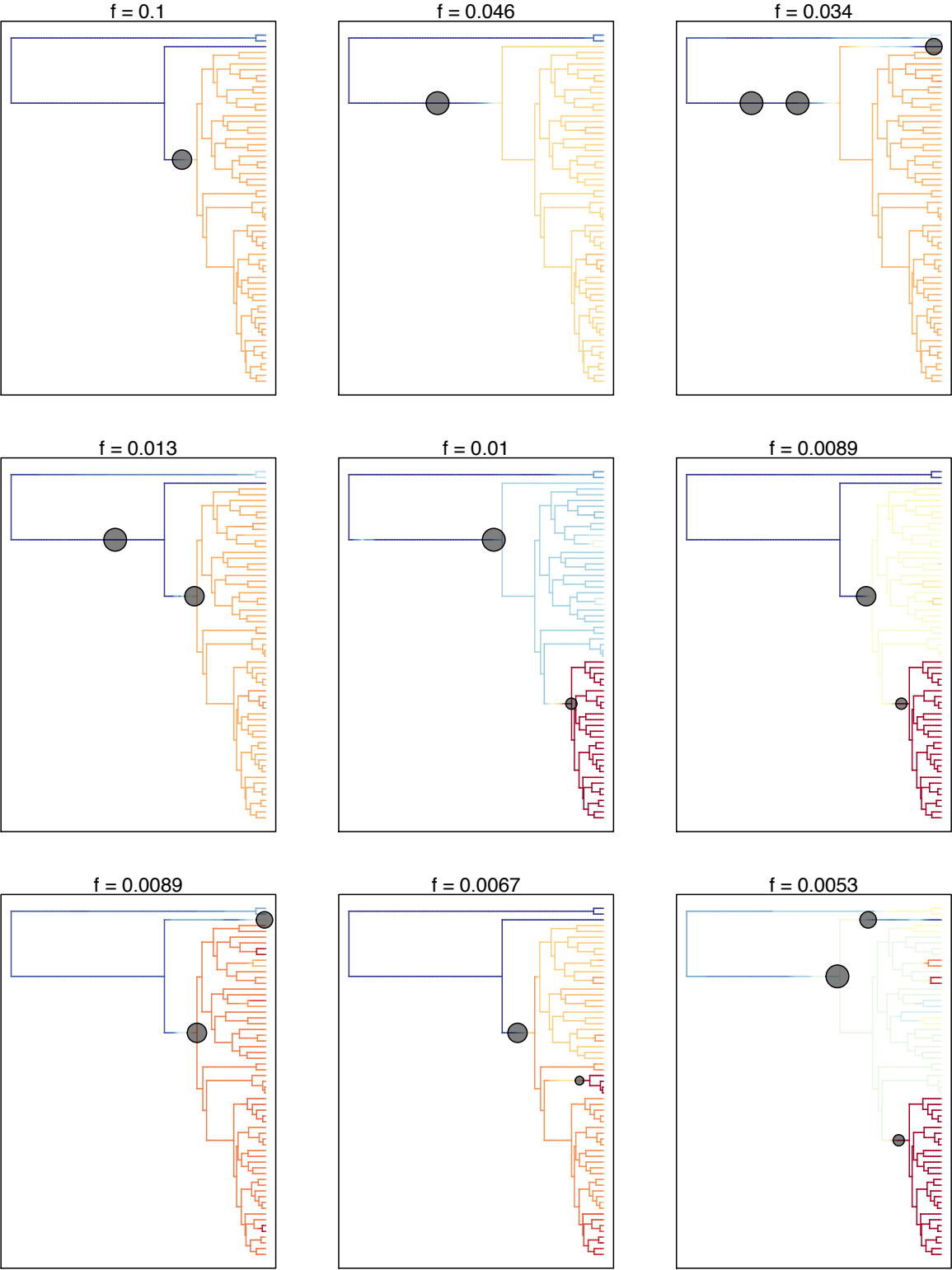


Fig. S23. 95% confidence set of diversification rate shift configurations inferred in BAMM using the MEDUSA-like model.



CHAPTER 3:

An updated phylogeny of Verbenaceae

ABSTRACT

- Premise of the study: Verbenaceae is family of ca. 770 species broadly distributed in the New World and with limited representation in Africa and Europe. The family is an important element in floras of the New World, but lacked extensive phylogenetic work until recently. In the last ten years, both family-wide phylogenetic studies and in-depth studies of major clades have been published. The available data from previous studies and new data were combined to produce an updated phylogeny of Verbenaceae including over 360 species, over three times as many species as included in previous family-wide studies.
- Methods: Twelve chloroplast regions, two nuclear ribosomal spacers, and eight low-copy nuclear loci were analyzed for 366 species of Verbenaceae. Phylogenetic analyses were conducted using maximum likelihood, Bayesian inference, and Bayesian multi-species coalescent approaches.
- Key results: Classification of genera into higher order groups was confirmed and relationships of unassigned genera were resolved. Discovery of a new genus in Verbenaceae was also confirmed. The genus *Scleröon* Benth in Lindl. was resurrected to classify *Citharexylum oleinum* and *C. tetramerum* as a new genus in Duranteae.
- Conclusions: Previous inferences of major clades were robust; continued study within clades is needed. The updated phylogeny of Verbenaceae provides a framework for further study of evolutionary patterns in the family.

Key words: classification, microfluidic PCR, molecular phylogenetics, systematics, *Scleröon*, Verbenaceae

INTRODUCTION

Verbenaceae s.s. comprises 28 genera and *ca.* 780 species of trees, shrubs, lianas, and herbs distributed primarily in the New World (Atkins, 2004; O’Leary et al., 2009; Marx et al. 2010, Thode et al., 2013; Lu-Irving et al., 2014; Frost et al., in prep.). Once considered to be much larger, over 50 genera classified in Verbenaceae s.l. were transferred to Lamiaceae after cladistic analyses of morphological characters (Cantino et al., 1992). Marx et al. (2010) produced a phylogeny of Verbenaceae s.s. including complete generic sampling and data from seven chloroplast regions for 109 species. The Marx et al. (2010) study provided a framework from which to describe major clades in the family and produced an updated classification of 8 tribes. Current generic and species diversity for tribes are as follows: Lantaneae (4 genera, *ca.* 275 spp.; Lu-Irving and Olmstead, 2012; Lu-Irving et al., 2014; O’Leary et al., 2016), Verbenaeae (5 genera, 177 spp.; O’Leary et al., 2007; Peralta et al., 2008; O’Leary et al., 2009; O’Leary et al., 2010; O’Leary, 2014; O’Leary and Mulgura, 2014), Neospartoneae (3 genera, 7 spp.), Priveae (2 genera, 21 spp.), Citharexyleae (2 genera, 72 spp.; Frost et al., 2017), Casselieae (3 genera, 14 spp.), Duranteae (5 genera, *ca.* 190 spp.; Thode et al., 2013), and Petreae (1 genus, 12 spp.). In addition to the eight tribes were two unassigned genera, *Dipyrena* (1 spp.) and *Rhaphithamnus* (2 spp.), which exhibited conflict in their placement between chloroplast (Marx et al., 2010) and nuclear (Yuan et al., 2010) datasets. *Coelocarpum*, a genus that was unassigned by Atkins (2004), nested within Lantaneae in Marx et al. (2010) with weak support and was tentatively described with Lantaneae. Later work (Lu-Irving and Olmstead, 2012; Lu-Irving et al., 2014) confirmed it’s placement outside Lantaneae.

Alongside or since the study by Marx et al. (2010), multi-locus phylogenetic studies of tribes within Verbenaceae have been conducted, namely on Verbeneae (Yuan and Olmstead, 2008a; Yuan and Olmstead, 2008b; O’Leary et al., 2009; Yuan et al., 2010; Frost et al., 2017), Lantaneae (Lu-Irving and Olmstead, 2012; Lu-Irving et al. 2014), Citharexyleae (Frost et al., 2017; Frost et al., in prep.), and Neospartoneae (Lu et al., in prep.). These studies provide a large pool of existing data from which to generate an updated phylogeny of Verbenaceae with increased taxonomic and molecular sampling. Additionally, novel results from these studies required further testing, which may be accomplished through an expanded family-wide study. Frost et al. (2017) discovered a potential new clade in Verbeneae, dubbed the Andean clade. The Andean clade of Verbeneae comprised three species of *Junellia* and *Verbena* (*Junellia fasciculata*, *Junellia occulta*, and *Verbena vilifolia*) for both chloroplast and nuclear datasets, but datasets varied on the relationship of these species to other clades of Verbeneae and on the inclusion or exclusion of *Hierobotana* (O’Leary, 2014), a monotypic genus endemic to Ecuador, in the Andean clade. Frost et al. (in prep.) discovered that two species of *Citharexylum*, *C. oleinum* and *C. tetramerum*, did not nest within Citharexyleae, but could not confidently place the species in Verbenaceae based only on outgroup sampling.

Through pooling of the available data from phylogenetic studies of Verbenaceae and generation of new data for this study, we generated an updated phylogeny of Verbenaceae including over 360 species. This phylogeny was used to confirm major clades of Verbenaceae, test conflicted relationships for unassigned genera and the novel Andean clade of Verbeneae, and place *C. oleinum* and *C. tetramerum* within Verbenaceae.

MATERIALS AND METHODS

Sampling—In total, 645 accessions representing 368 species of Verbenaceae were sampled. This study incorporates published data (Yuan and Olmstead, 2008a; Yuan and Olmstead, 2008b; O’Leary et al., 2009; Marx et al., 2010; Yuan et al., 2010; Lu-Irving and Olmstead, 2012; Thode et al., 2013; Lu-Irving et al., 2014; Frost et al., 2017) and newly generated data for 275 accessions. Because this study incorporates data from multiple sources using different molecular loci, new data was generated for 179 accessions included in those studies in order to create more overlapping data between datasets. Additionally, we included 96 new accessions representing 81 taxa. New accessions included two accessions (covering two spp.) of *Chascanum*, 11 (10 spp.) of *Duranta*, 31 (24 spp.) of *Glandularia*, 19 (15 spp.) of *Junellia*, four (three spp.) of *Lantana*, ten (ten spp.) of *Lippia*, one (one spp.) of *Mulgurea*, one (one spp.) of *Petrea*, one (one spp.) of *Stachytarpheta*, and 16 (14 spp.) of *Verbena*. Twenty-one molecular loci from the combined studies were utilized, including 12 chloroplast loci (*ccsA*, *matK*, *ndhF*, *psbZ*, *rbcL*, *rpl32*, *rpoC2*, *rps16*, *trnG-S*, *trnT*, *trnL-F*, and *trnY*), two nuclear ribosomal spacer regions (ETS and ITS), and eight low-copy nuclear genes (PPR11, PPR62, PPR70, PPR81, PPR90, PPR91, PPR97, and PPR123; PPR loci numbered sequentially as in Yuan et al., 2009). Generation of new sequence data was carried out using a subset of loci: *matK*, *ndhF*, *rbcL*, *rpl32*, *rpoC2*, *trnT*, *trnL-F*, ETS, and ITS. These loci were chosen for their broad use in studies and universality of primer sequences for family-wide use. For a table of vouchers, herbaria housing voucher specimens, and GenBank accession numbers accompanying sequence data used in this study, see

Appendix S1 (see the Supplementary Data with this article). Herbaria acronyms follow Index Herbariorum (Thiers, constantly updated: <http://sweetgum.nybg.org/science/ih/>).

DNA extraction, Microfluidic PCR, and sequencing—Genomic DNA was extracted from either field-collected, silica-gel-dried tissues or herbarium specimens using a modified CTAB method (Doyle and Doyle, 1987). Microfluidic PCR was performed on an Access Array System (Fluidigm) using two Juno 192.24 IFCs. For detailed primer information about targeted loci (*matK*, *ndhF*, *rbcL*, *rpl32*, *rpoC2*, *trnT*, *trnL-F*, ETS, and ITS), see Frost et al. (in prep.). Amplicons were harvested and pooled as described in Uribe-Convers et al. (2016). For each IFC, The resulting pools were multiplexed in an Illumina Miseq using the Reagent Kit v3 600 cycles. Microfluidic PCR in the Access Array System, downstream quality control, and Illumina sequencing were performed in the University of Idaho (Moscow, ID) Institute for Bioinformatics and Evolutionary Studies (ibest) Genomic Resources Core facility. Data processing follows Frost et al. (in prep.). Briefly, reads from the Illumina Miseq runs were processed using the Fluidigm2PURC pipeline (Blischak et al., in review). Reads were processed with clustering thresholds of 0.975, 0.99, 0.995, 0.997 and a size threshold of 5.

Phylogenetic analyses—Sequences were aligned using AliView ver. 1.18.1 (Larsson, 2014); alignments were inspected and manually adjusted where necessary. Individual alignments were analyzed with jModelTest 2.1.7 (Darriba et al., 2012; Guindon and Gascuel, 2003) to select the best-fit model of nucleotide substitution. The GTR + G

model was selected and applied to all analyses. For regions with shared evolutionary histories, alignments were concatenated using Geneious R7 7.0.6 (Biomatters, Auckland, New Zealand) and treated as a single dataset. Regions *ccsA*, *matK*, *ndhF*, *psbZ*, *rbcL*, *rpl32*, *rpoC2*, *rps16*, *trnG-S*, *trnT*, *trnL-F*, and *trnY* were combined as the chloroplast (cpDNA) dataset, and ETS and ITS were combined as the nuclear ribosomal (nrDNA) dataset. Ten independent datasets were analyzed: cpDNA, nrDNA, PPR11, PPR62, PPR70, PPR81, PPR90, PPR91, PPR97, and PPR123. The eight PPR genes were combined and analyzed as a low-copy nuclear dataset, and all of the data were concatenated for an “all combined” dataset.

Another dataset was constructed using one representative for each species and a subset of the data in order to reduce the amount of noise from missing data in the all combined dataset. For species with multiple individuals with overlapping data, the individual with the most data was retained as the representative for that species. For species with individuals with non-overlapping data, the non-overlapping sequences were combined to yield greater coverage; the combined sequence served as the representative for that species. The data set was reduced to the nine targeted loci in this study and PPR11, PPR70, and PPR123, which had the best taxonomic sampling of the PPR regions (>200 accessions).

Phylogenetic reconstructions were conducted for individual datasets, low-copy nuclear genes combined, and all data combined, both with all representatives and one representative, using maximum likelihood and Bayesian approaches, as implemented in RAxML and MrBayes ver. 3.2.6 (Ronquist & Huelsenbeck, 2003), respectively.

Maximum likelihood analyses consisted of bootstrap analyses with 500 replicates for each dataset. Datasets were partitioned into individual gene regions with individual parameters unlinked in Bayesian analyses. Analyses consisted of two replicate runs, each with four chains, which were run for at least one million generations, sampled every 100 generations. Runs were assessed for convergence and stationarity in Tracer v1.6.0 (Rambaut et al., 2014); runs were considered to have converged when effective sample sizes (ESS) for parameter values were above 200 for combined files. The first 20% of sampled trees were discarded as burn-in from each run; the remaining trees were summarized into a majority rule consensus tree with all compatible groups.

RESULTS

Dataset characteristics—Taxonomic sampling included 366 species of Verbenaceae, ca. half (47.5%) of the estimated species diversity (Table 1). The total concatenated dataset consisted of 27,794 aligned bp and 645 accessions (Table 2). Among the characters, 11,139 were variable, of which 7,270 were parsimony-informative. The reduced dataset with one representative per species was 15,630 aligned bp and included 368 accessions/species. The selected subset included less missing data than the all combined dataset, 57.56% and 74.00% missing data, respectively.

Phylogenetic analyses—The tribes described by Marx et al. (2010) were recovered for all datasets, except Casselieae with nrDNA (Fig. 1; supplementary). All analyses reconstructed a grade of Petreeae, Duranteae, Citharexyleae and Casselieae at the base.

The rest of the tree was composed of two large clades, Lantaneae and Verbenaeae, and several small clades including tribes Priveae and Neospartoneae and *Coelocarpum*, *Dipyrena*, and *Rhaphithamnus*, genera that are unassigned to tribes. Most datasets (cpDNA, low copy combined, and all combined) inferred *Coelocarpum* as sister to Lantaneae. *Coelocarpum* was reconstructed as sister to Verbenaeae by nrDNA with low support. Verbenaeae was reconstructed as sister to Lantaneae and *Coelocarpum* with high support for low-copy and all combined datasets. *Dipyrena* was inferred to be sister to a clade of Lantaneae, *Coelocarpum*, and Verbenaeae by nrDNA, low-copy, and all combined datasets. For cpDNA, *Dipyrena* was reconstructed as sister to Verbenaeae, as in Marx et al. (2010). For relationships within clades, see Fig. 2.

Rhaphithamnus, Priveae, Neospartoneae, and *Dipyrena* form a grade leading to the large clade including Lantaneae and Verbenaeae. All datasets reconstructed Neospartoneae as sister to the clade of Lantaneae, *Coelocarpum*, Verbenaeae, and *Dipyrena*. Relationships of Priveae and *Rhaphithamnus* relative to the aforementioned groups varied and/or were not well supported across analyses. Priveae, as sister to the clade including Neospartoneae and Lantaneae, and *Rhaphithamnus*, as sister to that, was reconstructed with high support by low-copy nuclear data and with low support by nrDNA and all combined datasets. The reversed relationship, *Rhaphithamnus* sister to the clade including Neospartoneae and Lantaneae and Priveae sister to that, was reconstructed with low support by cpDNA.

The clade of *Junellia fasciculata*, *Junellia occulta*, and *Verbena vilifolia*, was reconstructed by all datasets (Fig. 3); the relationship of this clade relative to other clades

Verbeneae and its relationship to *Hierobotana* varied across loci. These species nested with *Hierobotana* in nrDNA and all combined trees and separate from *Hierobotana* in cpDNA and low-copy nuclear combined trees. Chloroplast (Fig. 3A), low-copy nuclear (Fig. 3C), and all combined data (one representative dataset; Fig. 3D) reconstructed the clade as sister to *Verbena*; nrDNA (Fig. 3B) inferred it to be sister to *Verbena* and *Glandularia*.

Citharexylum oleinum and *C. tetramerum*, the two species that fell outside of *Citharexylum* in previous studies, nested in tribe *Duranteae* (Fig. 4). In all analyses, the two species were found to be sister to the clade of *Bouchea*, *Chascanum*, and *Stachytarpheta*. This relationship was highly supported by nrDNA and the all combined (one representative) dataset.

DISCUSSION

Relationships reconstructed by different sources of data (cpDNA, nrDNA, and low-copy nuclear genes) were, for the most part, concordant with each other and previously published studies of Verbenaceae. The eight tribes classified by Marx et al. (2010) were recovered by analyses, except for Casselleae for nrDNA, which may be an artifact of low sampling for that group in that dataset. Relationships between tribes were also mostly consistent with those reconstructed by Marx et al. (2010). Unassigned genera in Verbenaceae, *Coelocarpum*, *Dipyrena*, and *Rhaphithamnus*, are supported as independent lineages in this study and remain unassigned to tribes.

Unassigned genera—Additional nuclear loci support *Dipyrena* as sister to the clade including Lantaneae and Verbeneae, rather than sister to Verbeneae. Prior to this study, Marx et al. (2010) inferred *Dipyrena* to be sister to Verbeneae using chloroplast data. Yuan et al. (2010) using five PPR loci (PPR11, PPR62, PPR70, PPR91, and PPR123) reconstructed *Dipyrena* as sister to the clade including Verbeneae and Lantaneae with PPR11, PPR70, and PPR123. The same relationship to Verbeneae found with chloroplast data was reconstructed with PPR62 by Yuan et al. (2010) with low support. Expanded sampling of Verbenaceae for PPR62 in this study places *Dipyrena* sister to the clade including Verbena and Lantaneae as with other PPR loci. PPR91 reconstructed a different topology altogether. This study also includes a new source of evidence to resolve the conflict between chloroplast regions and PPR genes: nrDNA. Nuclear ribosomal data also infer *Dipyrena* as sister to the clade including Lantaneae and Verbeneae. While the chloroplast reconstructs a slightly different evolutionary history, nuclear data agree that *Dipyrena* is sister to Verbeneae plus Lantaeae.

Nuclear and combined data also support *Rhaphithamnus* as the earliest diverging lineage in the grade of *Rhaphithamnus*, Priveae, Neospartoneae, and *Dipyrena*. The relationship of *Rhaphithamnus* relative to Priveae was uncertain based on results of Marx et al. (2010). Similar to the case with *Dipyrena*, there was conflict between chloroplast and PPR datasets as to whether *Rhaphithamnus* was placed above or below Priveae in the grade. It was placed above Priveae in chloroplast (Marx et al., 2010) and PPR91 (Yuan et al., 2010) datasets and below for PPR11, PPR62, PPR70, and PPR123. Nuclear ribosomal

data in this study also reconstructs *Rhaphithamnus* below, as the earliest diverging lineage in the grade of these four small groups.

New clades

Verbeneae—Frost et al. (2017) discovered a new clade in Verbeaneae composed of three Andean species in *Verbena* and *Junellia*: *Junellia fasciculata*, *Junellia occulta*, and *Verbena vilifolia*. The study, which included data for three chloroplast regions and nuclear loci ETS, ITS, and PPR11, found that this clade, dubbed the Andean clade, along with monotypic *Hierobotana* was sister to *Verbena* and *Glandularia* in the nuclear tree, but nested within *Verbena* and *Glandularia* in the chloroplast tree. Additionally, in the nuclear tree, *Hierobotana*, which is endemic to the Ecuadorian Andes, was not inferred to be closely related to these other Andean species, but rather to North American *Verbena*.

Chloroplast results in this study were consistent with relationships found by Frost et al. (2017): *Hierobotana* was separate from the Andean clade and sister to North American *Verbena*. Nuclear ribosomal data (ETS and ITS) reconstructed the Andean clade plus *Hierobotana* as sister to a clade including *Verbena* and *Glandularia*, consistent with the nuclear tree in Frost et al. (2017). Only the results of nuclear loci combined (ETS, ITS, and PPR11; Frost et al., 2017) were presented in that paper. Incorporation of more low copy nuclear loci in this study and separate analyses of low copy nuclear data from nuclear ribosomal data provide new insights into the evolutionary history of these species. Low-copy nuclear genes combined inferred the Andean clade to be sister to all *Verbena* and *Hierobotana* to be nested within the North American *Verbena*. The all

combined (one representative) dataset found the Andean clade plus *Hierobotana* to be sister to all *Verbena*.

Species tree analyses are necessary to resolve discordant relationships among gene trees to determine (1) if *Hierobotana* is related to the Andean clade or distinct and (2) the relationship of the Andean clade relative to other genera in order to resolve classification. If the Andean taxa form a monophyletic group with *Verbena*, they could be included in *Verbena*. However, if they are reconstructed as paraphyletic to other genera, as in the nuclear ribosomal dataset where the Andean clade comes out sister to both *Verbena* and *Glandularia*, the Andean clade would need to be classified as a distinct genus.

Duranteae—*Citharexylum oleinum* and *C. tetramerum*, two species of shrubs with reduced inflorescences distributed in Mexico, were placed outside of *Citharexyleae* by Frost et al. (in prep.). All phylogenetic reconstructions inferred that these species form a small clade sister to *Bouchea*, *Chascanum*, and *Stachytarpheta* in tribe *Duranteae*.

Placement outside of and paraphyletic to other genera in the tribe necessitates classification of new genus in *Verbenaceae*. We propose to resurrect the genus *Scleröon* Benth in Lindl. for which *Scleröon oleinum* was designate the type (Edwards Botanical Register, 1843). *Citharexylum tetramerum* also belongs in *Scleröon*.

Scleröon Benth in Lindl., Edwards's Bot. Reg. 29 (Misc.): 65. 1843. Type: *Scleröon oleinum* Benth in Lindl.

i. *Scleröon tetramerum* (T.S. Brandeg.) L.A. Frost, **comb. nov**

Basionym: *Citharexylum tetramerum* T.S. Brandeg., Univ. Calif. Publ. Bot.
3: 390.1909.

CONCLUSIONS

Our work finds that higher level classification within Verbenaceae is robust, but there is still much to learn within major groups. Focused research on clades will continue to refine our understanding of relationships and revise classification. This updated family-wide phylogeny provides a framework from which to test broad patterns of evolution in a family that is an important element of the New World floras. Future work will explore the biogeographical history, via reconstructions of dispersal between continents and transitions from the tropics into temperate zone, and how patterns of diversification relate to biogeographic events, geologic events, and character evolution.

Acknowledgements—The authors thank the curators of the following herbaria for permitting us to sample specimens: F, HUH, MEX, MO, SI, TEX, USM, WTU; the following people for laboratory work: Samuel Frankel, Meng Lu, and Sarah Tyson; the following people for assistance in the field: Carlos Burelo-Ramos, Warren Cardinal-McTeague, Itzue Caviedes-Solis, Ross Furbush, David Garcia, Johan Home, Diego Morales-Briones, Lenis Prado, Sarah Tyson, and Simon Uribe-Convers; and anonymous reviewers. This study was supported by NSF grants DEB 0542493, DEB 0710026, and DEB 1020369 to RGO and DEB 1500919 to LAF and RGO.

REFERENCES

- Blischak, P. D., M. Latvis, D. F. Morales-Briones, J. C. Johnson, V. S. Di Stilio, A. D. Wolfe, and D. C. Tank. In Review. Fluidigm2PURC: automated processing and haplotype inference for double-barcoded PCR amplicons. bioRxiv. doi: 10.1101/242677.
- Darriba, D., G. L. Taboada, R. Doallo, and D. Posada. 2012. jModelTest 2: more models, new heuristics and high-performance computing. *Nature Methods* 9(8): 772.
- Doyle, J. J., and J. L. Doyle. 1987. A rapid isolation procedure for small quantities of fresh leaf tissue. *Phytochemical Bulletin* 19: 11–15.
- Guindon, S., and O. Gascuel. 2003. A simple, fast, and accurate algorithm to estimate large phylogenies by maximum likelihood. *Systematic Biology* 52(5): 696-704.
- Huelsenbeck, J. P., and F. Ronquist. 2001. MRBAYES: Bayesian inference of phylogenetic trees. *Bioinformatics* 17(8): 754-755.
- Frost, L. A., Tyson, S. M., Lu-Irving, P., O’Leary, N., & Olmstead, R. G. (2017). Origins of North American arid-land Verbenaceae: More than one way to skin a cat. *American journal of botany*, 104(11), 1708-1716.
- Lu-Irving, P., & Olmstead, R. G. (2012). Investigating the evolution of Lantaneae (Verbenaceae) using multiple loci. *Botanical Journal of the Linnean Society*, 171(1), 103-119.
- Lu-Irving, P., O’Leary, N., O’Brien, A., & Olmstead, R. G. (2014). Resolving the genera *Aloysia* and *Acantholippia* within tribe Lantaneae (Verbenaceae), using chloroplast and nuclear sequences. *Systematic Botany*, 39(2), 644-655.

- Marx, H. E., O'Leary, N., Yuan, Y. W., Lu-Irving, P., Tank, D. C., Múlgura, M. E., & Olmstead, R. G. (2010). A molecular phylogeny and classification of Verbenaceae. *American journal of Botany*, 97(10), 1647-1663.
- O'Leary, N. 2014. Hierobotana Briq., an intriguing monotypic genus of tribe Verbeneae (Verbenaceae). *Phytotaxa* 164: 286-290.
- O'Leary, N., M. E. Múlgura, and O. Morrone. 2007. Revisión taxonómica de las especies del género Verbena (Verbenaceae): serie Pachystachyae. *Annals of the Missouri Botanical Garden* 94: 571-621.
- O'Leary, N., Y.-W. Yuan, A. Chemisquy, and R. G. Olmstead. 2009. Reassignment of species of paraphyletic Junellia s.l. to the new genus Mulguraea (Verbenaceae) and new circumscription of genus Junellia: molecular and morphological congruence. *Systematic Botany* 34: 777-786.
- O'Leary, N., M. E. Múlgura, and O. Morrone. 2010. Revisión taxonómica de las especies del género Verbena L. (Verbenaceae) II: serie Verbena. *Annals of the Missouri Botanical Garden* 97: 369-428.
- O'Leary, N., and M. E. Múlgura. 2014. Synopsis of tribe Verbeneae Dumortier (Verbenaceae) in Peru. *Phytotaxa* 163: 121-148.
- O'Leary, N., P. Lu-Irving, P. Moroni, and S. Siedo. 2016. Recircumscription and taxonomic revision of Aloysia (Lantaneae: Verbenaceae) in South America. *Annals of the Missouri Botanical Garden* 101: 568-609.
- Olmstead, R. G. (2013). Phylogeny and biogeography in Solanaceae, Verbenaceae and Bignoniaceae: a comparison of continental and intercontinental diversification patterns. *Botanical Journal of the Linnean Society*, 171(1), 80-102.

- Peralta, P., M. E. Múlgura, S. S. Denham, and S. M. Botta. 2008. Revisión del género *Junellia* (Verbenaceae). *Annals of the Missouri Botanical Garden* 95: 338-390.
- Rambaut, A., M. A. Suchard, D. Xie, and A. J. Drummond. 2014. Tracer v1.6. Available from <http://beast.bio.ed.ac.uk/Tracer>.
- Thiers, B. [continuously updated]. Index Herbariorum: A global directory of public herbaria and associated staff. New York Botanical Garden's Virtual Herbarium. <http://sweetgum.nybg.org/science/ih/>.
- Thode, V. A., O'Leary, N., Olmstead, R. G., & Freitas, L. B. (2013). Phylogenetic position of the monotypic genus *Verbenoxylum* (Verbenaceae) and new combination under *Recordia*. *Systematic Botany*, 38(3), 805-817.
- Uribe-Convers, S., M. L. Settles, and D. C. Tank. 2016. A Phylogenomic Approach Based on PCR Target Enrichment and High Throughput Sequencing: Resolving the Diversity within the South American Species of *Bartsia* L. (Orobanchaceae). *PLOS ONE* 11(2): e0148203. doi: 10.1371/journal.pone.0148203
- Yuan, Y. W., & Olmstead, R. G. (2008a). A species-level phylogenetic study of the *Verbena* complex (Verbenaceae) indicates two independent intergeneric chloroplast transfers. *Molecular Phylogenetics and Evolution*, 48(1), 23-33.
- Yuan, Y. W., & Olmstead, R. G. (2008b). Evolution and phylogenetic utility of the *PHOT* gene duplicates in the *Verbena* complex (Verbenaceae): dramatic intron size variation and footprint of ancestral recombination. *American Journal of Botany*, 95(9), 1166-1176.

Yuan, Y.-W., C. Liu, H. E. Marx, and R. G. Olmstead. 2009. The PPR (pentatricopeptide repeat) gene family, a tremendous resource for plant phylogenetic studies. *New Phytologist* 182: 272-283.

Yuan, Y. W., Liu, C., Marx, H. E., & Olmstead, R. G. (2010). An empirical demonstration of using pentatricopeptide repeat (PPR) genes as plant phylogenetic tools: Phylogeny of Verbenaceae and the Verbena complex. *Molecular Phylogenetics and Evolution*, 54(1), 23-35.

TABLES

Table 1. Taxonomic sampling

Taxon	Sampling: spp. sampled (estimated species diversity)	Taxon	Sampling: spp. sampled (estimated species diversity)
Petreeae	6 (12)	Neospartoneae	5 (7)
<i>Petrea</i>	6 (12)	<i>Diostea</i>	1 (1)
Duranteae	33 (191)	<i>Lampayo</i>	2 (2)
<i>Bouchea</i>	5 (10)	<i>Neosparton</i>	2 (4)
<i>Chascanum</i>	6 (27)	Verbeneae	124 (177)
<i>Duranta</i>	13 (20)	<i>Glandularia</i>	52 (84)
<i>Recordia</i>	2 (2)	<i>Hierobotana</i>	1 (1)
<i>Stachytarpheta</i>	7 (130)	<i>Junellia</i>	27 (37)
Casselieae	6 (14)	<i>Mulguraea</i>	5 (11)
<i>Casselia</i>	3 (6)	<i>Verbena</i>	39 (44)
<i>Parodianthus</i>	1 (2)	Lantaneae	121 (270)
<i>Tamonea</i>	2 (6)	<i>Aloysia</i>	28 (36)
Citharexyleae	61 (72)	<i>Acantholippia</i>	1 (1)
<i>Citharexylum</i>	59 (70)	<i>Lantana</i>	34 (100)
<i>Rehdera</i>	2 (2)	<i>Lippia</i>	58 (125)
Priveae	3 (21)	Unassigned genera	
<i>Pitrea</i>	1 (1)	<i>Coelocarpum</i>	2 (5)
<i>Priva</i>	2 (20)	<i>Dipyrena</i>	1 (1)
		<i>Rhaphithamnus</i>	2 (2)

Table 2. Characteristics of individual datasets

Alignment	No. of taxa	Proportion of taxa	Alignment length (bp)	% missing data	No. of variable sites	Proportion of variable sites	No. of parsimony informative sites	Proportion of parsimony informative sites	GC content
all comb.	645	1.000	27794	74.00	11139	0.401	7270	0.262	0.392
cpDNA	627	0.972	16961	69.45	5176	0.305	3175	0.187	0.358
nrDNA	580	0.899	1401	43.94	906	0.647	764	0.545	0.592
lowcopy	400	0.620	9948	74.957	5142	0.517	3417	0.343	0.398
PPR11	204	0.316	1461	29.76	866	0.593	621	0.425	0.401
PPR62	151	0.234	1452	44.65	717	0.494	457	0.315	0.411
PPR70	202	0.313	1128	52.35	697	0.618	464	0.411	0.382
PPR81	123	0.191	1180	7.96	652	0.553	433	0.367	0.395
PPR90	72	0.112	986	3.29	314	0.318	182	0.185	0.405
PPR91	45	0.070	1306	8.74	524	0.401	335	0.257	0.394
PPR97	62	0.096	747	5.47	266	0.356	158	0.212	0.41
PPR123	241	0.374	1394	31.18	739	0.53	533	0.382	0.405

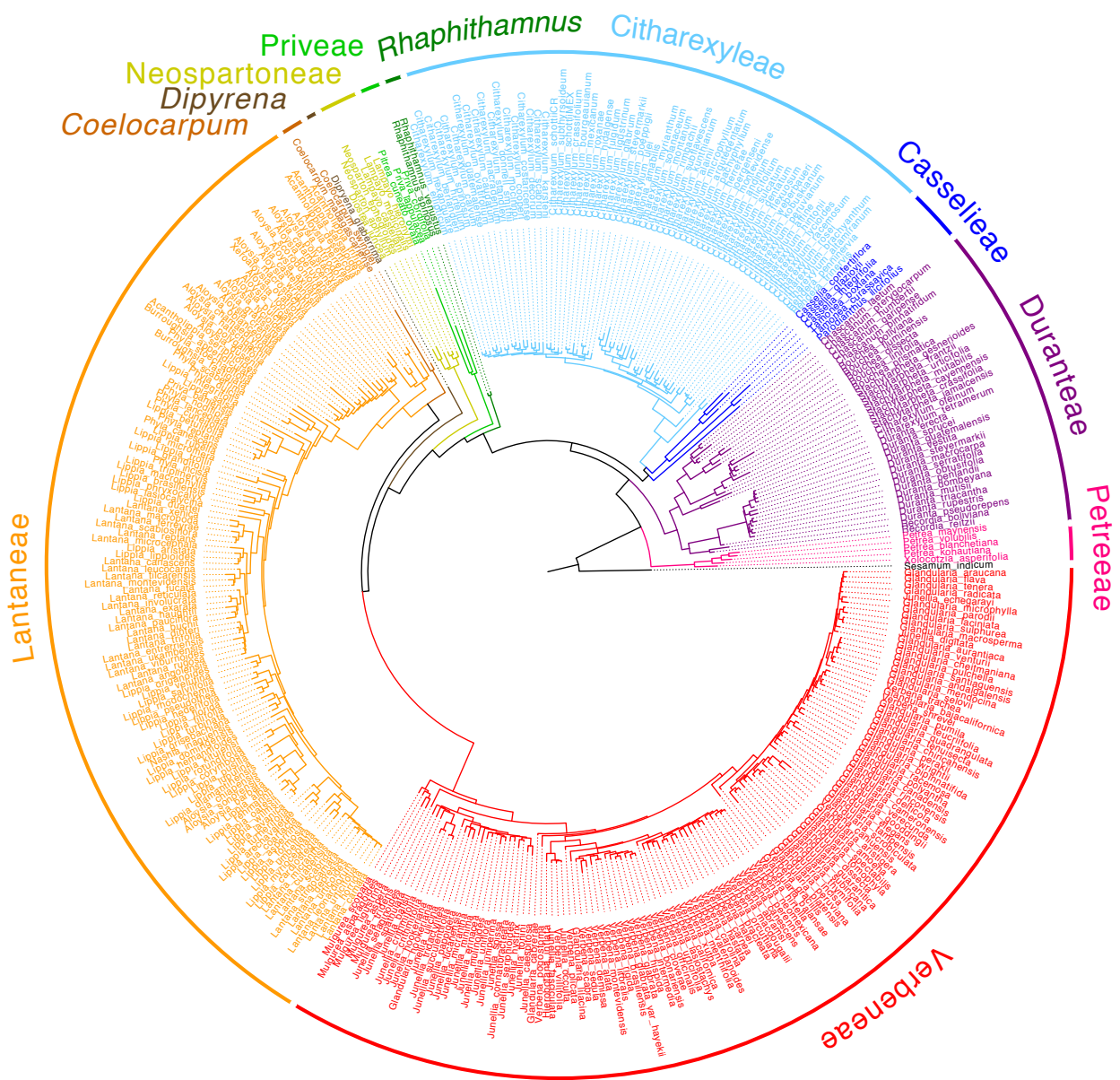
FIGURE CAPTIONS

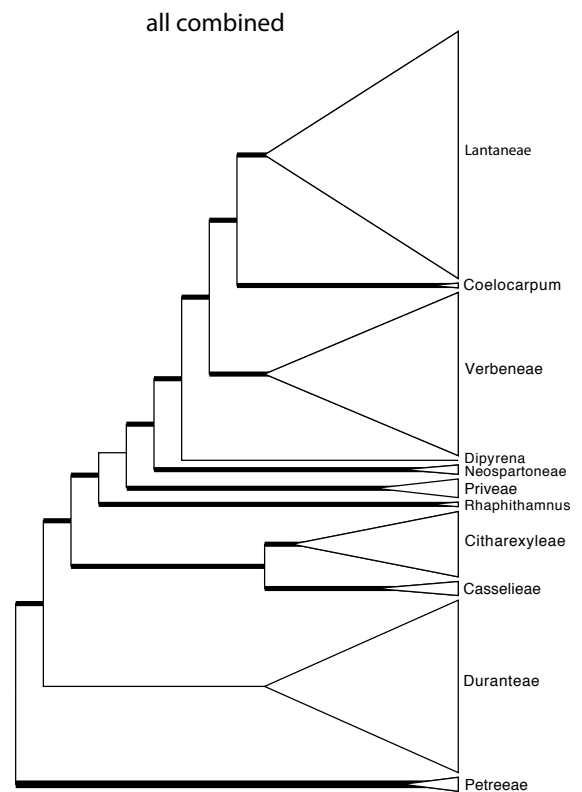
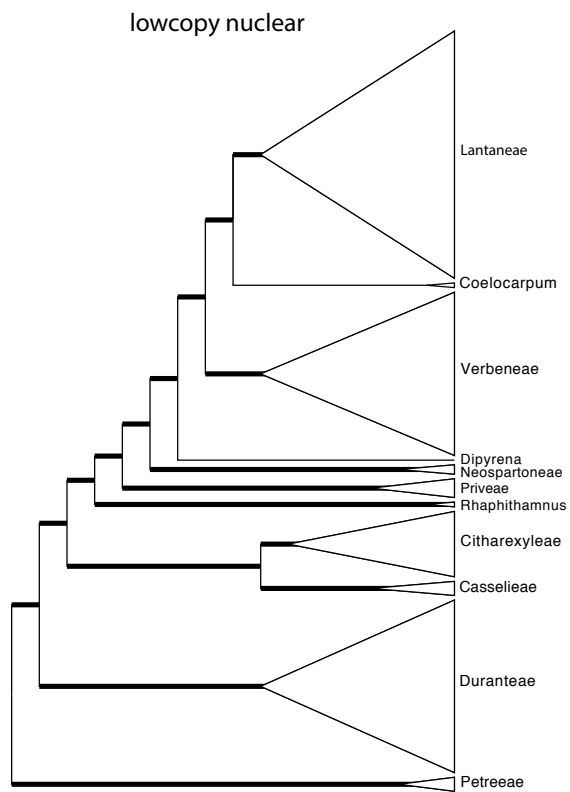
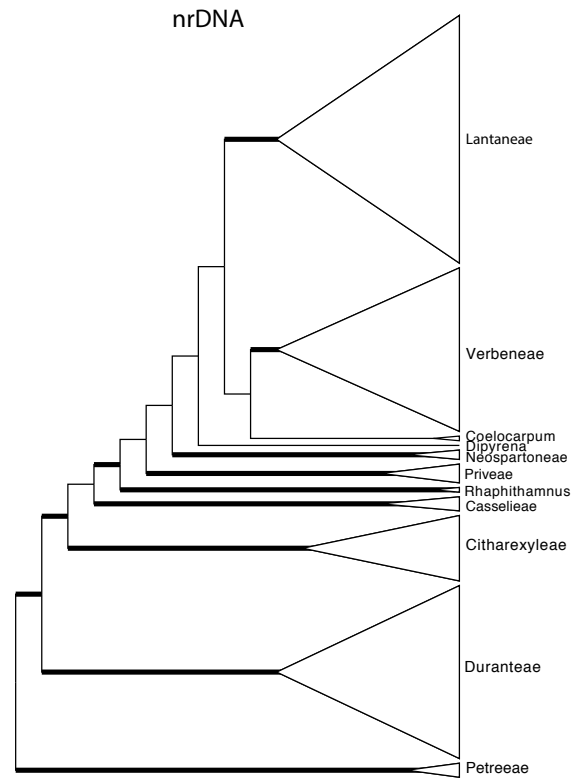
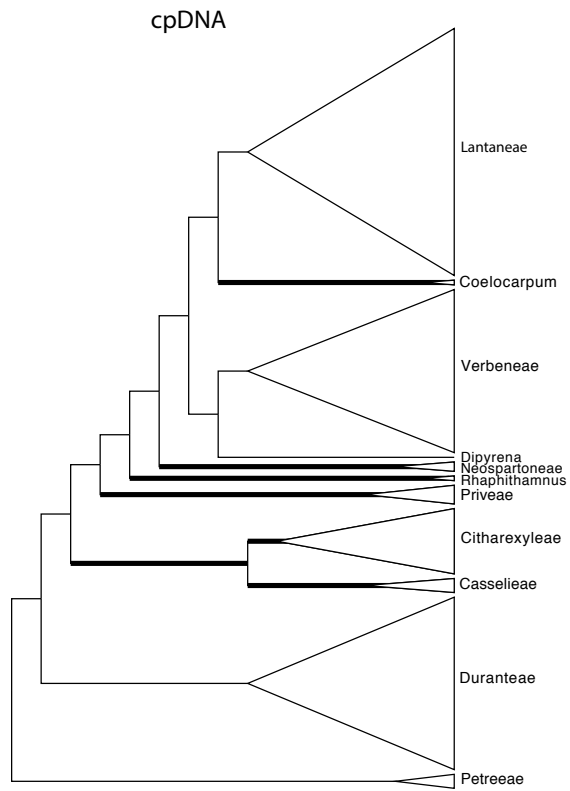
Fig. 1. Cartoon trees for cp, nr, lowcopy nuclear combined, and all combined (one representative) datasets showing topological differences among trees and support for relationships. Thickened branches indicate high support (≥ 70 bootstrap support from maximum likelihood (ML) analyses or ≥ 95 % posterior probability from Bayesian inference (BI)).

Fig. 2. Bayesian phylogenetic reconstructions for the all combined (one representative) dataset with tribes/major clades labelled and color coded.

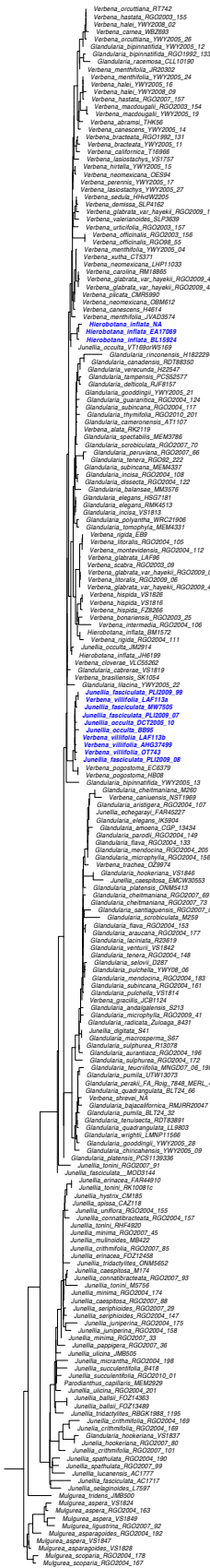
Fig. 3. Bayesian phylogenetic reconstructions for tribe Verbenae showing relationships of the Andean clade (*Junellia fasciculata*, *Junellia occulta*, and *Verbena villifolia*) and *Hierobotana inflata* (highlighted blue) from (A) cpDNA, (B) nrDNA, (C) low-copy nuclear combined, and (D) all combined (one representative dataset).

Fig. 4. Bayesian phylogenetic reconstructions for tribe Duranteae showing relationship of *C. oleinum* and *C. tetramerum* (highlighted blue) from the all combined (one representative) dataset. The same relationships were recovered by other datasets. Numbers indicate support values for high supportably nodes (≥ 95 % posterior probability).

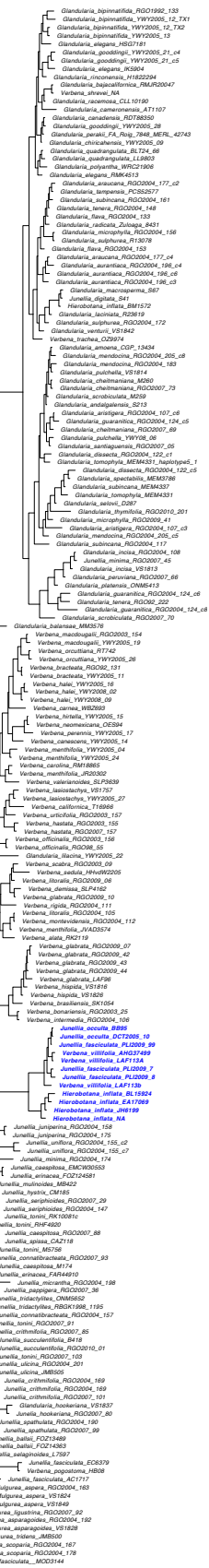


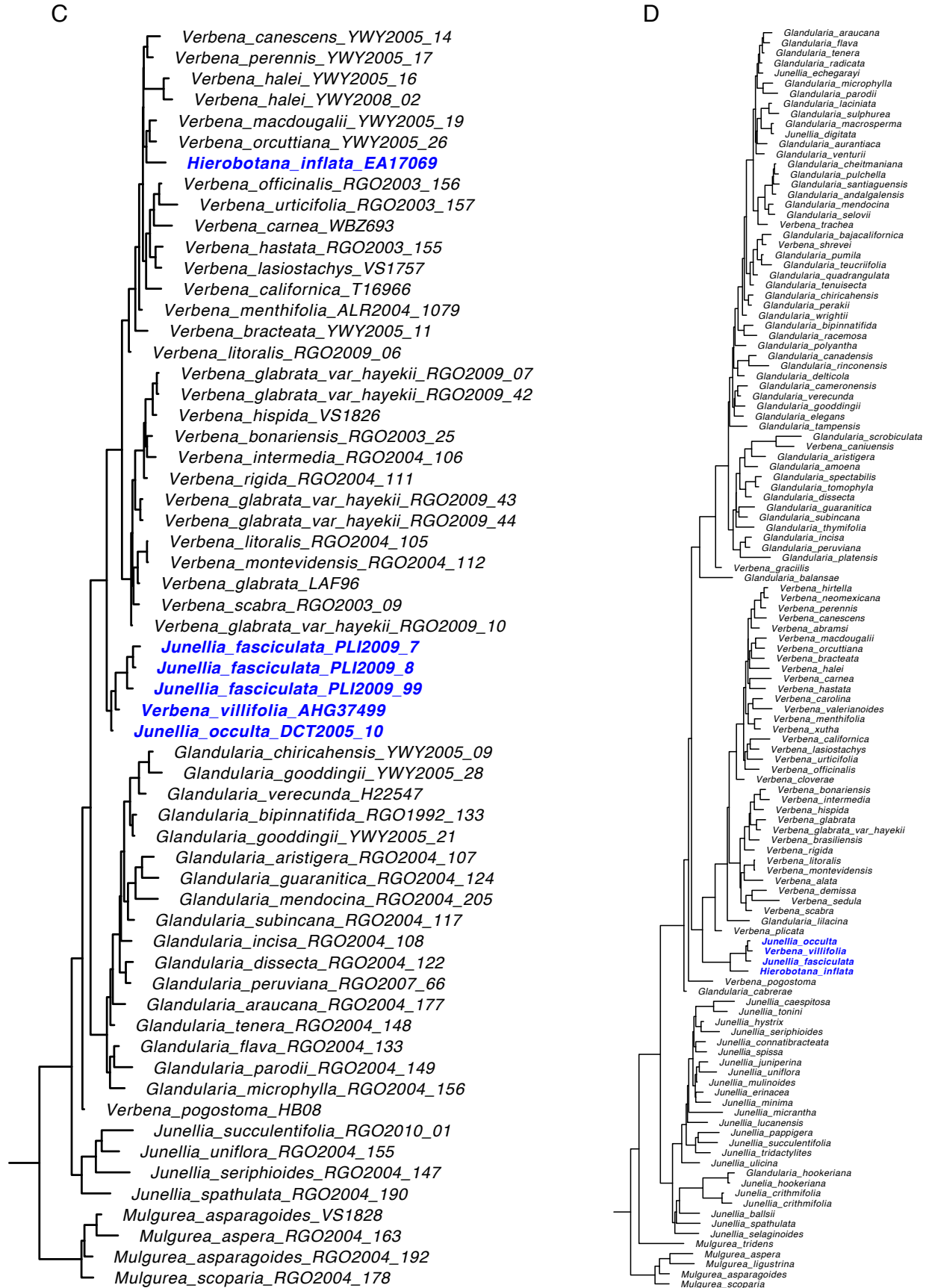


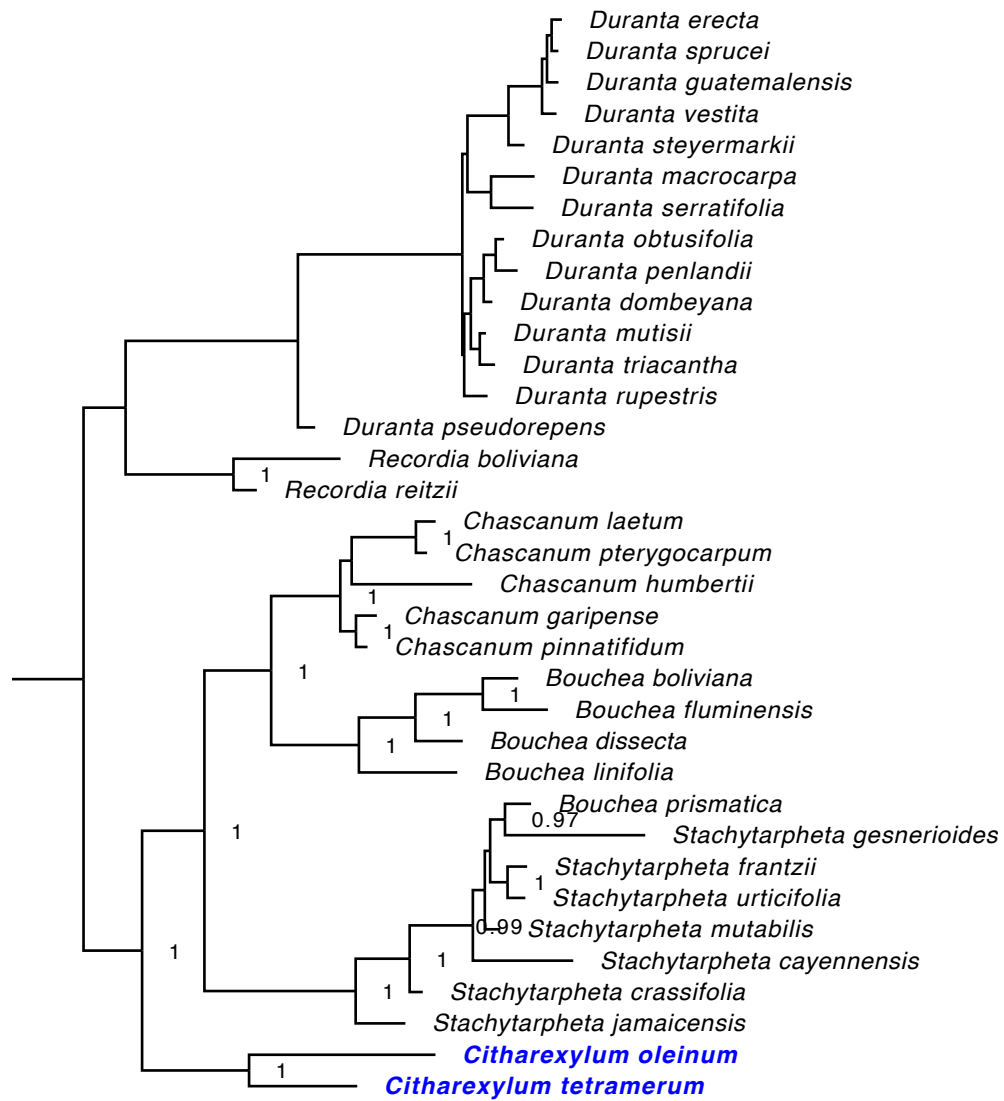
A



B







APPENDICES

Appendix S1. Specimens included in this study with voucher information

Taxon	Tip label	Voucher (Herbarium)
<i>Acantholippia deserticola</i>	Acantholippia_deserticola_FB4963	F. Biurrun 4963 (SI)
<i>Acantholippia deserticola</i>	Acantholippia_deserticola_RK8847	R. Keisling 8847 (SI)
<i>Acantholippia salsoloides</i>	Acantholippia_salsoloides_RGO2007_28	R.G. Olmstead 2007-28 (WTU)
<i>Acantholippia salsoloides</i>	Acantholippia_salsoloides_RGO2007_23	R.G. Olmstead 2007-23 (WTU)
<i>Acantholippia salsoloides</i>	Acantholippia_salsoloides_RGO2007_52	R.G. Olmstead 2007-52 (WTU)
<i>Acantholippia seriphioides</i>	Acantholippia_seriphioides_C10152	Correa et al. 10152 (SI)
<i>Acantholippia seriphioides</i>	Acantholippia_seriphioides_RGO2004_146	R.G. Olmstead 2004-146 (WTU)
<i>Acantholippia seriphioides</i>	Acantholippia_seriphioides_RGO2004_152	R.G. Olmstead 2004-152 (WTU)
<i>Acantholippia trifida</i>	Acantholippia_trifida_B7706	Biurrun 7706 (SI)
<i>Aloysia axillaris</i>	Aloysia_axillaris_WA21575	Wood & Atahuachi 21575 (KEW)
<i>Aloysia barbata</i>	Aloysia_barbata_CF3902	Carter & Ferris 3902 (US)
<i>Aloysia castellanosii</i>	Aloysia_castellanosii_F41191	Ferriencia 41191 (MERL)
<i>Aloysia catamarcensis</i>	Aloysia_catamarcensis_RGO2007_82	R.G. Olmstead 2007-82 (WTU)
<i>Aloysia chamaedryfolia</i>	Aloysia_chamaedryfolia_HR1131	H. Rimpler 1131 (FB)
<i>Aloysia chamaedryfolia</i>	Aloysia_chamaedryfolia_VT102	V. Thode 102 (ICN)
<i>Aloysia chiapensis</i>	Aloysia_chiapensis_M932	Martinez 932 (TEX)
<i>Aloysia citriodora</i>	Aloysia_citriodora_RGO2003_24	R.G. Olmstead 2003-24 (WTU)
<i>Aloysia citriodora</i>	Aloysia_citriodora_RGO2007_13	R.G. Olmstead 2007-13 (WTU)
<i>Aloysia crenata</i>	Aloysia_crenata_ALC29106	A. L. Cabrera 29106 (SI)
<i>Aloysia dusenii</i>	Aloysia_dusenii_KS38344	Krapocikas & Schinini 38344 (TEX)
<i>Aloysia dusenii</i>	Aloysia_dusenii_RGO2010_217	R.G. Olmstead 2010-217
<i>Aloysia gratissima</i>	Aloysia_gratissima_BLT26_28	B.L. Turner 26-28 (TEX)
<i>Aloysia gratissima</i>	Aloysia_gratissima_KJK12803	K.-J. Kim 12803 (TEX)
<i>Aloysia gratissima</i>	Aloysia_gratissima_PLI2008_17	P. Lu-Irving 08-17 (WTU)
<i>Aloysia gratissima</i>	Aloysia_gratissima_RGO2004_103	R.G. Olmstead 2004-103 (WTU)
<i>Aloysia gratissima</i>	Aloysia_gratissima_RGO2004_109	R.G. Olmstead 2004-109 (WTU)
<i>Aloysia hatschbachii</i>	Aloysia_hatschbachii_GH51897	G. Hatschbach 51897 (US)
<i>Aloysia herrerae</i>	Aloysia_herrerae_RGO2009_30	R.G. Olmstead 2009-30 (WTU)
<i>Aloysia herrerae</i>	Aloysia_herrerae_WS14658	Wood & Serrano 14658 (KEW)
<i>Aloysia looseri</i>	Aloysia_looseri_FAR9847	F.A. Roig 9847 (MERL)
<i>Aloysia lycioides</i>	Aloysia_lycioides_46000	#460-00 (VAL)
<i>Aloysia lycioides</i>	Aloysia_lycioides_RBGK2517602169	251-76-02169 (KEW)
<i>Aloysia macrostachya</i>	Aloysia_macrostachya_PLI2008_14	P. Lu-Irving 2008-14 (WTU)
<i>Aloysia macrostachya</i>	Aloysia_macrostachya_PLI2008_19	P. Lu-Irving 08-19 (WTU)
<i>Aloysia oblanceolata</i>	Aloysia_oblanceolata_VT96	Thode 96 (ICN)
<i>Aloysia peruviana</i>	Aloysia_peruviana_RGO2009_45	R.G. Olmstead 2009-45 (WTU)
<i>Aloysia polygalifolia</i>	Aloysia_polygalifolia_VT398	Thode 398 (ICN)
<i>Aloysia polystachya</i>	Aloysia_polystachya_K817	Kranz 817 (CESJ)
<i>Aloysia pulchra</i>	Aloysia_pulchra_RGO2004_129	R.G. Olmstead 2004-129 (WTU)
<i>Aloysia pulchra</i>	Aloysia_pulchra_VT157	Thode 157 (ICN)
<i>Aloysia scorodonioides</i>	Aloysia_scorodonioides_PLI2009_62	P. Lu-Irving 09-62 (WTU)
<i>Aloysia scorodonioides</i>	Aloysia_scorodonioides_RGO2009_40	R.G. Olmstead 09-40 (WTU)
<i>Aloysia scorodonioides</i>	Aloysia_scorodonioides_S1591	Saravia 1591 (SI)
<i>Aloysia sonorensis</i>	Aloysia_sonorensis_R85_1108	Reichenbacher 85-1108 (TEX)
<i>Aloysia virgata</i>	Aloysia_virgata_RGO2004_133	R.G. Olmstead 2004-133 (WTU)
<i>Aloysia virgata</i>	Aloysia_virgata_RGO2007_68	R.G. Olmstead 07-68 (WTU)
<i>Aloysia virgata</i>	Aloysia_virgata_VJB232_97	Valencia J. B. #232-97

Appendix S1. (cont.) Specimens included in this study with voucher information

Taxon	Tip label	Voucher (Herbarium)
<i>Aloysia wrightii</i>	Aloysia_wrightii_O1765	Ocampo 1765 (WTU)
<i>Aloysia wrightii</i>	Aloysia_wrightii_RGO1991_04	R.G. Olmstead 1991-004 (WTU)
<i>Baillonia amabilis</i>	Baillonia_amabilis_GM2188	Guaglianon & Mulgura 2188 (SI)
<i>Baillonia amabilis</i>	Baillonia_amabilis_MC4522	M. Cardenas 4522 (US)
<i>Bouchea boliviana</i>	Bouchea_boliviana_AAM2573	A. Arauja-M et.al. 2573 (MO)
<i>Bouchea dissecta</i>	Bouchea_dissecta_ALRG2004_951	A.L. Reina G. et al., 2004-951 (TEX)
<i>Bouchea fluminensis</i>	Bouchea_fluminensis_HR1141	H. Rimpler 1141 (FB)
<i>Bouchea linifolia</i>	Bouchea_linifolia_BLT20_423	B.L. Turner 20-423 (TEX)
<i>Bouchea prismatica</i>	Bouchea_prismatica_JRA10965	J.R. Abbott 10965 (MO)
<i>Burroughsia appendiculata</i>	Burroughsia_appendiculata_JH14254	James Henrickson 14254 (TEX)
<i>Burroughsia appendiculata</i>	Burroughsia_appendiculata_JH14273	James Henrickson 14273 (LL)
<i>Burroughsia fastigiata</i>	Burroughsia_fastigiata_LLW7847	LL Wiggins 7847 (US)
<i>Burroughsia fastigiata</i>	Burroughsia_fastigiata_SB294	Sikes & Babcock 294 (TEX)
<i>Casselia confertiflora</i>	Casselia_confertiflora_RCM2859	R.C. Mendonca et al. 2859 (US)
<i>Casselia glaziovii</i>	Casselia_glaziovii_MAdS3630	M.A. de Silva et al. 3630 (US)
<i>Casselia integrifolia</i>	Casselia_integrifolia_JRP3449	J.R. Pirani et.al. 3449 (US)
<i>Chascanum garipense</i>	Chascanum_garipense_LS11230	L. Smook 11230 (MO)
<i>Chascanum humbertii</i>	Chascanum_humbertii_BL505	B. Lewis et al. 505 (MO)
<i>Chascanum humbertii</i>	Chascanum_humbertii_MR6127	Miller & Randrianasola 6127 (MO)
<i>Chascanum laetum</i>	Chascanum_laetum_JD6923	J. DeWilde 6923 (MO)
<i>Chascanum marrubifolium</i>	Chascanum_marrubifolium_MGMT1099	M. Gilbert & M. Thulin 1099 (MO)
<i>Chascanum marrubiifolium</i>	Chascanum_marrubiifolium_JL15802	J.J. Lavranos 15802 (MO)
<i>Chascanum pinnatifidum</i>	Chascanum_pinnatifidum_JLBP12207	J. Lanvranos & B. Pehlemann 12207 (MO)
<i>Chascanum pterygocarpum</i>	Chascanum_pterygocarpum_BV759S	B. Verdcourt 759S (MO)
<i>Citharexylum affine</i>	Citharexylum_affine_TW3014	T. Wendt et al. 3014 (F)
<i>Citharexylum affine</i>	Citharexylum_affine_V6743	Villanueva 6743 (MEXU)
<i>Citharexylum affine</i>	Citharexylum_affine_VS	Velasco-Sinaca (MEXU)
<i>Citharexylum alainii</i>	Citharexylum_alainii_VSR2959A	Veloz, Salazar, Reyes 2959-A (FTG)
<i>Citharexylum altamiranum</i>	Citharexylum_altamiranum_EC2609	E. Carranza 2609 (MEXU)
<i>Citharexylum altamiranum</i>	Citharexylum_altamiranum_GJD9971	G. and J. Davidse 9971 (MO)
<i>Citharexylum altamiranum</i>	Citharexylum_altamiranum_M12032	Magaña 12032
<i>Citharexylum altamiranum</i>	Citharexylum_altamiranum_OH9864	Orozoco H. 9864 (MEXU)
<i>Citharexylum altamiranum</i>	Citharexylum_altamiranum_RH4704	R. Hernandez 4704 (MO)
<i>Citharexylum andinum</i>	Citharexylum_andinum_BB981	B. Becker 981 (TEX)
<i>Citharexylum andinum</i>	Citharexylum_andinum_F2628	E. Fernandez et al 2628 (MO)
<i>Citharexylum argutedentatum</i>	Citharexylum_argutedentatum_RGO2009_32	R.G. Olmstead 2009-32 (WTU)
<i>Citharexylum argutedentatum</i>	Citharexylum_argutedentatum_RGO2009_36	R.G. Olmstead 2009-36 (WTU)
<i>Citharexylum berlandieri</i>	Citharexylum_berlandieri_JT674	J. Trusty 674 (FTG)
<i>Citharexylum berlandieri</i>	Citharexylum_berlandieri_LAF65	L.A. Frost 65 (WTU)
<i>Citharexylum berlandieri</i>	Citharexylum_berlandieri_LW803	L. Woodbury 803 (FTG)
<i>Citharexylum berlandieri</i>	Citharexylum_berlandieri_RHM11926	R.H. Magaña 11926 (MEXU)
<i>Citharexylum bourgeauianum</i>	Citharexylum_bourgeauianum_W20066	Webster et al 20066 (HUH)
<i>Citharexylum brachyanthum</i>	Citharexylum_brachyanthum_FC9112	F. Chiang 9112 (F)
<i>Citharexylum brachyanthum</i>	Citharexylum_brachyanthum_JAE2609	J.A. Encina 2609 (MEXU)
<i>Citharexylum brachyanthum</i>	Citharexylum_brachyanthum_JWC11623	Johnston, Wendt, Chiang 11623 (F)
<i>Citharexylum brachyanthum</i>	Citharexylum_brachyanthum_RTC17479	R.T. Colin 17479 (MEXU)
<i>Citharexylum calvum</i>	Citharexylum_calvum_LAF79	L.A. Frost 79 (WTU)

Appendix S1. (cont.) Specimens included in this study with voucher information

Taxon	Tip label	Voucher (Herbarium)
<i>Citharexylum calvum</i>	Citharexylum_calvum_LAF80	L.A. Frost 80 (WTU)
<i>Citharexylum caudatum</i>	Citharexylum_caudatum_CSM2352	Clase, Santana Montilla 2352 (FTG)
<i>Citharexylum caudatum</i>	Citharexylum_caudatum_RGO96_73	R.G. Olmstead 1996-73A (WTU)
<i>Citharexylum cooperi</i>	Citharexylum_cooperi_BH25538	B. Hammel 25538 (INB)
<i>Citharexylum costaricense</i>	Citharexylum_costaricense_E626	Espinoza 626
<i>Citharexylum costaricense</i>	Citharexylum_costaricense_LAF2014_01	L.A. Frost 14-01 (WTU)
<i>Citharexylum costaricense</i>	Citharexylum_costaricense_RL1136	R. Lawton 1136 (F)
<i>Citharexylum crassifolium</i>	Citharexylum_crassifolium_RW733	R. Wanderlin et al. 733 (MO)
<i>Citharexylum decorum</i>	Citharexylum_decorum_IA1252	I. Aldo 1252 (MO)
<i>Citharexylum decorum</i>	Citharexylum_decorum_LAF142	L.A. Frost 142 (WTU)
<i>Citharexylum decorum</i>	Citharexylum_decorum_LAF143	L.A. Frost 143 (WTU)
<i>Citharexylum decorum</i>	Citharexylum_decorum_LAF144	L.A. Frost 144 (WTU)
<i>Citharexylum decorum</i>	Citharexylum_decorum_LAF145	L.A. Frost 145 (WTU)
<i>Citharexylum decorum</i>	Citharexylum_decorum_LAF146	L.A. Frost 146 (WTU)
<i>Citharexylum decorum</i>	Citharexylum_decorum_LAF147	L.A. Frost 147 (WTU)
<i>Citharexylum dentatum</i>	Citharexylum_dentatum_BS2014	B. Stein et al. 2014 (F)
<i>Citharexylum dentatum</i>	Citharexylum_dentatum_D3130	Dillon et al. 3130 (F)
<i>Citharexylum dentatum</i>	Citharexylum_dentatum_LAF90	L.A. Frost 090 (WTU)
<i>Citharexylum dentatum</i>	Citharexylum_dentatum_PLI09_09	P. Lu-Irving 2009-09 (WTU)
<i>Citharexylum donnell-smithii</i>	Citharexylum_donnel_smithii_BH26607	B. Hammel 26607 (INB)
<i>Citharexylum donnell-smithii</i>	Citharexylum_donnel_smithii_LAF2014_10	L.A. Frost 14-10 (WTU)
<i>Citharexylum donnell-smithii</i>	Citharexylum_donnel_smithii_LAF2014_11	L.A. Frost 14-11 (WTU)
<i>Citharexylum donnell-smithii</i>	Citharexylum_donnell_smithii_UWBG	cultivated UWBG, seed from CR
<i>Citharexylum ellipticum</i>	Citharexylum_ellipticum_EC14571	E. Cabrera 14571 (MO)
<i>Citharexylum ellipticum</i>	Citharexylum_ellipticum_LAF74	L.A. Frost 74 (WTU)
<i>Citharexylum ellipticum</i>	Citharexylum_ellipticum_LAF75	L.A. Frost 75 (WTU)
<i>Citharexylum ellipticum</i>	Citharexylum_ellipticum_LAF77	L.A. Frost 77 (WTU)
<i>Citharexylum ellipticum</i>	Citharexylum_ellipticum_LAF78	L.A. Frost 78 (WTU)
<i>Citharexylum flabellifolium</i>	Citharexylum_flabellifolium_F85_903B	Felger 85-903B (TEX)
<i>Citharexylum flabellifolium</i>	Citharexylum_flabellifolium_FS6115	F. Shreve 6115 (F)
<i>Citharexylum flabellifolium</i>	Citharexylum_flabellifolium_TRVD93_818	VanDevender et al. 93-818 (MO)
<i>Citharexylum flexuosum</i>	Citharexylum_flexuosum_LAF109	L.A. Frost 109 (WTU)
<i>Citharexylum flexuosum</i>	Citharexylum_flexuosum_LAF110	L.A. Frost 110 (WTU)
<i>Citharexylum flexuosum</i>	Citharexylum_flexuosum_LAF111	L.A. Frost 111 (WTU)
<i>Citharexylum flexuosum</i>	Citharexylum_flexuosum_LAF117	L.A. Frost 117 (WTU)
<i>Citharexylum flexuosum</i>	Citharexylum_flexuosum_LAF118	L.A. Frost 118 (WTU)
<i>Citharexylum flexuosum</i>	Citharexylum_flexuosum_LAF89	L.A. Frost 089 (WTU)
<i>Citharexylum flexuosum</i>	Citharexylum_flexuosum_PLI2009_13	P. Lu-Irving 2009-13 (WTU)
<i>Citharexylum flexuosum</i>	Citharexylum_flexuosum_PLI2009_19	P. Lu-Irving 2009-19 (WTU)
<i>Citharexylum fulgidum</i>	Citharexylum_fulgidum_MRR544	M. Rosas R. 544 (HUH-Arnold Arboretum)
<i>Citharexylum glabrum</i>	Citharexylum_glabrum_GM10169	Garcia-Mendoza 10169 (MEXU)
<i>Citharexylum glabrum</i>	Citharexylum_glabrum_JAM5312	J.A. Machuca 5312 (MO)
<i>Citharexylum glabrum</i>	Citharexylum_glabrum_JCSN17646	J.C. Soto N. 17646 (MEXU)
<i>Citharexylum glabrum</i>	Citharexylum_glabrum_RCD3121	R.C. Durán 3121 (MEXU)
<i>Citharexylum guatemalense</i>	Citharexylum_guatemalense_IC1827	I. Coronado et al. 1827 (MO)
<i>Citharexylum herrerae</i>	Citharexylum_herrerae_RGO09_11	R.G. Olmstead 2009-11 (WTU)
<i>Citharexylum herrerae</i>	Citharexylum_herrerae_RGO09_21	R.G. Olmstead 2009-21 (WTU)

Appendix S1. (cont.) Specimens included in this study with voucher information

<i>Taxon</i>	<i>Tip label</i>	<i>Voucher (Herbarium)</i>
<i>Citharexylum hexangulare</i>	Citharexylum_hexangulare_C22275	Calzada 22275 (MEXU)
<i>Citharexylum hexangulare</i>	Citharexylum_hexangulare_C27709	Chagata 27709 (MEXU)
<i>Citharexylum hexangulare</i>	Citharexylum_hexangulare_LAF51	L.A. Frost 51 (WTU)
<i>Citharexylum hexangulare</i>	Citharexylum_hexangulare_LAF73	L.A. Frost 73 (WTU)
<i>Citharexylum hexangulare</i>	Citharexylum_hexangulare_LAF86	L.A. Frost 86 (WTU)
<i>Citharexylum hexangulare</i>	Citharexylum_hexangulare_LAF87	L.A. Frost 87 (WTU)
<i>Citharexylum hexangulare</i>	Citharexylum_hexangulare_M20	Martinez 20
<i>Citharexylum hidalgense</i>	Citharexylum_hidalgense_A1971	Ayala 1971
<i>Citharexylum hidalgense</i>	Citharexylum_hidalgense_BBG740291	Berkley Botanical Garden 740291
<i>Citharexylum hidalgense</i>	Citharexylum_hidalgense_JR22356	J. Rzedowski 22356 (F)
<i>Citharexylum hidalgense</i>	Citharexylum_hidalgense_PT530	P. Tenorio 530 (MO)
<i>Citharexylum hintonii</i>	Citharexylum_hintonii_GH7534	G. Hinton 7531 (MO)
<i>Citharexylum hirtellum</i>	Citharexylum_hirtellum_EMMS	E.M. Martínez Salas (MO)
<i>Citharexylum hirtellum</i>	Citharexylum_hirtellum_LAF82	L.A. Frost 82 (WTU)
<i>Citharexylum hirtellum</i>	Citharexylum_hirtellum_LAF84	L.A. Frost 84 (WTU)
<i>Citharexylum ilicifolium</i>	Citharexylum_ilicifolium_KEW	cultivated Royal Botanic Gardens, Kew
<i>Citharexylum ilicifolium</i>	Citharexylum_ilicifolium_LAF135	L.A. Frost 135 (WTU)
<i>Citharexylum ilicifolium</i>	Citharexylum_ilicifolium_LAF137	L.A. Frost 137 (WTU)
<i>Citharexylum ilicifolium</i>	Citharexylum_ilicifolium_LAF152	L.A. Frost 152 (WTU)
<i>Citharexylum joergenseni</i>	Citharexylum_joergenseni_EF1711	E. Fernandez et al. 1711 (MO)
<i>Citharexylum karsteni</i>	Citharexylum_karsteni_LAF2013_03	L.A. Frost 13-03 (WTU)
<i>Citharexylum karsteni</i>	Citharexylum_karsteni_LAF2013_15	L.A. Frost 13-15 (WTU)
<i>Citharexylum karsteni</i>	Citharexylum_karsteni_LAF2013_16	L.A. Frost 13-16 (WTU)
<i>Citharexylum kobuskianum</i>	Citharexylum_kobuskianum_LAF114	L.A. Frost 114 (WTU)
<i>Citharexylum kobuskianum</i>	Citharexylum_kobuskianum_LAF115	L.A. Frost 115 (WTU)
<i>Citharexylum kobuskianum</i>	Citharexylum_kobuskianum_LAF116	L.A. Frost 116 (WTU)
<i>Citharexylum kunthianum</i>	Citharexylum_kunthianum_LAF140	L.A. Frost 13-19 B (WTU)
<i>Citharexylum kunthianum</i>	Citharexylum_kunthianum_LAF141	L.A. Frost 13-23 A (WTU)
<i>Citharexylum kunthianum</i>	Citharexylum_kunthianum_LAF2013_19B	L.A. Frost 13-26 (WTU)
<i>Citharexylum kunthianum</i>	Citharexylum_kunthianum_LAF2013_23A	L.A. Frost 140 (WTU)
<i>Citharexylum kunthianum</i>	Citharexylum_kunthianum_LAF2013_26	L.A. Frost 141 (WTU)
<i>Citharexylum ligustrinum</i>	Citharexylum_ligustrinum_RGBK0006951235	cultivated Royal Botanic Gardens, Kew
<i>Citharexylum ligustrinum</i>	Citharexylum_ligustrinum_V18711	Ventura 18711 (MO)
<i>Citharexylum lycioides</i>	Citharexylum_lycioides_C154	Chávez et al. rjchm 154
<i>Citharexylum lycioides</i>	Citharexylum_lycioides_S955	Spellman et al. 955 (F)
<i>Citharexylum macradenium</i>	Citharexylum_macradenium_BH26602	B. Hammel 26602 (INB)
<i>Citharexylum mexicanum</i>	Citharexylum_mexicanum_FC_F243	F. Chiang et al. F-243 (MO, MEXU)
<i>Citharexylum mexicanum</i>	Citharexylum_mexicanum_GP2165	Gomez Pompa 2165 (MEXU)
<i>Citharexylum mexicanum</i>	Citharexylum_mexicanum_S625	Salinas 625
<i>Citharexylum mexicanum</i>	Citharexylum_mexicanum_TN318	Taylor and Nee 318 (MO)
<i>Citharexylum microphyllum</i>	Citharexylum_microphyllum_ARSG8502	Acasado-Rdgz., Siaca, Garcia 8502 (FTG)
<i>Citharexylum microphyllum</i>	Citharexylum_microphyllum_RGNR4084	R. Garcia, N. Ramirez 4084 (F)
<i>Citharexylum mocinnoi</i>	Citharexylum_mocinnoi_LAF54	L.A. Frost 54 (WTU)
<i>Citharexylum mocinnoi</i>	Citharexylum_mocinnoi_LAF59	L.A. Frost 59 (WTU)
<i>Citharexylum mocinnoi</i>	Citharexylum_mocinnoi_LAF60	L.A. Frost 60 (WTU)
<i>Citharexylum mocinnoi</i>	Citharexylum_mocinnoi_LAF71	L.A. Frost 71 (WTU)
<i>Citharexylum mocinnoi</i>	Citharexylum_mocinnoi_longibracteolata_LAF71	L.A. Frost 71 (WTU)
<i>Citharexylum montanum</i>	Citharexylum_montanum_LAF129	L.A. Frost 129 (WTU)

Appendix S1. (cont.) Specimens included in this study with voucher information

Taxon	Tip label	Voucher (Herbarium)
<i>Citharexylum montanum</i>	Citharexylum_montanum_LAF131	L.A. Frost 131 (WTU)
<i>Citharexylum montanum</i>	Citharexylum_montanum_LAF132	L.A. Frost 132 (WTU)
<i>Citharexylum montanum</i>	Citharexylum_montanum_LAF133	L.A. Frost 133 (WTU)
<i>Citharexylum montanum</i>	Citharexylum_montanum_LAF2013_10	L.A. Frost 13-10 (WTU)
<i>Citharexylum montanum</i>	Citharexylum_montanum_LAF2013_25	L.A. Frost 13-25 (WTU)
<i>Citharexylum montevidensis</i>	Citharexylum_montevidensis_RGO2004_101	R.G. Olmstead 2004-101 (WTU)
<i>Citharexylum montevidensis</i>	Citharexylum_montevidensis_RGO2004_102	R.G. Olmstead 2004-102 (WTU)
<i>Citharexylum myrianthum</i>	Citharexylum_myrianthum_AK578	A. Kegler 578 (MO)
<i>Citharexylum oleinum</i>	Citharexylum_oleinum_B3587	Bartholomew et al. 3587 (HUH-Gray)
<i>Citharexylum oleinum</i>	Citharexylum_oleinum_DN2473	Diggs & Nee 2473 (F)
<i>Citharexylum ovatifolium</i>	Citharexylum_ovatifolium_GW11813	G. Webster et al. 11813 (F)
<i>Citharexylum ovatifolium</i>	Citharexylum_ovatifolium_MY00781	M. Yáñez 00781 (MO)
<i>Citharexylum pachyphyllum</i>	Citharexylum_pachyphyllum_BV471	B. Vuilleumier 471 (HUH)
<i>Citharexylum pachyphyllum</i>	Citharexylum_pachyphyllum_D1655	E.W. Davis et al. 1655 (F)
<i>Citharexylum pachyphyllum</i>	Citharexylum_pachyphyllum_H1066	Hudson 1066 (MO)
<i>Citharexylum peruvianum</i>	Citharexylum_peruvianum_LAF100	L.A. Frost 100 (WTU)
<i>Citharexylum peruvianum</i>	Citharexylum_peruvianum_LAF121	L.A. Frost 121 (WTU)
<i>Citharexylum peruvianum</i>	Citharexylum_peruvianum_LAF123	L.A. Frost 123 (WTU)
<i>Citharexylum peruvianum</i>	Citharexylum_peruvianum_LAF99	L.A. Frost 99 (WTU)
<i>Citharexylum peruvianum</i>	Citharexylum_peruvianum_S17122	Segastegui 17122 (USM)
<i>Citharexylum poeppigii</i>	Citharexylum_poeppigii_LAF2013_11	L.A. Frost 13-11 (WTU)
<i>Citharexylum poeppigii</i>	Citharexylum_poeppigii_LAF2013_12	L.A. Frost 13-12 (WTU)
<i>Citharexylum racemosum</i>	Citharexylum_racemosum_EC5797	E. Carrauzo 5797 (TEX)
<i>Citharexylum racemosum</i>	Citharexylum_racemosum_M5997	Martinez 5997
<i>Citharexylum reticulatum</i>	Citharexylum_reticulatum_AA581	A. Arajo et al. 581 (MO)
<i>Citharexylum rimbachii</i>	Citharexylum_rimbachii_LAF138	L.A. Frost 138 (WTU)
<i>Citharexylum rimbachii</i>	Citharexylum_rimbachii_LAF139	L.A. Frost 139 (WTU)
<i>Citharexylum rosei</i>	Citharexylum_rosei_CWJ8180	Chiang, Wendt, Johnston 8180 (F)
<i>Citharexylum roxanae</i>	Citharexylum_roxanae_AC5083	A. Carter 5083 (F)
<i>Citharexylum roxanae</i>	Citharexylum_roxanae_RM23834	R. Moran 23834 (MO)
<i>Citharexylum scabrum</i>	Citharexylum_scabrum_SLF359_94	Friedman 359-94
<i>Citharexylum schottiiCR</i>	Citharexylum_schottiiCR_LAF2014_04	L.A. Frost 14-04 (WTU)
<i>Citharexylum schottiiCR</i>	Citharexylum_schottiiCR_LAF2014_07	L.A. Frost 14-07 (WTU)
<i>Citharexylum schottiiCR</i>	Citharexylum_schottiiCR_LAF2014_09	L.A. Frost 14-09 (WTU)
<i>Citharexylum schottiiMEX</i>	Citharexylum_schottiiMEX_LAF62	L.A. Frost 62 (WTU)
<i>Citharexylum schottiiMEX</i>	Citharexylum_schottiiMEX_LAF63	L.A. Frost 63 (WTU)
<i>Citharexylum solanaceum</i>	Citharexylum_solanaceum_RW341	R. Wasum 341 (MO)
<i>Citharexylum spinosum</i>	Citharexylum_spinosum_JCS5727	J.C. Solomon 5727 (TEX)
<i>Citharexylum spinosum</i>	Citharexylum_spinosum_RGO14_04	R.G. Olmstead 2014-04 (WTU)
<i>Citharexylum spinosum</i>	Citharexylum_spinosum_RGO96_113	R.G. Olmstead 1996-113 (WTU)
<i>Citharexylum standleyi</i>	Citharexylum_standleyi_AM3011	A. Magallanes 3011 (F)
<i>Citharexylum standleyi</i>	Citharexylum_standleyi_L1797	Lott 1796
<i>Citharexylum standleyi</i>	Citharexylum_standleyi_LAPJ2182b	LAPJ 2182b
<i>Citharexylum steyermarkii</i>	Citharexylum_steyermarkii_DEB40360	D.E. Breedlove 40360 (MO)
<i>Citharexylum subflavescens</i>	Citharexylum_subflavescens_LAF2013_01	L.A. Frost 13-01 (WTU)
<i>Citharexylum subflavescens</i>	Citharexylum_subflavescens_LAF2013_06	L.A. Frost 13-06 (WTU)
<i>Citharexylum subflavescens</i>	Citharexylum_subflavescens_LAF2013_27	L.A. Frost 13-27 (WTU)

Appendix S1. (cont.) Specimens included in this study with voucher information

Taxon	Tip label	Voucher (Herbarium)
<i>Citharexylum subthyrsoideum</i>	Citharexylum_subthyrsoideum_MGG30	M. Gabriela Gomez 30 (MO)
<i>Citharexylum sulcatum</i>	Citharexylum_sulcatum_LAF2013_07B	L.A. Frost 13-07 B (WTU)
<i>Citharexylum sulcatum</i>	Citharexylum_sulcatum_LAF2013_08	L.A. Frost 13-08 (WTU)
<i>Citharexylum tetramerum</i>	Citharexylum_tetramerum_M8638	Mendoza 8638
<i>Citharexylum tetramerum</i>	Citharexylum_tetramerum_PT4717	P. Teuoria 4717 (F)
<i>Citharexylum tristachyum</i>	Citharexylum_tristachyum_G11484	Gillis 11484 (FTG)
<i>Citharexylum ulei</i>	Citharexylum_ulei_LAF128	L.A. Frost 128 (WTU)
<i>Citharexylum ulei</i>	Citharexylum_ulei_LAF130	L.A. Frost 130 (WTU)
<i>Citharexylum weberbaueri</i>	Citharexylum_weberbaueri_LAF103	L.A. Frost 103 (WTU)
<i>Citharexylum weberbaueri</i>	Citharexylum_weberbaueri_LAF105	L.A. Frost 105 (WTU)
<i>Citharexylum weberbaueri</i>	Citharexylum_weberbaueri_LAF106	L.A. Frost 106 (WTU)
<i>Citharexylum weberbaueri</i>	Citharexylum_weberbaueri_LAF120	L.A. Frost 120 (WTU)
<i>Citharexylum weberbaueri</i>	Citharexylum_weberbaueri_LAF124	L.A. Frost 124 (WTU)
<i>Citharexylum weberbaueri</i>	Citharexylum_weberbaueri_LAF125	L.A. Frost 125 (WTU)
<i>Citharexylum weberbaueri</i>	Citharexylum_weberbaueri_LAF126	L.A. Frost 126 (WTU)
<i>Citharexylum weberbaueri</i>	Citharexylum_weberbaueri_PLI09_04	P. Lu-Irving 2009-04 (WTU)
<i>Coelocarpum madagascariense</i>	Coelocarpum_madagascariense_GES2977	G.E. Schatz 2977 (MO)
<i>Coelocarpum madagascariense</i>	Coelocarpum_madagascariense_PM3569	Phillipson and Milijaona 3569 (MO)
<i>Coelocarpum swinglei</i>	Coelocarpum_swinglei_PBP3443	Phillipson et al. 3443 (MO)
<i>Diostea juncea</i>	Diostea_juncea_RBGK1969_35347	RBG Kew 1969-35347
<i>Diostea juncea</i>	Diostea_juncea_RGBE19300262	RBG Edinburgh 19300262
<i>Diostea juncea</i>	Diostea_juncea_RGO2010_3	R.G. Olmstead 2010-03 (WTU)
<i>Dipryena glaberrima</i>	Dipryena_glaberrima_RGO2004_179	R.G. Olmstead 2004-179 (WTU)
<i>Duranta costaricana</i>	Duranta_costaricana_EA2025	E. Alfaro 2025 (MO)
<i>Duranta dombeyana</i>	Duranta_dombeyana_AS9723	A. Sagastegui 9723 (TEX)
<i>Duranta erecta</i>	Duranta_erecta_RGO1992_211	R.G. Olmstead 1992-211 (WTU)
<i>Duranta erecta</i>	Duranta_erecta_RGO1996_100	R.G. Olmstead 1996-100 (WTU)
<i>Duranta erecta</i>	Duranta_erecta_RGO2009_39	R.G. Olmstead 2009-39 (WTU)
<i>Duranta erecta variegata</i>	Duranta_erecta_variegata_RGO92_206	R.G. Olmstead 92-206 (WTU)
<i>Duranta fletcheriana</i>	Duranta_fletcheriana_1996_71	R.G. Olmstead 1996-71 (WTU)
<i>Duranta guatemalensis</i>	Duranta_guatemalensis_SOG4741	S. Ochoa Gaona 4741 (TEX)
<i>Duranta macrocarpa</i>	Duranta_macrocarpa_ML88672	M. Lewis 88672 (MO)
<i>Duranta mutisii</i>	Duranta_mutisii_LAF2013_09	L.A. Frost 13-09 (WTU)
<i>Duranta mutisii</i>	Duranta_mutisii_PJ1666	P. Jorgensen et al. 1666 (MO)
<i>Duranta obtusifolia</i>	Duranta_obtusifolia_AM1048	A. Macurdy 1048 (MO)
<i>Duranta obtusifolia</i>	Duranta_obtusifolia_LAF2013_28	L.A. Frost 13-28 (WTU)
<i>Duranta penlandii</i>	Duranta_penlandii_BS10673	B. Sparre 10673 (US) (Maybe 18673)
<i>Duranta pseudorepens</i>	Duranta_pseudorepens_C12474	Can et al. 12474 (USOR)
<i>Duranta rupestris</i>	Duranta_rupestris_RGO2009_12	R.G. Olmstead 2009-12 (WTU)
<i>Duranta rupestris</i>	Duranta_rupestris_RGO2009_33	R.G. Olmstead 2009-33 (WTU)
<i>Duranta serratifolia</i>	Duranta_serratifolia_RGO2007_09	R.G. Olmstead 2007-09 (WTU)
<i>Duranta sprucei</i>	Duranta_sprucei_RGO1992_221	R.G. Olmstead 1992-221 (WTU)
<i>Duranta steyermarkii</i>	Duranta_steyermarkii_SLP2767	S. Lopez-Palacios 2767 (TEX)
<i>Duranta triacantha</i>	Duranta_triacantha_CA432	C. Antezama 432 (MO)
<i>Duranta triacantha</i>	Duranta_triacantha_IP2046	I. Padilla 2046 (MO)
<i>Duranta triacantha</i>	Duranta_triacantha_RGO2009_20	R.G. Olmstead 2009-20 (WTU)
<i>Duranta vestita</i>	Duranta_vestita_MRRW50	M. Rossato & R. Wasum 50 (MO)

Appendix S1. (cont.) Specimens included in this study with voucher information

Taxon	Tip label	Voucher (Herbarium)
<i>Duranta vestita</i>	Duranta_vestita_RW1624	R. Wasum 1624 (US)
<i>Glandularia amoena CGP</i>	Glandularia_amoena_CGP_13434	C.G. Pringle 13434
<i>Glandularia andalgalensis</i>	Glandularia_andalgalensis_S213	Solomon 213
<i>Glandularia araucana</i>	Glandularia_araucana_RGO2004_177	R.G. Olmstead 2004-177 (WTU)
<i>Glandularia aristigera</i>	Glandularia_aristigera_RGO2004_107	R.G. Olmstead 2004-107 (WTU)
<i>Glandularia aurantiaca</i>	Glandularia_aurantiaca_RGO2004_196	R.G. Olmstead 2004-196 (WTU)
<i>Glandularia bajacalifornica</i>	Glandularia_bajacalifornica_RMJRR20047	R. Moran & J. Reveal 20047 (US)
<i>Glandularia balansae</i>	Glandularia_balansae_MM3576	M.E. Mulgara 3576 (CTES,FCQ, SI)
<i>Glandularia bipinnatifida</i>	Glandularia_bipinnatifida_RGO1992_133	R.G. Olmstead 1992-133 (WTU)
<i>Glandularia bipinnatifida</i>	Glandularia_bipinnatifida_YWY2005_12	Y.-W. Yuan 2005-12 (WTU)
<i>Glandularia bipinnatifida</i>	Glandularia_bipinnatifida_YWY2005_13	Y.-W. Yuan 2005-13 (WTU)
<i>Glandularia cabreriae</i>	Glandularia_cabreriae_VS1819	V. Soza 1819 (WTU)
<i>Glandularia cameronensis</i>	Glandularia_cameronensis_AT1107	A. Traverse 1107
<i>Glandularia canadensis</i>	Glandularia_canadensis_RDT88350	R. Dale Thomas 88350 (US)
<i>Glandularia cheitmaniana</i>	Glandularia_cheitmaniana_M260	Marazzi 260 (SI)
<i>Glandularia cheitmaniana</i>	Glandularia_cheitmaniana_RGO2007_69	R.G. Olmstead 2007-69 (WTU)
<i>Glandularia cheitmaniana</i>	Glandularia_cheitmaniana_RGO2007_73	R.G. Olmstead 2007-73 (WTU)
<i>Glandularia chiricahensis</i>	Glandularia_chiricahensis_YWY2005_09	Y.-W. Yuan 2005-09 (WTU)
<i>Glandularia delticola</i>	Glandularia_delticola_RJF8157	Raymond J. Fleetwood 8157 (US)
<i>Glandularia dissecta</i>	Glandularia_dissecta_RGO2004_122	R.G. Olmstead 2004-122 (WTU)
<i>Glandularia elegans</i>	Glandularia_elegans_HSG7181	H. S. Gentry 7181
<i>Glandularia elegans</i>	Glandularia_elegans_IK5904	I. Knobloch 5904
<i>Glandularia elegans</i>	Glandularia_elegans_RMK4513	R. M. King 4513
<i>Glandularia flava</i>	Glandularia_flava_RGO2004_133	R.G. Olmstead 2004-133 (WTU)
<i>Glandularia flava</i>	Glandularia_flava_RGO2004_153	R.G. Olmstead 2004-153 (WTU)
<i>Glandularia gooddingii</i>	Glandularia_gooddingii_YWY2005_21	Y.-W. Yuan 2005-21 (WTU)
<i>Glandularia gooddingii</i>	Glandularia_gooddingii_YWY2005_28	Y.-W. Yuan 2005-28 (WTU)
<i>Glandularia guaranítica</i>	Glandularia_guaranítica_RGO2004_124	R.G. Olmstead 2004-124 (WTU)
<i>Glandularia hookeriana</i>	Glandularia_hookeriana_VS1837	V. Soza 1837 (WTU)
<i>Glandularia hookeriana</i>	Glandularia_hookeriana_VS1846	V. Soza 1846 (WTU)
<i>Glandularia incisa</i>	Glandularia_incisa_RGO2004_108	R.G. Olmstead 2004-108 (WTU)
<i>Glandularia incisa</i>	Glandularia_incisa_VS1813	V. Soza 1813
<i>Glandularia laciniata</i>	Glandularia_laciniata_R23619	Reughol 23619 (MERL)
<i>Glandularia lilacina</i>	Glandularia_lilacina_YWY2005_22	Y.-W. Yuan 2005-22 (WTU)
<i>Glandularia macrosperma</i>	Glandularia_macrosperma_S67	Solomon 67
<i>Glandularia mendocina</i>	Glandularia_mendocina_RGO2004_183	R.G. Olmstead 2004-183 (WTU)
<i>Glandularia mendocina</i>	Glandularia_mendocina_RGO2004_205	R.G. Olmstead 2004-205 (WTU)
<i>Glandularia microphylla</i>	Glandularia_microphylla_RGO2004_156	R.G. Olmstead 2004-156 (WTU)
<i>Glandularia microphylla</i>	Glandularia_microphylla_RGO2009_41	R.G. Olmstead 2009-41 (WTU)
<i>Glandularia parodii</i>	Glandularia_parodii_RGO2004_149	R.G. Olmstead 2004-149 (WTU)
<i>Glandularia perakii</i>	Glandularia_perakii_FA_Roig_7848_MERL_42743	F.A. Roig 7848 (MERL 42743)
<i>Glandularia peruviana</i>	Glandularia_peruviana_RGO2007_66	R.G. Olmstead 2007-66 (WTU)
<i>Glandularia platensis</i>	Glandularia_platensis_ONM5413	O.N. Morrone 5413
<i>Glandularia platensis</i>	Glandularia_platensis_PCS1139336	P. C. Standley 1139336 (US)
<i>Glandularia polyantha</i>	Glandularia_polyantha_WRC21906	W.R. Carr 21906
<i>Glandularia pulchella</i>	Glandularia_pulchella_VS1814	V. Soza 1814
<i>Glandularia pulchella</i>	Glandularia_pulchella_YWY08_06	Y.-W. Yuan 08-06

Appendix S1. (cont.) Specimens included in this study with voucher information

Taxon	Tip label	Voucher (Herbarium)
<i>Glandularia pumila</i>	Glandularia_pumila_BLT24_32	B.L. Turner 24-32
<i>Glandularia pumila</i>	Glandularia_pumila_UTW13073	U. T. Waterfall 13073 (US)
<i>Glandularia quadrangulata</i>	Glandularia_quadrangulata_BLT24_66	Lundell & Lundell 9803
<i>Glandularia quadrangulata</i>	Glandularia_quadrangulata_LL9803	B.L. Turner 24-66
<i>Glandularia racemosa</i>	Glandularia_racemosa_CLL10190	C.L. Lundell 10190 (US)
<i>Glandularia radicata Zuloaga</i>	Glandularia_radicata_Zuloaga_8431	F.O. Zuloaga 8431
<i>Glandularia rinconensis</i>	Glandularia_rinconensis_H1822294	H. et al. (US 1822294)
<i>Glandularia santiaguensis</i>	Glandularia_santiaguensis_RGO2007_05	R.G. Olmstead 2007-05 (WTU)
<i>Glandularia scrobiculata</i>	Glandularia_scrobiculata_M259	Marazzi 259 (SI)
<i>Glandularia scrobiculata</i>	Glandularia_scrobiculata_RGO2007_70	R.G. Olmstead 2007-70 (WTU)
<i>Glandularia selovii</i>	Glandularia_selovii_D287	Denham s.s. 287
<i>Glandularia spectabilis</i>	Glandularia_spectabilis_MEM3786	M.E. Mulgara et al 3786
<i>Glandularia subincana</i>	Glandularia_subincana_MEM4337	M.E. Mulgara et al 4337
<i>Glandularia subincana</i>	Glandularia_subincana_RGO2004_117	R.G. Olmstead 2004-117 (WTU)
<i>Glandularia subincana</i>	Glandularia_subincana_RGO2004_161	R.G. Olmstead 2004-161 (WTU)
<i>Glandularia sulphurea</i>	Glandularia_sulphurea_R13078	Reughol 13078 (MERL)
<i>Glandularia sulphurea</i>	Glandularia_sulphurea_RGO2004_172	R.G. Olmstead 2004-172 (WTU)
<i>Glandularia tampensis</i>	Glandularia_tampensis_PCS52577	P. C. Standley 52577 (US)
<i>Glandularia tenera</i>	Glandularia_tenera_RGO1992_222	R.G. Olmstead 92-222 (WTU)
<i>Glandularia tenera</i>	Glandularia_tenera_RGO2004_148	R.G. Olmstead 2004-148 (WTU)
<i>Glandularia tenuisecta</i>	Glandularia_tenuisecta_RDT83891	R. Dale Thomas 83891
<i>Glandularia teucrifolia</i>	Glandularia_teucrifolia_MNGD07_06_1982	M. Nee & G. Diggs 07/06/1982 (US)
<i>Glandularia thymifolia</i>	Glandularia_thymifolia_RGO2010_201	R.G. Olmstead 2010-201 (WTU)
<i>Glandularia tomophyla</i>	Glandularia_tomophyla_MEM4331	M.E. Mulgara et al 4331
<i>Glandularia venturii</i>	Glandularia_venturii_VS1842	V. Soza 1842 (WTU)
<i>Glandularia verecunda</i>	Glandularia_verecunda_H22547	Henrickson 22547 (US)
<i>Glandularia wrightii</i>	Glandularia_wrightii_LMNP11566	Lehto, McGill, Nash & Pinkava 11566 (US)
<i>Hierobotana inflata</i>	Hierobotana_inflata_BL15924	B. Lojtant 15924 (MO)
<i>Hierobotana inflata</i>	Hierobotana_inflata_BM1572	B. MacBryde 1572 (MO)
<i>Hierobotana inflata</i>	Hierobotana_inflata_EA17069	E. Asplund 17069 US
<i>Hierobotana inflata</i>	Hierobotana_inflata_JH6199	Jack Humbles 6199 (TEX)
<i>Hierobotana inflata</i>	Hierobotana_inflata_NA	No Voucher
<i>Junellia crithmifolia</i>	Junellia_crithmifolia_RGO2004_169	R.G. Olmstead 2004-169 (WTU)
<i>Junellia hookeriana</i>	Junellia_hookeriana_RGO2007_80	R.G. Olmstead 2007-80 (WTU)
<i>Junellia ballsii</i>	Junellia_ballsii_FOZ13489	F.O. Zuloaga 14363
<i>Junellia ballsii</i>	Junellia_ballsii_FOZ14363	F.O. Zuloaga 13489
<i>Junellia caespitosa</i>	Junellia_caespitosa EMCW30553	E. Mendez & C. Waillond 30553 (MERL)
<i>Junellia caespitosa</i>	Junellia_caespitosa_M174	Meglioli 174 (SI)
<i>Junellia caespitosa</i>	Junellia_caespitosa_RGO2007_88	R.G. Olmstead 2007-88 (WTU)
<i>Junellia connatibracteata</i>	Junellia_connatibracteata_RGO2004_157	R.G. Olmstead 2004-157 (WTU)
<i>Junellia connatibracteata</i>	Junellia_connatibracteata_RGO2007_93	R.G. Olmstead 2007-93 (WTU)
<i>Junellia crithmifolia</i>	Junellia_crithmifolia_RGO2004_169	R.G. Olmstead 2004-169 (WTU)
<i>Junellia crithmifolia</i>	Junellia_crithmifolia_RGO2007_101	R.G. Olmstead 2007-101 (WTU)
<i>Junellia crithmifolia</i>	Junellia_crithmifolia_RGO2007_85	R.G. Olmstead 2007-85 (WTU)
<i>Junellia digitata</i>	Junellia_digitata_S41	Solomon 41
<i>Junellia echegarayi</i>	Junellia_echegarayi_FAR45227	F.A. Roig et al 45227 (MERL)
<i>Junellia erinacea</i>	Junellia_erinacea_FAR44910	F.A. Roig et al 44910 (MERL)

Appendix S1. (cont.) Specimens included in this study with voucher information

<i>Taxon</i>	<i>Tip label</i>	<i>Voucher (Herbarium)</i>
<i>Junellia erinacea</i>	Junellia_erinacea_FOZ12458	F.O. Zuloaga 12458
<i>Junellia fasciculata</i>	Junellia_fasciculata_AC1717	A. Cano 1717 (MO)
<i>Junellia fasciculata</i>	Junellia_fasciculata_EC6379	E. Cerrate 6379 (USM)
<i>Junellia fasciculata</i>	Junellia_fasciculata_MOD3144	M.O. Dillon et al. 3144 (USM)
<i>Junellia fasciculata</i>	Junellia_fasciculata_MW7505	M. Weigand et al. 7505 (USM)
<i>Junellia fasciculata</i>	Junellia_fasciculata_PLI2009_07	P. Lu-Irving 2009-07 (WTU)
<i>Junellia fasciculata</i>	Junellia_fasciculata_PLI2009_08	P. Lu-Irving 2009-08 (WTU)
<i>Junellia fasciculata</i>	Junellia_fasciculata_PLI2009_99	P. Lu-Irving 2009-99 (WTU)
<i>Junellia hystrix</i>	Junellia_hystrix_CM185	C. Meglioli et al 185 (WTU)
<i>Junellia juniperina</i>	Junellia_juniperina_RGO2004_158	R.G. Olmstead 2004-158 (WTU)
<i>Junellia juniperina</i>	Junellia_juniperina_RGO2004_175	R.G. Olmstead 2004-175 (WTU)
<i>Junellia lucanensis</i>	Junellia_lucanensis_AC1777	A. Cano 1777 (MO)
<i>Junellia micrantha</i>	Junellia_micrantha_RGO2004_198	R.G. Olmstead 2004-198 (WTU)
<i>Junellia minima</i>	Junellia_minima_RGO2004_174	R.G. Olmstead 2004-174 (WTU)
<i>Junellia minima</i>	Junellia_minima_RGO2007_33	R.G. Olmstead 2007-33 (WTU)
<i>Junellia minima</i>	Junellia_minima_RGO2007_45	R.G. Olmstead 2007-45 (WTU)
<i>Junellia mulinoides</i>	Junellia_mulinoides_MB422	M. Bonifacino 422
<i>Junellia occulta</i>	Junellia_occulta_BB95	B. Becker et al. 95 (TEX)
<i>Junellia occulta</i>	Junellia_occulta_DCT2005_10	D.C. Tank 2005-10 (WTU)
<i>Junellia occulta</i>	Junellia_occulta_JM2914	J. Mostacero et al. 2914 (MO)
<i>Junellia occulta</i>	Junellia_occulta_VT169orW5169	VT 169 or Weigand 5169
<i>Junellia pappigera</i>	Junellia_pappigera_RGO2007_36	R.G. Olmstead 2007-36 (WTU)
<i>Junellia selaginoides</i>	Junellia_selaginoides_L7597	Lammers et al., 7597 (US)
<i>Junellia seriphioides</i>	Junellia_seriphioides_RGO2004_147	R.G. Olmstead 2004-147 (WTU)
<i>Junellia seriphioides</i>	Junellia_seriphioides_RGO2007_29	R.G. Olmstead 2007-29 (WTU)
<i>Junellia spathulata</i>	Junellia_spathulata_RGO2004_190	R.G. Olmstead 2004-190 (WTU)
<i>Junellia spathulata</i>	Junellia_spathulata_RGO2007_99	R.G. Olmstead 2007-99 (WTU)
<i>Junellia spissa</i>	Junellia_spissa_CAZ118a	C.A. Zanotti 118
<i>Junellia succulentifolia</i>	Junellia_succulentifolia_B418	Bonifacino 418 (US)
<i>Junellia succulentifolia</i>	Junellia_succulentifolia_RGO2010_01	R.G. Olmstead 2010-01 (WtU)
<i>Junellia tonini</i>	Junellia_tonini_M5756	Morrone 5756 (SI)
<i>Junellia tonini</i>	Junellia_tonini_RGO2007_103	R.G. Olmstead 2007-103 (WTU)
<i>Junellia tonini</i>	Junellia_tonini_RGO2007_91	R.G. Olmstead 2007-91 (WTU)
<i>Junellia tonini</i>	Junellia_tonini_RHF4920	R.H. Fortunato 4920
<i>Junellia tonini</i>	Junellia_tonini_RK10081c	R. Kiesling 10081c (SI)
<i>Junellia tridactylites</i>	Junellia_tridactylites_ONM5652	O.N. Morrone et al. 5652
<i>Junellia tridactylites</i>	Junellia_tridactylites_RBGK1988_1195	RBG Kew #1988-1195; Voucher unknown
<i>Junellia ulicina</i>	Junellia_ulicina_JMB505	J.M. Bonifacino 505
<i>Junellia ulicina</i>	Junellia_ulicina_RGO2004_201	R.G. Olmstead 2004-201 (WTU)
<i>Junellia uniflora</i>	Junellia_uniflora_RGO2004_155	R.G. Olmstead 2004-155 (WTU)
<i>Lampayo castellani</i>	Lampayo_castellani_BV386	B.Vuilleumier 386 (TEX)
<i>Lampayo castellani</i>	Lampayo_castellani_RGO2007_63	R.G. Olmstead 2007-063 (WTU)
<i>Lampayo hieronymi</i>	Lampayo_hieronymi EMC2092	E. Marilienz Carretero 2092 (MERL)
<i>Lampayo hieronymi</i>	Lampayo_hieronymi_FB4960	F. Biurran et al. 4960 (SI)
<i>Lampayo medicinalis</i>	Lampayo_medicinalis_BGHNR311	BGHNR 311 (RGBE)
<i>Lantana angolensis</i>	Lantana_angolensis_H915	Hines 915 (PRE)
<i>Lantana angolensis</i>	Lantana_angolensis_LR572	Long & Rae 572 (MO)

Appendix S1. (cont.) Specimens included in this study with voucher information

Taxon	Tip label	Voucher (Herbarium)
<i>Lantana buchii</i>	Lantana_buchii_PLI2012_107	P. Lu-Irving 12-107 (WTU)
<i>Lantana camara</i>	Lantana_camara_PLI2012_37	P. Lu-Irving 12-37 (WTU)
<i>Lantana camara</i>	Lantana_camara_PLI2012_3A	P. Lu-Irving 2012-3A (WTU)
<i>Lantana camara</i>	Lantana_camara_RGO1992_140	R.G. Olmstead 92-140 (WTU)
<i>Lantana canascens</i>	Lantana_canascens_RGO2007_06	R.G. Olmstead 2007-06 (WTU)
<i>Lantana cujabensis</i>	Lantana_cujabensis_PLI2010_19	P. Lu-Irving 10-19 (WTU)
<i>Lantana depressa</i>	Lantana_depressa_PLI2012_1	P. Lu-Irving 12-1 (WTU)
<i>Lantana dinteri</i>	Lantana_dinteri_MG30347	Merxmuller & Gress 30347 (PRE)
<i>Lantana entrerriensis</i>	Lantana_entrerriensis_RGO2004_126	R.G. Olmstead 2004-126 (WTU)
<i>Lantana exarata</i>	Lantana_exarata_PLI2012_49	P. Lu-Irving 12-49 (WTU)
<i>Lantana ferreyrae</i>	Lantana_ferreyrae_PLI05_06_2010	P. Lu-Irving s.n. May 6, 2010 (WTU)
<i>Lantana fucata</i>	Lantana_fucata_FRGS2952	F.R.G. Salimena 2952 (CESJ)
<i>Lantana haughtii</i>	Lantana_haughtii_PLI2009_34	P. Lu-Irving 09-34 (WTU)
<i>Lantana horrida</i>	Lantana_horrida_KJK12808	K.-J. Kim 12808 (TEX)
<i>Lantana horrida</i>	Lantana_horrida_PLI2012_61	P. Lu-Irving 12-61 (WTU)
<i>Lantana involucrata</i>	Lantana_involucrata_PLI2012_13	P. Lu-Irving 12-13
<i>Lantana involucrata</i>	Lantana_involucrata_RGO1996_124	R.G. Olmstead 1996-124 (WTU)
<i>Lantana leonardiorum</i>	Lantana_leonardiorum_PLI2012_102	P. Lu-Irving 12-102 (WTU)
<i>Lantana leucocarpa</i>	Lantana_leucocarpa_PLI2012_70	P. Lu-Irving 12-70 (WTU)
<i>Lantana macropoda</i>	Lantana_macropoda_NM7355	Nesom & Mayfield 7355 (TEX)
<i>Lantana micrantha</i>	Lantana_micrantha_RGO2007_08	R.G. Olmstead 2007-08 (WTU)
<i>Lantana microcephala</i>	Lantana_microcephala_PLI2008_07	P. Lu-Irving 2008-07 (WTU)
<i>Lantana montevidensis</i>	Lantana_montevidensis_PLI2008_15	P. Lu-Irving 2008-15 (WTU)
<i>Lantana montevidensis</i>	Lantana_montevidensis_RGO2010_203	R.G. Olmstead 2010-203 (WTU)
<i>Lantana pauciflora</i>	Lantana_pauciflora_PLI2012_106	P. Lu-Irving 2012-106
<i>Lantana reptans</i>	Lantana_reptans_PLI2009_14	P. Lu-Irving 2009-14 (WTU)
<i>Lantana reticulata</i>	Lantana_reticulata_PLI2012_66	P. Lu-Irving 2012-66 (WTU)
<i>Lantana rugosa</i>	Lantana_rugosa_PLI2008_25	P. Lu-Irving 2008-25 (WTU)
<i>Lantana rugosa</i>	Lantana_rugosa_VWV389	VW. Vos 389 (NU)
<i>Lantana scabiosiflora</i>	Lantana_scabiosiflora_PLI2009_01	P. Lu-Irving 2009-1 (WTU)
<i>Lantana scabrida</i>	Lantana_scabrida_PLI2012_89	P. Lu-Irving 2012-89 (WTU)
<i>Lantana strigocamara</i>	Lantana_strigocamara_PLI2012_22	P. Lu-Irving 2012-22 (WTU)
<i>Lantana tilcarensis</i>	Lantana_tilcarensis_RGO2007_18	R.G. Olmstead 2007-18 (WTU)
<i>Lantana trifolia</i>	Lantana_trifolia_PLI2009_59	P. Lu-Irving 2009-59 (WTU)
<i>Lantana trifolia</i>	Lantana_trifolia_PLI2012_90	P. Lu-Irving 2012-90 (WTU)
<i>Lantana trifolia</i>	Lantana_trifolia_RGO1996_98	R.G. Olmstead 1996-98 (WTU)
<i>Lantana ukambensis</i>	Lantana_ukambensis_FM80	Mawi 80 (MO)
<i>Lantana urticifolia</i>	Lantana_urticifolia_RGO1996_75	R.G. Olmstead 1996-75 (WTU)
<i>Lantana urticoides</i>	Lantana_urticoides_PLI2008_02	P. Lu-Irving 2008-2 (WTU)
<i>Lantana viburnoides</i>	Lantana_viburnoides_M991013R29	Miyazaki 991013R29 (TEX)
<i>Lantana viburnoides</i>	Lantana_viburnoides_PK23167	P. Kuchar 23167 (MO)
<i>Lantana xenica</i>	Lantana_xenica_VS1838	V. Soza 1838 (WTU)
<i>Lippia alba</i>	Lippia_alba_FTG71293A	FTG 71293A (FTG)
<i>Lippia alba</i>	Lippia_alba_RGO2004_110	RGO 04-110 (WTU)
<i>Lippia arechavaletae</i>	Lippia_arechavaletae_NA	No Voucher
<i>Lippia aristata</i>	Lippia_aristata_PLI2010_05	PLI 2010-5 (WTU)
<i>Lippia asperrima</i>	Lippia_asperrima_ERG3282	E.R. Guaglianone et al. 3282

Appendix S1. (cont.) Specimens included in this study with voucher information

Taxon	Tip label	Voucher (Herbarium)
<i>Lippia asperrima</i>	Lippia_asperrima_RGO2004_140	RGO 04-140
<i>Lippia betulifolia</i>	Lippia_betulifolia_WH4841	W. Hahn 4841 (US)
<i>Lippia brasiliensis</i>	Lippia_brasiliensis_PLI2010_17	PLI 2010-17 (WTU)
<i>Lippia coartacta</i>	Lippia_coartacta_ONM5253	O.N. Morrone 5253
<i>Lippia corymbosa</i>	Lippia_corymbosa_PLI2010_13	PLI 2010-13 (WTU)
<i>Lippia diamantinensis</i>	Lippia_diamantinensis_FRGS2943	F.R.G. Salimena 2943 (CESJ)
<i>Lippia domingensis</i>	Lippia_domingensis_PLI2012_80	PLI 2012-80 (WTU)
<i>Lippia duartei</i>	Lippia_duartei_PLI2010_11	PLI 2010-11 (WTU)
<i>Lippia dulcis</i>	Lippia_dulcis_NA	No Voucher
<i>Lippia filifolia</i>	Lippia_filifolia_VT352	V. Thode 352 (ICN)
<i>Lippia florida</i>	Lippia_florida_FRGS2945	F.R.G. Salimena 2945 (CESJ)
<i>Lippia formosa</i>	Lippia_formosa_O1764	Ocampo 1764
<i>Lippia grandifolia</i>	Lippia_grandifolia_MR5249	M. Reekmans 5249 (PRE)
<i>Lippia grisebachiana</i>	Lippia_grisebachiana_C382	Caldella et al. 382
<i>Lippia hederifolia</i>	Lippia_hederifolia_PLI2010_14	PLI 10-14 (WTU)
<i>Lippia hemanioides</i>	Lippia_hemanioides_VT389	V. Thode 389 (ICN)
<i>Lippia integrifolia</i>	Lippia_integrifolia_RGO2007_78	RGO 2007-78 (WTU)
<i>Lippia javanica</i>	Lippia_javanica_PLI2012_1a	PLI 2012-1a (WTU)
<i>Lippia javanica</i>	Lippia_javanica_WV390	W. Vos 390 (NU)
<i>Lippia kituensi</i>	Lippia_kituensi_LF917	L. Festo et al 917 (MO)
<i>Lippia lasiocalycina</i>	Lippia_lasiocalycina_VT363	Thode 363 (WTU)
<i>Lippia lippoides</i>	Lippia_lippoides_MEM4185	M.E. Mulgara et al 4185
<i>Lippia lupulina</i>	Lippia_lupulina_FRGS2941	F.R.G. Salimena 2941 (CESJ)
<i>Lippia macrophylla</i>	Lippia_macrophylla_TS13474	Thomas & Sant'Ana 13474 (CESJ)
<i>Lippia micromera</i>	Lippia_micromera_RGO1992_225	RGO 92-225 (WTU)
<i>Lippia myriocephala</i>	Lippia_myriocephala_SOG144	SOG 144 (HULE)
<i>Lippia oatesii</i>	Lippia_oatesii_B4199	Biegel 4199 (PRE)
<i>Lippia origanoides</i>	Lippia_organoides_PLI2010_18	PLI 10-18 (WTU)
<i>Lippia origanoides</i>	Lippia_organoides_RGO1992_210	RGO 92-210 (WTU)
<i>Lippia phryxocalyx</i>	Lippia_phryxocalyx_GE4506	G. Eiten 4506 (US)
<i>Lippia pseudothea</i>	Lippia_pseudothea_FS2940	FS 2940 (CESJ)
<i>Lippia pusilla</i>	Lippia_pusilla_VT337	V. Thode 337 (ICN)
<i>Lippia rehmannii</i>	Lippia_rehmannii_HHWP92	HHW Pearson 2/12/92
<i>Lippia rehmannii</i>	Lippia_rehmannii_PLI2008_20	PLI 2008-20 (WTU)
<i>Lippia rhodocnemis</i>	Lippia_rhodocnemis_PLI2010_06	PLI 2010-6 (WTU)
<i>Lippia rotundifolia</i>	Lippia_rotundifolia_FRGS2958	F.R.G. Salimena 2958 (CESJ)
<i>Lippia rubella</i>	Lippia_rubella_PLI2010_3	PLI 10-3 (WTU)
<i>Lippia salsa</i>	Lippia_salsa_RGO2004_180	RGO 04-180 (WTU)
<i>Lippia salviifolia</i>	Lippia_salviifolia_FRGS2975	F.R.G. Salimena 2975 (CESJ)
<i>Lippia salviifolia</i>	Lippia_salviifolia_RGO2004_131	RGO 2004-131 (WTU)
<i>Lippia triplinervis</i>	Lippia_tripplinervis_M2456	Mota 2456 (WTU)
<i>Lippia trollii</i>	Lippia_trollii_FOZ11537	F.O. Zuloaga 11537
<i>Lippia turbinata</i>	Lippia_turbinata_RGO2007_74	RGO 2007-74 (WTU)
<i>Lippia turnerifolia</i>	Lippia_turnerifolia_RGO2004_121	RGO 2004-121 (WTU)
<i>Lippia ukambensis</i>	Lippia_ukambensis_PJG9915	P.J. Greenway 9915 (PRE)
<i>Lippia umbellata</i>	Lippia_umbellata_VD06_194	Van Devender 06-194 (TEX)
<i>Lippia velutina</i>	Lippia_velutina_PLI2010_16	PLI 10-16 (WTU)

Appendix S1. (cont.) Specimens included in this study with voucher information

Taxon	Tip label	Voucher (Herbarium)
<i>Lippia wilmsii</i>	Lippia_wilmsii_PLI2012_11	PLI 12-11 (WTU)
<i>Mulgurea asparagoides</i>	Mulgurea_asparagoides_RGO2004_192	R.G. Olmstead 2004-192 (WTU)
<i>Mulgurea asparagoides</i>	Mulgurea_asparagoides_VS1828	V. Soza 1828 (WTU)
<i>Mulgurea aspera</i>	Mulgurea_aspera_RGO2004_163	R.G. Olmstead 2004-163 (WtU)
<i>Mulgurea aspera</i>	Mulgurea_aspera_VS1824	V. Soza 1824 (WTU)
<i>Mulgurea aspera</i>	Mulgurea_aspera_VS1849	V. Soza 1849 (WTU)
<i>Mulgurea ligustrina</i>	Mulgurea_ligustrina_RGO2007_92	R.G. Olmstead 2007-92 (WTU)
<i>Mulgurea scoparia</i>	Mulgurea_scoparia_RGO2004_167	R.G. Olmstead 2004-167 (WTU)
<i>Mulgurea scoparia</i>	Mulgurea_scoparia_RGO2004_178	R.G. Olmstead 2004-178 (WTU)
<i>Mulgurea tridens</i>	Mulgurea_tridens_JMB500	J.M. Bonifacio 500 (US)
<i>Nashia inaguensis</i>	Nashia_inaguensis_FTG8655	Fairchild Tropical Gardens 8655
<i>Nashia inaguensis</i>	Nashia_inaguensis_Hirts	cultivated Hirt's Gardens
<i>Nashia inaguensis</i>	Nashia_inaguensis_WTG13097	William T. Gillis 13097 (TEX)
<i>Neosparton aphyllum</i>	Neosparton_aphyllum_RGO2004_150	RGO 2004-150 (WTU)
<i>Neosparton aphyllum</i>	Neosparton_aphyllum_RGO2004_193	RGO 2004-193 (WTU)
<i>Neosparton ephedroides</i>	Neosparton_ephedroides_RGO2004_194	RGO 2004-194 (WTU)
<i>Neosparton ephedroides</i>	Neosparton_ephedroides_RGO2007_77	RGO 2007-077 (WTU)
<i>Parodianthus capillaris</i>	Parodianthus_capillaris_MEM2929	M.E. Mulgara 2929 (SI)
<i>Parodianthus ilicifolius</i>	Parodianthus_ilicifolius_RGO2004_181	RGO 2004-181 (WTU)
<i>Petrea blanchetiana</i>	Petrea_blanchetiana_GdN5812	G. de Nevers 5812 (MO)
<i>Petrea bracteata</i>	Petrea_bracteata_AHG13325	A.H. Gentry 13325 (MO)
<i>Petrea kohautiana</i>	Petrea_kohautiana_JLC6554	J.L. Clark 6554 (US)
<i>Petrea maynensis</i>	Petrea_maynensis_GV856	G. Villa 856 (MO)
<i>Petrea maynensis</i>	Petrea_maynensis_RB1765	R. Burnham 1765 (MO)
<i>Petrea volubilis</i>	Petrea_volubilis_RBGK3267503134	RBGK #326.75.03134
<i>Petrea volubilis</i>	Petrea_volubilis_RBGK0007317818	W. Ramirez et al. 17 (MO)
<i>Petrea volubilis</i>	Petrea_volubilis_RGO2011_07	RGO 2011-07
<i>Phyla canascens</i>	Phyla_canascens_RGO2004_159	RGO 2004-159 (WTU)
<i>Phyla cuneifolia</i>	Phyla_cuneifolia_RGO1992_134	RGO 1992-134 (WTU)
<i>Phyla dulcis</i>	Phyla_dulcis_RGO1998_56	RGO 1998-56 (WTU)
<i>Phyla incisa</i>	Phyla_incisa_KJK12801	K.-J. Kim 12801 (TEX)
<i>Phyla lanceolata</i>	Phyla_lanceolata_M4090	McCormac 4090 (OS)
<i>Phyla lanceolata</i>	Phyla_lanceolata_PLI2008_16	PLI 2008-16 (WTU)
<i>Phyla nodiflora</i>	Phyla_nodiflora_PLI2008_03	PLI 2008-03 (WTU)
<i>Phyla nodiflora</i>	Phyla_nodiflora_PLI2008_04	PLI 2008-04 (WTU)
<i>Phyla reptans</i>	Phyla_reptans_RGO2007_65	RGO 2007-65 (WTU)
<i>Phyla scaberrima</i>	Phyla_scaberrima_R168	Rothschild 168 (TEX)
<i>Phyla stoechadifolia</i>	Phyla_stoechadifolia_C43312	Correll 43312 (TEX)
<i>Pitrea cuneato-ovata</i>	Pitrea_cuneato_ovata_RGO2004_186	RGO 2004-186 (WTU)
<i>Pitrea cuneato-ovata</i>	Pitrea_cuneato_ovata_RGO2007_81	RGO 2007-81 (WTU)
<i>Priva bahiensis</i>	Priva_bahiensis_MS6025	M. Sobral et al 6025 (SI)
<i>Priva cordifolia</i>	Priva_cordifolia_WV391	W. Vos 391 (NU)
<i>Priva lappulacea</i>	Priva_lappulacea_RGO1996_86	RGO 1996-86 (WTU)
<i>Priva lappulacea</i>	Priva_lappulacea_TSC8651	T.S. Cochrane 8651 (TEX)
<i>Recordia boliviana</i>	Recordia_boliviana_MN42092	M. Nee 42092 (TEX)
<i>Recordia boliviana</i>	Recordia_boliviana_NRJW2932	N. Ritter, J. Wood 2932 (MO)
<i>Recordia reitzii</i>	Recordia_reitzii_166756	166756 (ICN)

Appendix S1. (cont.) Specimens included in this study with voucher information

Taxon	Tip label	Voucher (Herbarium)
<i>Rehdera penninervia</i>	Rehdera_penninervia_CLLEC19938	C.L. Lundell, Elias Contreras 19938 (TEX)
<i>Rehdera penninervia</i>	Rehdera_penninervia_MPCNB1378	M. Pena-Chocarro & N. Bonilla 1378 (MO)
<i>Rehdera trinervis</i>	Rehdera_trinervis_DN2386	D. Neil 2386 (MO)
<i>Rehdera trinervis</i>	Rehdera_trinervis_EM31706	E. Martinez et al, 31706 (TEX)
<i>Rehdera trinervis</i>	Rehdera_trinervis_EMS30531	E.Martinez S. 30531 (TEX)
<i>Rhaphithamnus spinosus</i>	Rhaphithamnus_spinosus_RBGK1288301596	Kew 128-83.01596
<i>Rhaphithamnus venustus</i>	Rhaphithamnus_venustus_TFS11855	T.F. Stuessy 11855 (OS)
<i>Stachytarpheta cayannensis</i>	Stachytarpheta_cayannensis_RGO951	RGO 951 (WTU)
<i>Stachytarpheta cayannensis</i>	Stachytarpheta_cayannensis_RGO2004_113	RGO 2004-113 (WTU)
<i>Stachytarpheta crassifolia</i>	Stachytarpheta_crassifolia_PT10	P. Tavares et al 10 (MO)
<i>Stachytarpheta frantzii</i>	Stachytarpheta_frantzii_FTG2001_0533B	Fairchild Tropical Gardens 2001-0533B
<i>Stachytarpheta gesnerioides</i>	Stachytarpheta_gesnerioides_WWT5915	W.W.Thomas et al. 5915 (MO)
<i>Stachytarpheta jamaicensis</i>	Stachytarpheta_jamaicensis_RGO1996_68	RGO 1996-68 (WTU)
<i>Stachytarpheta jamaicensis</i>	Stachytarpheta_jamaicensis_RGO2003_20	RGO 2003-20 (WTU)
<i>Stachytarpheta mutabilis</i>	Stachytarpheta_mutabilis_RGO1992_207	RGO 1992-207 (WTU)
<i>Stachytarpheta urticifolia</i>	Stachytarpheta_urticifolia_JT673	J Trusty 673 (FTG)
<i>Tamonea boxiana</i>	Tamonea_boxiana_RGO2003_12	RGO 2003-12 (WTU)
<i>Tamonea curassavica</i>	Tamonea_curassavica_HR1917	H. Rimpler 1917 (FB)
<i>Tamonea juncea</i>	Tamonea_juncea_EM14514	E. Martinez 14514 (MO)
<i>Verbena abramsii</i>	Verbena_abramsii_THK56	T.H. Kearney 56
<i>Verbena alata</i>	Verbena_alata_RK2119	R. Kurmorow 2119 (TEX)
<i>Verbena bonariensis</i>	Verbena_bonariensis_RGO2003_25	R.G. Olmstead 2003-25 (WTU)
<i>Verbena bracteata</i>	Verbena_bracteata_RGO1992_131	R.G. Olmstead 92-131 (WTU)
<i>Verbena bracteata</i>	Verbena_bracteata_YWY2005_11	Y.-W. Yuan 2005-11 (WTU)
<i>Verbena brasiliensis</i>	Verbena_brasiliensis_SK1054	Strong & Kelloff 1054
<i>Verbena californica</i>	Verbena_californica_T16966	Taylor 16966 (UC/JEPS)
<i>Verbena canescens</i>	Verbena_canescens_H4614	Hinckley 4614 (TEX)
<i>Verbena canescens</i>	Verbena_canescens_YWY2005_14	Y.-W. Yuan 2005-14 (WTU)
<i>Verbena caniuensis</i>	Verbena_caniuensis_NST1969	N.S. Troneso 1969 (TEX)
<i>Verbena carnea</i>	Verbena_carnea_WBZ693	W.B. Zomlefer 693 (WTU)
<i>Verbena carolina</i>	Verbena_carolina_RM18865	R. McVaugh 18865
<i>Verbena cloverae</i>	Verbena_cloverae_VLC55262	V.L. Cory 55262
<i>Verbena demissa</i>	Verbena_demissa_SLP4162	S. Lopez-Palacios 4162 (TEX)
<i>Verbena glabrata</i>	Verbena_glabrata_LAF96	LAF 96 (WTU)
<i>Verbena glabrata var. hayekii</i>	Verbena_glabrata_var_hayekii_RGO2009_07	R.G. Olmstead 2009-07 (WTU)
<i>Verbena glabrata var. hayekii</i>	Verbena_glabrata_var_hayekii_RGO2009_10	R.G. Olmstead 2009-10 (WTU)
<i>Verbena glabrata var. hayekii</i>	Verbena_glabrata_var_hayekii_RGO2009_42	R.G. Olmstead 2009-42 (WTU)
<i>Verbena glabrata var. hayekii</i>	Verbena_glabrata_var_hayekii_RGO2009_43	R.G. Olmstead 2009-43 (WTU)
<i>Verbena glabrata var. hayekii</i>	Verbena_glabrata_var_hayekii_RGO2009_44	R.G. Olmstead 2009-44 (WTU)
<i>Verbena graciliis</i>	Verbena_graciliis_JCB1124	J.C. Blumer 1124
<i>Verbena halei</i>	Verbena_halei_YWY2005_16	Y.-W. Yuan 2005-16 (WTU)
<i>Verbena halei</i>	Verbena_halei_YWY2008_02	Y.-W. Yuan 2008-02 (WTU)
<i>Verbena halei</i>	Verbena_halei_YWY2008_09	Y.-W. Yuan 2008-09 (WTU)
<i>Verbena hastata</i>	Verbena_hastata_RGO2003_155	R.G. Olmstead 2003-155 (WTU)
<i>Verbena hastata</i>	Verbena_hastata_RGO2007_157	R.G. Olmstead 2007-157 (WTU)
<i>Verbena hirtella</i>	Verbena_hirtella_YWY2005_15	Y.-W. Yuan 2005-15 (WTU)
<i>Verbena hispida</i>	Verbena_hispida_FZ8266	F. Zuloaga 8266 (SI)

Appendix S1. (cont.) Specimens included in this study with voucher information

Taxon	Tip label	Voucher (Herbarium)
<i>Verbena hispida</i>	Verbena_hispida_VS1816	V. Soza 1816 (WTU)
<i>Verbena hispida</i>	Verbena_hispida_VS1826	V. Soza 1826 (WTU)
<i>Verbena intermedia</i>	Verbena_intermedia_RGO2004_106	R.G. Olmstead 2004-106 (WTU)
<i>Verbena lasiostachys</i>	Verbena_lasiostachys_VS1757	Soza 1757 (WTU)
<i>Verbena lasiostachys</i>	Verbena_lasiostachys_YWY2005_27	Y.-W. Yuan 2005-27 (WTU)
<i>Verbena litoralis</i>	Verbena_litoralis_RGO2004_105	R.G. Olmstead 2004-105 (WTU)
<i>Verbena litoralis</i>	Verbena_litoralis_RGO2009_06	RGO 2009-06 (WTU)
<i>Verbena macdougalii</i>	Verbena_macdougalii_RGO2003_154	RGO 2003-154 (WTU)
<i>Verbena macdougalii</i>	Verbena_macdougalii_YWY2005_19	Y.-W. Yuan 2005-19 (WTU)
<i>Verbena menthifolia</i>	Verbena_menthifolia_ALR2004_1079	A. L. Reina G. 2004-1079 (TEX)
<i>Verbena menthifolia</i>	Verbena_menthifolia_JR20302	J. Rzedowski 20302 (MICH)
<i>Verbena menthifolia</i>	Verbena_menthifolia_JVAD3574	Jennie V. A. Dieterle 3574 (MICH)
<i>Verbena menthifolia</i>	Verbena_menthifolia_YWY2005_04	Y.-W. Yuan 2005-04 (WTU)
<i>Verbena menthifolia</i>	Verbena_menthifolia_YWY2005_24	Y.-W. Yuan 2005-24 (WTU)
<i>Verbena montevidensis</i>	Verbena_montevidensis_RGO2004_112	R.G. Olmstead 2004-112 (WTU)
<i>Verbena neomexicana</i>	Verbena_neomexicana_LHP11033	Lehto, Hensel & Pinkava 11033
<i>Verbena neomexicana</i>	Verbena_neomexicana_OBM612	O.B. Metcalfe 612
<i>Verbena neomexicana</i>	Verbena_neomexicana_OES94	O.E. Sperry 94
<i>Verbena officinalis</i>	Verbena_officinalis_RGO2003_156	R.G. Olmstead 2003-156 (WTU)
<i>Verbena officinalis</i>	Verbena_officinalis_RGO98_55	RGO 98-55 (WTU)
<i>Verbena orcuttiana</i>	Verbena_orcuttiana_RT742	R. Tallent 742 (MICH)
<i>Verbena orcuttiana</i>	Verbena_orcuttiana_YWY2005_26	Y.-W. Yuan 2005-26 (WTU)
<i>Verbena perennis</i>	Verbena_perennis_YWY2005_17	Y.-W. Yuan 2005-17 (WTU)
<i>Verbena plicata</i>	Verbena_plicata_CMR5990	C.M. Rogers 5990
<i>Verbena pogostoma</i>	Verbena_pogostoma_EC6379	E. Carrate 6379 (USM)
<i>Verbena pogostoma</i>	Verbena_pogostoma_HB08	H. Beltran 08 (USM)
<i>Verbena rigida</i>	Verbena_rigida_EB9	Erixon & Bremer 9 (UPS)
<i>Verbena rigida</i>	Verbena_rigida_RGO2004_111	R.G. Olmstead 2004-111 (WTU)
<i>Verbena scabra</i>	Verbena_scabra_RGO2003_09	R.G. Olmstead 2003-09 (WTU)
<i>Verbena sedula</i>	Verbena_sedula_HHvdW2205	H. H. van der Werff 2205 (TEX)
<i>Verbena shrevei</i>	Verbena_shrevei_NA	No Voucher
<i>Verbena trachea</i>	Verbena_trachea_OZ9974	O. Zollner 9974 (TEX)
<i>Verbena urticifolia</i>	Verbena_urticifolia_RGO2003_157	R.G. Olmstead 2003-157 (WTU)
<i>Verbena valerianoides</i>	Verbena_valerianoides_SLP3639	S. Lopez-Palacios 3639 (TEX)
<i>Verbena villifolia</i>	Verbena_villifolia_AHG37499	A. Gentry et al. 37499 (TEX)
<i>Verbena villifolia</i>	Verbena_villifolia_LAF113A	LAF 113A (WTU)
<i>Verbena villifolia</i>	Verbena_villifolia_LAF113B	LAF 113B (WTU)
<i>Verbena villifolia</i>	Verbena_villifolia_OT743	O. Tovar 743 (TEX)
<i>Verbena xutha</i>	Verbena_xutha_CT5371	Clansen & Trapido 5371
<i>Xeroaloyisia ovatifolia</i>	Xeroaloyisia_ovatifolia_RGO2004_184	RGO 2004-184 (WTU)
<i>Xolocotzia asperifolia</i>	Xolocotzia_asperifolia_DN5477	David Neill 5477 (MO)
<i>Xolocotzia asperifolia</i>	Xolocotzia_asperifolia_WDS22332	W.D. Stevens 22332 (MO)